8-2009

Histone Deacetylase Inhibitors for Selective Anti-Cancer Therapeutics

Shambhunath Choudhary
University of Tennessee - Knoxville

To the Graduate Council:

I am submitting herewith a dissertation written by Shambhunath Choudhary entitled "Histone Deacetylase Inhibitors for Selective Anti-Cancer Therapeutics." I have examined the final electronic copy of this dissertation for form and content and recommend that it be accepted in partial fulfillment of the requirements for the degree of Doctor of Philosophy, with a major in Comparative and Experimental Medicine.

Hwa-Chain Robert Wang, Major Professor

We have read this dissertation and recommend its acceptance:

Karla J Matteson, Seung J Baek, Stephen A Kania

Accepted for the Council:

Carolyn R. Hodges

Vice Provost and Dean of the Graduate School

(Original signatures are on file with official student records.)

To the Graduate Council:

I am submitting herewith a dissertation written by Shambhunath Choudhary entitled "Histone Deacetylase Inhibitors for Selective Anticancer Therapeutics". I have examined the final electronic copy of this dissertation for form and content and recommend that it be accepted in partial fulfillment of the requirements for the degree of Doctor of Philosophy, with a major in Comparative and Experimental Medicine.

Hwa-Chain Robert Wang
Major Professor

We have read this dissertation
and recommend its acceptance:

Karla J Matteson

Seung J Baek

Stephen A Kania

Accepted for the Council:

Carolyn R. Hodges
Vice Provost and Dean of the Graduate School

(Original signatures are on file with official student records.)

HISTONE DEACETYLASE INHIBITORS FOR SELECTIVE ANTICANCER THERAPEUTICS

A Dissertation
Presented for the
Doctor of Philosophy
Degree
The University of Tennessee, Knoxville

Shambhunath Choudhary
August 2009

DEDICATION

This dissertation is dedicated to my parents, Govind Choudhary and Trivani Choudhary with love.

ACKNOWLEDGEMENTS

I would like to thank the people who helped me to make this research and degree possible. First my sincere appreciation goes to my PhD mentor, Dr. Hwa Chain Robert Wang, who has served as a father figure to me over the last four and half years and has helped and supported me in achieving my short-term scientific goals. In due course of time, he honed my abilities to identify unresolved problems in the field of cancer biology and solve them with great zeal and zest. Additionally, I would like to extend my sincere thanks to the members of my committee, Dr Karla J Matteson, Dr. Stephan A Kania, and Dr. Seung J Baek, for all their time and needful guidance. I also thank my collaborator Dr. Kenneth K Chan of Ohio State University for providing FR901228 for my thesis work and Ms. Dianne J Trent for technique support in flow cytomerty.

I express my thanks to all the members of my lab for providing a stimulating and fun environment to learn and grow. Specifically, I would like to thank Dr. Yong Fang Chen, Dr. Nalin Siriwardhana, Kusum Rathore, Joyce Song, and Nayna Kotadia for their help and time in my projects. Special thanks to Kusum Rathore for all the technical help she has given me during my projects.

I appreciate and thank the College of Veterinary Medicine, University of Tennessee, Knoxville, for the opportunity and the financial support for this study.

Finally, I express my deepest gratitude to my mother, father and brothers who were always beside me and motivated me to come this far. I am eternally grateful for their everlasting support and faith in all my strength and capability.

ABSTRACT

Activating mutations of *ras* genes are frequently found in human cancers. Since Ras proteins and their functions play an important role in tumorigenesis, it is important to develop targeted anticancer therapeutics against Ras-related human cancers. We observed that in addition to tumorigenic ability, oncogenic H-Ras possesses a novel proapoptotic ability to facilitate the induction of apoptosis by histone deacetylase inhibitors (HDACIs), such as FR901228 and trichostatin A (TSA). HDACIs make up a new class of structurally diverse anticancer agents and have been shown to exhibit antimetastatic and antiangiogenic activities toward malignantly transformed cells. We detected that expression of oncogenic H-Ras potentiated intracellular reactive oxygen species (ROS) in human and mouse cells to enhance HDACI-induced ROS, thereby contributing to the induction of selective apoptosis and caspase activation.

The first part (Part I) of this dissertation focuses on the understanding of Ras proteins, their role in normal and transformed cell physiology, and current treatment options against Ras-related human cancers, as well as the role of HDACIs and ROS in anticancer therapeutics. The next three parts (Part II-IV) focus on revealing the mechanisms for the novel pro-apoptotic ability of oncogenic H-Ras that allow HDACIs to induce selective apoptosis of the oncogenic H-Ras expressing cells. Results in Part II & III verify the pro-apoptotic activity of oncogenic H-Ras in the increased susceptibility of human cancer cells to HDACIs. The caspase pathways, the B-Raf and extracellular signal regulated kinase pathway, $p21^{Cip1}$ and $p27^{Kip1}$, and core histone contents are regulated differently by FR901228 in oncogenic H-Ras–expressed cells than their counterparts in parental cells, contributing to the increased susceptibility to the induction of selective apoptosis. Results in Part IV describe the role of reactive oxygen species in the pro-apoptotic ability of

oncogenic H-Ras to enhance the cell susceptibility to HDACIs. Intracellular ROS was cooperatively up-regulated by oncogenc H-Ras and HDACI treatment to induce selective apoptosis of oncogenic H-Ras-expressing cells. The last section (Part V) summarizes the findings with their importance and discusses future directions.

Table of Contents

ABBREVIATIONS

Ac-DEVD-CHO	Ac-Asp-Glu-Val-Asp-CHO
AEBSF	4-(2-Aminoethyl)benzenesulfonylfluoride
BrdU	5-bromo-2'-deoxyuridine
CM-H2DCF-DA	Chloromethyl-dichlorodihydrofluorescin-diacetate
CDK	Cyclin-dependent kinase
ERK	Extracellular signal regulatory kinase
FITC	Fluorescein isothiocyanate
FLIP	FLICE inhibitory protein
FTI	Farnesyltransferase inhibitor
GAP	GTPase activating protein
GEF	Guanine nucleotide exchange factors
HAT	Histone acetyl transferase
HDAC	Histone deacetylase
HDACI	Histone deacetylase inhibitor
HIF	Hypoxia inducible factors
H_2O_2	Hydrogen peroxide
·OH	Hydroxyl radical
IAP	Inhibitor of apoptosis
IC_{50}	50% inhibitory concentration
ICMT1	Isoprenylcysteine carboxyl methyltransferase-1
MTT	Methyl Thiazolyl Tetrazolium

NAC	N-acetyl-L-cysteine
NAO	10-N-nonyl Acridine Orange
NF-κB	Nuclear factor-kappa B
PARP	poly(ADP-ribose) polymerase
PI3-K	phosphatidylinositol 3-kinase
PTEN	Phosphatidylinositol 3 kinase phosphatase with tensin homology
RCE1	Ras-converting enzyme-1
Rho-123	Rhodamine-123
ROS	Reactive oxygen species
ROT	Rotenone
RTK	Receptor tyrosine kinase
SAPK	Stress-activated protein kinase
O_2^-	Superoxide anion radical
TSA	Trichostatin A
VEGF	Vascular endothelial growth factor

PART-I

BACKGROUND AND OVERVIEW

ras oncogene in human cancer

Cancer and Oncogene

Cancer is characterized by uncontrolled cell growth and differentiation where a normal cell becomes progressively transformed to a malignant one. This transformation results from sequential acquisition of mutations in the cellular genome that causes changes in the gene functions responsible for maintaining a balance between cell proliferation and cell death. These mutational damages can cause (i) activation of oncogenes, which stimulate proliferation or protect against cell death, and (ii) the inactivation of the tumor suppressor genes, which would normally inhibit proliferation. These genetic changes in tumor tissue lead to excessive cell proliferation as compared to cell death. In normal tissue, on the other hand, a strict balance between cell proliferation and cell death is always maintained.

Oncogenes are activated proto-oncogenes that promote cellular transformation. Normally their products will perform different essential functions inside a cell such as transmission of growth-promoting signals from cell surface to the nucleus (e.g. *src, ras*), transcription regulation (e.g. *myc, c-jun*), or regulation of cell death (e.g. *bcl2*). These genes are dominantly acting since only one copy of the gene has to undergo mutation to produce a change in cellular control. On the other hand, both copies of the tumor suppressor gene (e.g. *Rb*, *p53)* must be lost, mutated or inactivated for malignant transformation.

The next hurdle for an aspiring cancer cell after overcoming the controls on cell birth and cell death is telomere erosion that sets the limit for endless cell division. Telomeres are non-transcribed regions at the end of chromosomes that shortens with every cell division. This process induces replicative senescence and blocks cell division. Telomerase, the enzyme that

repairs the eroded telomeres, is expressed in limited fashion in somatic cells; therefore the somatic cells are allowed only a limited number of cell divisions (1). Telomerase upregulation has been observed in most of human malignancies and helps the cancer cells to maintain telomere length in order to become immortal (2). Once immortalized, these continuously dividing cells need enough supplies of nutrients and oxygen to maintain a high rate of proliferation. To meet this demand a solid tumor may start the process of angiogenesis by stimulating the release of several growth factors e.g. vascular endothelial growth factor (VEGF) from tumor cells as well as the surrounding normal cells (3,4).

Much of the current molecular research is directed towards identifying genes that are altered in various types of tumors and elucidating the role of these genes in carcinogenesis. A family of genes that is frequently found to harbor a mutation in human tumors is that of the *ras* oncogenes.

ras oncogene

ras is a family of genes that is widely activated in human cancer. In fact *ras* was the first oncogene to be discovered in human cancer (from a bladder tumor) (5). In humans there are three functional genes in this family; H-*ras*, K-*ras*, and N-*ras*. The Ras genes encode four highly similar 188-189 amino acid proteins with molecular weights of 21,000 (H-Ras, N-Ras, K-Ras4A and K-Ras4B). The two forms of K-Ras diverge solely in their COOH-terminal 25 amino acids as a consequence of alternate exon utilization (Figure 1). Mutated *ras* genes in human tumors can be detected by their ability to transform NIH/3T3 cells into immortalized cells (NIH/3T3 transfection assay). In early research, this assay was used in combination with nude mouse

tumorigenicity test to reveal the positions at which activating point mutations occurred. Such point mutations are mostly seen in codons 12, 13 and 61 of the three *ras* genes. The most frequent alteration is a codon 12 G → T transversion causing a glycine → valine amino acid substitution (6). Currently the incidence of mutated *ras* genes in various human tumors can be easily detected by detecting point mutations with the help of various biochemical assays such as selective hybridization with synthetic oligodeoxynucleotide probes specific for a known mutation, RNase mismatch cleavage or by sequence analysis after PCR amplification of the *ras* gene segments known to contain point mutations. These assays have provided information on the presence and incidence of mutated *ras* genes in a variety of tumor types. Specific associations have been found between the various *ras* oncogenes and particular types of human cancer (Table 1). K-*ras* mutations are found mainly in pancreatic and colonic carcinomas, H-*ras* mutations are frequent in bladder carcinomas, and N-*ras* mutations are linked primarily to lymphoid malignancies and melanomas. Some tumor types, like thyroid tumors, seem to lack any specificity and activating mutations are seen in all three *ras* oncogenes (7,8).

Regulation of Ras functioning

Post-translational modifications

Ras proteins are small GTPases and act as signal transduction molecules at the inner surface of plasma membrane in response to various extracellular stimuli. After their synthesis, cytoplasmic Ras proteins must undergo post-translational modification (lipid processing) at their C terminus that facilitates their association with the plasma membrane in order to carry out

intracellular functions. Hence, post-translational modification of Ras proteins is the key determinant of their functioning. The C terminus is highly divergent among the Ras family members and contains the membrane-targeting sequences (Figure 1). Three enzymes that sequentially modify the C-terminal CAAX motif of Ras proteins catalyze post-translational lipid processing, where C is cysteine, A is usually an aliphatic residue and X is any amino acid (Figure 1). First a farnesyl isoprenoid lipid is attached to Ras proteins by the enzyme farnesyltransferase (FTase). In the presence of FTase inhibitors, both K-Ras-4A and N-Ras can become prenylated by geranylgeranyl transferase (9). This prenylation reaction is followed, in the endoplasmic reticulum, by the proteolytic cleavage of the last three amino-acid residues (AAX) by Ras-converting enzyme-1 (RCE1), and by the carboxymethylation of the now terminal Cys residue by isoprenylcysteine carboxyl methyltransferase-1 (ICMT1). The C-terminal Lys residues in K-Ras-4B are sufficient to anchor it in the membrane, whereas H-, N- and K-Ras-4A require a palmitoylation step in which a palmitoyl moiety is attached to the C-terminal upstream Cysteine residues by palmitoyltransferase (PTase) before their insertion in the membrane is stabilized (10,8).

GTPase cycle and GAP- and GEF-mediated regulation

At inner surface of the plasma membrane Ras proteins serve as binary molecular switches to transduce extracellular ligand-mediated stimuli into the cytoplasm to control signal transduction pathways that influence cell growth, differentiation and apoptosis. As shown in figure 2, biological activity of Ras is controlled by a regulated GDP/GTP cycle. The binding of GTP to Ras proteins locks them in their active states, which enables high affinity interactions

with downstream targets that are called effectors. Subsequently, a slow intrinsic GTPase activity cleaves off the gamma-phosphate, leading to Ras functional inactivation and thus the termination of signaling. Since the intrinsic GDP/GTP exchange and GTP hydrolytic activity of Ras is very low, two types of regulatory proteins modulate cellular control of GDP/GTP cycling. Guanine nucleotide exchange factors (GEFs) or GTP-releasing proteins/factors (GRPs/GRFs), such as RasGRF and son of sevenless (SOS), promote formation of the active GTP-bound state whereas Ras GTPase activating proteins (GAPs), such as p120GAP or neurofibromin (NF1), promote formation of the inactive GDP-bound state. Oncogenic Ras mutant proteins are locked in the active GTP-bound state, as point mutations at 12, 13 or 61 codons render them insensitive to GAP stimulation leading to constitutive, deregulated activation of Ras function (11).

Downstream effector signaling

In general, Ras mediated signaling involves its activation and recruitment to the plasma membrane following receptor Tyrosine kinase (RTK) stimulation by growth factors (GF). Activated Ras then initiate several signal-transduction cascades by engaging effector molecules from multiple effector families to mediate its various functions (Figure 2). Ras effectors are proteins that interact with RAS-GTP/activated Ras.

Raf and the MEK/ERK cascade. Raf is a key effector of Ras. The mammalian Raf protein family consists of three Serine/Threonine kinases: Raf-1, A-Raf and B-Raf (11). Raf-1 was the first bona fide mammalian Ras effector to be identified. It mediates the signal from Ras to nucleus through mitogen-activated protein kinase (MAPK)/extracellular signal-regulated kinase (ERK) kinase (MEK), ERK1/2, and the E26-transcription factor proteins (ETS). MAPK

signaling has been shown to be both sufficient and necessary for Ras-induced transformation of murine cell lines. In addition, activating mutation of B-Raf is found in human cancers, in non-overlapping frequencies with Ras mutations (for example, in melanoma and colon cancer). This further emphasizes an important role for aberrant Raf–MEK–ERK signaling in oncogenesis (12,8).

Ras signals through PI3K. Another Ras effector is p110 catalytic subunit of the class I phosphoinositide 3-kinases (PI3Ks) which generate the second messenger lipid phosphatidylinositol (3,4,5) triphosphate or PIP_3 upon activation. PIP_3 recruits phosphatidyl inositol-dependent kinase 1 (PDK1) and Ser/Thr kinase AKT/Protein kinase B to the plasma membrane, where PDK1 phosphorylates and activates AKT. The anti-apoptotic effects of Ras have been mainly attributed to the pro-survival activities of activated PI3K signaling through a pathway that involves the Ser/Thr kinase AKT/protein kinase B and the transcription factor nuclear factor-κB (NF-κB), both of which have crucial roles in preventing anoikis (detachment induced cell death or suspension induced apoptosis). High activity of PI3K is seen in many tumor cells and in most cases this is attributed to the loss of the phosphatidylinositol 3 kinase phosphatase with tensin homology (PTEN) lipid phosphatase. PTEN catalyzes the removal of the D3 phosphate from PIP3 to terminate downstream signaling, and is now thought to be the most commonly mutated tumor suppressor in humans, after p53 (8,13).

Ras signals through RAL–GEFs. Ras interacts with guanine nucleotide-exchange factors for the Ras-like (RalA and RalB) small GTPases (Ral guanine nucleotide-dissociation stimulator (RalGDS) and RalGDS-like protein (RGL)). RAL–GEFs serve as a link between the RAS and the Ral family of GTPases. Recent studies in human cells have suggested that activation of the

RalGEF–Ral pathway alone, but not the PI3K or the Raf pathways, is sufficient to promote Ras transformation of human kidney epithelial cells (14). RAL signaling has been implicated in tumor cell growth and cell survival, regulation of endocytosis or excocytosis, actin organization, cell migration, and gene expression (15,8).

Additional Ras effectors. Several other Ras effectors have been described, which include a number of proteins with diverse roles in cell physiology. These include phospholipase C-ε (PLCε), T-cell lymphoma invasion and metastasis-1 (TIAM1), Ras interaction/interference protein-1 (RIN1), ALL (acute lymphoblastic leukaemia)-1 fused gene on chromosome 6 (AF-6, also known as afadin) proteins, and the Ras association domain-containing family (RASSF) proteins (8).

Targeting oncogenic Ras in human cancer treatment

Current Ras-related anticancer approaches mainly focus on targeting RAS proteins or RAS effector pathways (16). Blocking Ras function by inhibiting the enzymes that catalyze post-translational modification of Ras proteins in order to prevent its association with plasma membrane was one of the earliest strategies adopted. This led to the development of farnesyltransferase inhibitors (FTIs) that simulate the CAAX motif of Ras proteins and compete with Ras for its post-translational processing enzymes, thus blocking the first step of Ras modification (prenylation) and thereby inhibiting its activity (17). However later on it was found that in the presence of FTase inhibitors, K-Ras and N-Ras can become prenylated by geranylgeranyl transferase thereby rendering them refractory to inactivation by FTIs (9). Alternative strategy to block Ras function involved pharmacological inhibition of enzymes that

catalyzes other steps of the Ras processing pathway such as Ras-converting enzyme-1 (RCE1) and isoprenylcysteine carboxyl methyltransferase (ICMT1). However due to extensive number of other CAAX-terminating proteins that serve as substrates, these two enzymes may not be selective for Ras proteins. Additional approaches have been developed over the years such as inhibition of Ras expression by anti-sense RNA-based technology, the use of anti-Ras ribozymes, or application of anti-Ras retroviral therapy to counter Ras function (8).

Approaches focusing on targeting Ras effector pathways involve developing inhibitors of downstream effector of Ras such as MEK, Akt, and mTOR. For example, inhibition of MEK by CI-1040 has been shown to inhibit the growth of some cell lines expressing Q61R NRAS (18). However, despite substantial effort, there are currently no agents that effectively counter the biochemical consequences of oncogenic Ras.

Recent studies have shown the pro-apoptotic activity of oncogenic H-Ras(V12) that allows HDACI FR901228 to induce selective apoptosis of mouse embryo fibroblast 10T1/2 cells (105,106). However, mechanisms behind the pro-apoptotic activity of oncogenic H-Ras are not clear. Histone deacetylase inhibitors (HDACIs) are a new class of anticancer agents and growing evidence indicates that transformed cells are much more sensitive than normal cells to growth-inhibitory and apoptotic effects of (44,47).

Expression of oncogenic Ras has also been shown to elevate intracellular ROS (64). ROS have broad range of responses inside the cell depending upon magnitude of level and duration of exposure. Excessive accumulation of intracellular ROS may cause cell death. Cells with activating mutation of *ras* genes will be under increased ROS stress and will be more susceptible to further oxidative insults than normal cells, leading to cell death. Hence any agent that directly

or indirectly causes ROS accumulation will preferentially kill cancer cells. For example, HDACIs have been shown to cause increased intracellular ROS leading to apoptosis (84). Excessive accumulation of intracellular ROS caused by oncogenic Ras and HDACI treatment may cause selective apoptosis of cells harboring activating mutation of *ras* genes.

Apoptosis in cancer

Apoptosis

Apoptosis is a genetically encoded, highly regulated natural process for removing unwanted cells such as those with potentially harmful mutations, aberrant sub-stratum attachment, or alterations in cell-cycle control. Defective apoptosis can disrupt the delicate balance between cell proliferation and cell death and can lead to diseases such as cancer. Hence evasion of apoptosis has been recognized as one of the six essential alterations in cell physiology that dictate malignant growth and is a hallmark of most, and maybe all, types of cancer (19). Defective cell cycle regulation, growth factor autonomy, defective senescence, sustained angiogenesis, and metastasis and tissue invasion are other five fundamental hallmarks of cancer. Moreover, defective apoptosis can also interfere with the anticancer drugs, which act primarily by inducing apoptosis. Hence, over the years many efforts have been made to design the drugs, which can restore apoptosis in order to treat cancer (20).

Apoptotic cell death phenotype is characterized by features such as cytoplasmic shrinkage, membrane blebbing, nuclear fragmentation, intranucleosomal DNA fragmentation, phosphatidylserine exposure due to changes in the plasma membrane, and finally fragmentation

into membrane enclosed apoptotic bodies sequestered by macrophages or other engulfing cells (21,22).

Mechanism of Apoptosis

The core machinery of apoptosis in mammals consists of a large family of cysteine proteases, termed caspases, Apaf-1 and BCL2-family members. Activation of caspases is responsible for the cleavage of vital components of the cell leading to the formation of characteristic morphological features of apoptosis (described above) (23).

Apoptotic signaling pathways that activate caspases can be divided into two components — those that involve the mitochondria (intrinsic pathway) and those that signal through death receptors (extrinsic pathway) (Figure 3)

The intrinsic pathway involves the release of cytochrome c from the intermembrane space of the mitochondria due to mitochondrial membrane permeabilization (MMP). Though exact mechanism of MMP is not yet clear, defective inner transmembrane potential ($\Delta\Psi m$) has been observed before, during and after MMP (24). The mitochondrial respiratory chain produces energy, which is stored as an electrochemical gradient or the $\Delta\Psi m$, negative inside of about 180-200 mV. This energy source pumps protons (H^+) that drive ATP synthesis. Loss of $\Delta\Psi m$ is a result of the ion equilibration across the inner membrane. This loss of $\Delta\Psi m$ could lead to swelling of the matrix as water enters, which can result in sufficient swelling to break the outer membrane to produce MMP. MMP contributes to cell death in several different ways; in apoptosis by releasing cytochrome c, in caspase independent cell death by releasing factors like

apoptosis inducing factor (AIF) (25) and Htra2/Omi (26) and, by disrupting mitochondrial functions that are essential for cell survival such as electron transport chain (27).

Once in cytosol, cytochrome c interacts with apoptotic protease-activating factor 1 (APAF1) and, together with dATP (2'-deoxyadenosine 5'-triphosphate), forms a multimeric complex that recruits and activates caspase 9, leading to the activation of downstream executer caspases and the death response (20).

In the extrinsic pathway, ligands such as tumour-necrosis factor (TNF), FAS ligand (also known as CD95L), or TNF-related apoptosis-inducing ligand (TRAIL, also known as APO2 ligand (APO2L) or TNF ligand superfamily member 10 (TNFSF10)) interact with and activate their respective death receptors (TNF receptor 1 (TNFR1), FAS (also known as CD95) and death receptor 4 (DR4, also known as TRAIL receptor 1 (TRAILR1)) or DR5 (also known as TRAILR2), respectively. Activated receptors then initiate recruitment of the FAS-associated death domain (FADD) and the activation of the protease caspase 8, which then cleaves and activate downstream executer caspases (28). The death receptor pathway also contributes to the mitochondrial cytochrome c release through the activation of caspase 8 and its down stream target BID (29). Caspase 8 induces BID-cleavage leading to the formation of truncated BID (tBID), which then translocates from cytoplasm to mitochondria and causes cytochrome c release. Finally both mechanisms converge into cleavage and activation of executioner caspases 3, 6 and 7, which carry out the proteolysis of death substrates (Figure 3) (23).

Caspases

Caspases are a family of cysteine proteases that are responsible for the execution of apoptosis. As the name implies ('c' stand for cysteine and 'aspase' is for aspartate) these enzymes cleave the protein after an aspartic acid residue. Each caspase is initially synthesized as a pro-caspase and requires a cleavage at specific site (which also is an aspartate) by another caspase to generate active enzyme. Multiple caspases are involved in mammals during different phases of apoptosis (23). Currently, 11 human caspases have been identified: caspase 1-10 and caspase 14. The protein initially named caspase 13 was found to be the bovine homologue of caspase 4. Caspase 11 and 12 are murine homologues of human caspase 4 and 5. Caspases are classified in several ways. Most important of those is the function-based classification where all caspases fit into three subfamilies i.e. initiators of apoptosis and inflammation (caspase 1, 5, 11), initiators of apoptosis (caspase 2, 8, 9, 10, 12) and effectors /executors of apoptosis (caspase 3, 6, 7) which are activated by initiator caspases (21).

Regulation of Apoptosis

Apoptotic signaling pathways are tightly regulated by pro and anti-apoptotic mechanisms and the balance between them may govern the orderly demise of the cell. Proteins of BCL2 family members (30) that localize to the mitochondria can either prevent or cause the release of cytochrome c from the mitochondria to either inhibit or promote apoptosis. For example, anti-apoptotic BCL2 family members BCL2 and BCL-X_L inhibit programmed cell death by preventing the release of cytochrome c, whereas pro-apoptotic BCL2 family members (such as BAK, BAX, BAD and BID) promote the release of cytochrome c. Inhibitor of apoptosis proteins

(IAPs) are another important protein family that regulates apoptosis. IAPs bind to and inhibit both intrinsic and extrinsic caspases and thereby block apoptotic signaling (31). IAPs in turn are regulated by another mitochondrial released protein called SMAC (second mitochondria-derived activator of caspase (32), also known as DIABLO, direct IAP-binding protein with low pI (33)). SMAC is released from mitochondria once the cell has received a death signal. SMAC then binds to IAP and antagonizes their anti-apoptotic activity.

Other important regulators of apoptosis are MDM2 and p53. On sensing DNA damage, p53 induces cell-cycle arrest and apoptosis. Importance of disrupting the p53 pathway in cancer development can assess by the fact that p53 is mutated and inactivated in half of all cancers analyzed. MDM2 can also inactivate p53 mediated apoptotic pathway by binding to p53 and causing its degradation by the proteasome (34).

Protein components and regulators of the apoptosis signaling pathways are possible drug targets for modulating apoptosis and are promising targets for cancer drug discovery. Some of the apoptosis targets that are currently being explored for cancer drug discovery include the tumor-necrosis factor (TNF)-related apoptosis-inducing ligand (TRAIL) receptors, the BCL2 family of anti-apoptotic proteins, inhibitor of apoptosis (IAP) proteins and MDM2 (20).

Histone deacetylase inhibitors in cancer research

Acetylation, Deacetylation, and Chromatin Remodeling

While the base sequence of DNA provides the genetic code for proteins, remodeling of the chromatin proteins around which the DNA is wrapped is the fundamental epigenetic mechanism along with DNA methylation for regulating gene expression. All of the human

genome is packaged into chromatin which is a complex structure made up of DNA, histones, and non-histone proteins. The basic repeating unit of chromatin is the nucleosome, composed of approximately 146 bp of DNA wrapped around the histone octamer composed of two copies of each of four core histones, H2A, H2B and H3 and H4 (Figure 4). In addition to the core histone molecules, the linker histone H1 is also contained in chromatin, which in combination with other proteins helps in DNA condensation. Histones are small basic proteins consisting of a globular domain and a more flexible and charged NH2-terminus (histone "tail") that protrudes from the nucleosome (35,36). Chromatin remodeling involves the reversible post-translational modification of amino acids in the histone tails by acetylation of lysines, methylation of lysines and arginines, phosphorylation of serines, and ubiquination and sumoylation of lysines (Figure 4). These modifications affect the histones' ability to bind DNA and each other, which in turn affects gene expression. It has been hypothesized that histone modifications acting alone or in combination represent a ''code'' that can be read and translated into biological functions by non-histone proteins forming complexes involved in the regulation of gene expression (37-39).

Among these various covalent modifications of histone tail histone acetylation has been the most studied and appreciated. The acetylation status of histones and non-histone proteins is determined by two groups of enzymes, histone deacetylases (HDACs) and histone acetyl-transferases (HATs). HATs add acetyl groups to lysine residues and acetylation of histone in general promotes a more relaxed chromatin structure, allowing transcriptional activation. HDACs remove the acetyl groups from lysine residues and consequently promote chromatin condensation and hence can act as transcription repressors (40).

The correlation between histone acetylation and transcriptional activation is due to intrinsic HAT activity of several groups of transcriptional co-activator proteins. These include GCN5-related N-acetyltransferase, MYST, and cAMP response element binding protein (CREB/p300) families (41). HATs are recruited to sites in the promoter region of genes by DNA-binding transcription factors and they function in association with protein complexes that can include an array of other HATs, transcription coactivators and co-repressors. HATs also target non-histone protein substrates, in particular TFs such as p53, GATA-1, E2F, estrogen receptor (ER), and various cell-cycle regulatory proteins with variable functional consequences (40).

In humans, 18 HDAC enzymes have been identified and classified into four classes, based on homology to yeast HDACs (42,43). Class I HDACs are related to yeast RPD3 deacetylase and can be further divided into classes Ia (HDAC1 and -2), Ib (HDAC3) and Ic (HDAC8). They have high homology in their catalytic sites. Class I HDACs are primarily nuclear in localization and ubiquitously expressed. Class II HDACs are related to yeast Hda1 (histone deacetylase 1) and include class IIa, consisting of HDAC4, -5, -7 and -9, and class IIb, consisting of HDAC6 and -10, which contain two catalytic sites. Class II HDACs have tissue-specific expression and can be primarily cytoplasmic in location and/or migrate between the cytoplasm and nucleus. All HDACs under class I and II are zinc-dependent enzymes and their activity is inhibited by compounds such as varinostat or trichostatin A (TSA). Members of class III HDAC, also called a sirtuins, require NAD+ for their enzymatic activity. Among them, SIRT1 is orthologous to yeast silent information regulator 2. Unlike class I and class II deacetylases, the enzymatic activity of class III HDACs is not inhibited by compounds such as

vorinostat or TSA. Class IV HDAC is represented by HDAC11, which has conserved residues in its catalytic center that are shared by both class I and class II deacetylases. Apart from histone, the HDACs have many non-histone proteins substrates such as hormone receptors, chaperone proteins and cytoskeleton proteins, which regulate cell proliferation and cell death (Table 2). Hence these enzymes may more properly be referred to as "lysine deacetylases" (43).

Histone deacetylases and Cancer

HATs and HDACs are involved in acetylation and deacetylation not only of chromatin proteins, disruption of which can lead to altered regulation of transcription of genes (epigenetic regulation), but also of non-histone proteins controlling cell-cycle progression, differentiation, and/or apoptosis. Hence altered expression or mutation of genes that encode HATs and HDACs can disrupt the highly ordered differentiation program leading to proliferation of undifferentiated cells and cancer.

Alterations in both HATs and HDACs are found in many human cancers. Genes encoding HATs have been found translocated, amplified, overexpressed, and/or mutated in many human cancers. For example, loss of heterozygosity in *p300* gene has been described in 80% of glioblastomas whereas loss of heterozygosity in CREB binding protein locus has been observed in a subset of lung cancers (44). Structural mutations in HDACs associated with cancers are rare. However, overexpression of different HDACs has been reported in various cancers. HDAC2 and HDAC3 proteins are increased in colon cancer samples (45). Again in many cases of lymphomas and leukemias HDACs are functionally recruited in oncogenic translocation protein complexes (46).

Histone deacetylase inhibitors

HDACIs are a new class of structurally diverse anticancer agents and have been shown to exhibit antimetastatic and antiangiogenic activities toward malignantly transformed cells in vitro and *in vivo* (47,42). They selectively alter gene transcription by chromatin remodeling and by changing the structure of proteins in transcription factor complexes. HDACs have many non-histone proteins as their target substrate apart from histones, which regulate cell proliferation and cell death thus HDACI-induced transformed cell death involves both transcription-dependent and transcription-independent mechanisms (Table 3) (42,47,48).

HDACIs are structurally diverse group of molecules derive from both natural sources (e.g TSA, FK228) and from synthetic route (e.g. MS-275, Tubacin). With few exceptions they all have been divided into chemical classes including hydroxamates such as Trichostatin A (TSA), aliphatic acids such as phenyl butyrate, benzamides such as MS-275, and electrophilic ketones such as trifuoromethyl ketones, and depsipeptides such as FK228 (Table 3) (47).

FR901228

FR901228, also known as FK228 and romidepsin (NSC-630176), (E)-(1S,4S,10S,21R)-7-[(Z)-ethylidene]-4,21-diisopropyl-2-oxa-12,13-dithia-5,8,20,23-tetraazabicyclo[8,7,6]-tricos-16-ene-3,6,9,19,22-pentanone, is a bicyclic depsipeptide isolated from *Chromobacterium violaceum* cultures (49,50). FR901228 has been shown to exhibit strong activity inhibiting Class I histone deacetylases, mild activity inhibiting Class II, assayed *in vitro* (51). Some studies have suggested that Class I HDACs are important in regulating proliferation and survival in cancer

cells (42,52). Selective inhibition of Class I HDACs by FR901228 has been postulated to play an important role in the selectivity of FR901228 in control of cancer cells. As such, FR901228 is a pro-drug and has a stable molecular hydrophobic structure that facilitates its entry through the cell membrane into cells. Its internal disufide bond can be reduced by intracellular glutathione to form two active, free sulfhydryl groups to chelate the zinc in the HDAC active site (53). Increased intracellular glutathione is associated with multidrug resistance; therefore, FR901228 is potentially effective for treating tumor cells with glutathione-mediated drug resistance.

Trichostatin A (TSA)

Trichostatin A (TSA) was first isolated from cultures of *Streptomyces hygroscopicus* as antifungal antibiotics active against Trichophyton species (54). It was the first natural product hydroxamate discovered to inhibit HDACs. It is an inhibitor of class I and II HDACs. TSA, has relatively high reactivity and instability, and has been extensively used as a tool for the study HDAC function. TSA contains a cap group, an aliphatic chain and a terminal hydroxamic acid functional group. TSA act as substrate mimics and inhibit the HDAC by inserting its aliphatic chain into catalytic site of the enzyme. This insertion and binding in the catalytic site blocks substrate access to the active zinc ion and, thereby, inhibits the deacetylase activity (40).

The cellular effects of HDACI

HDACIs have been shown to induce growth arrest, differentiation, cell death and inhibition of angiogenesis. Normal cells are almost always considerably more resistant than tumor cells. Mechanisms of their action are complex and not completely understood. Effects of HDACIs can be attributed to the accumulation of acetylated histones and many nonhistone proteins that have been shown to involve in regulation of gene expression, cell proliferation, cell migration, and cell death. For example HDACIs can affect transcription by inducing acetylation of histones, transcription factors and other proteins regulating transcription and thereby selectively altering the gene expressions. Up to 20% of all known genes are affected by HDACI (48). The cyclin-dependent kinase (CDK) inhibitor p21 (WAF1/CIP1) and p27 (KIP1) are the most common genes induced by HDACIs which are responsible for HDACI-mediated cell cycle arrest in both normal and transformed cells (43).

HDACIs have been shown to induce transformed cell death by activating the intrinsic and extrinsic apoptotic pathway, mitotic failure, autophagic cell death, polyploidy, and senescence, and reactive oxygen species–facilitated cell death (43). In addition, HDACI such as TSA, FK229 have been shown to block tumor angiogenesis by inhibition of transcription factors of angiogenesis namely hypoxia inducible factors (HIF) (43). HDACI also cause hyper-acetylation of HSP90 and its inactivation, leading to the degradation of proteins that require the chaperone function of HSP90 leading to inactivation of anti-apoptotic pathway (55). The response to HDACI depends upon on the nature of HDACI, concentration and time of exposure, and the cell context (cell type, cell stage, and normal or pathological state of the cell).

HDACI have shown synergistic or additive antitumor effects with a wide range of antitumor reagent, including chemotherapeutic drugs (e.g. cisplatin, VP-16), HSP90 inhibitor

(e.g. 17-ally-amino-demethoxy geldanamycin), proteasome inhibitor (e.g. bortezomib), kinase inhibitors (e.g. phosphatidylinocitol 3 kinase inhibitor LY294002, MEK1/2 inhibitor PD184352) and radiotherapy (42,52).

Clinical development of HDACI

Various HDACIs are in phase I/II clinical trials with the main aim being to analyze/exclude unwanted toxicity and to find optimal doses/schedules. At least 14 different HDACI are in some phase of clinical trials as monotherapy or in combination with various other antitumor agents such as gemcitabine, radiation, etc, in patients with hematologic and solid tumors (Table 3) (43).

Resistance has been observed in clinical trials with some HDACIs in different tumors. However the basis of resistance to HDACIs is not well understood. High level of Bcl-2 and thioredoxin (Trx), which has been associated with resistance of transformed cells to chemotherapy, may play a role in the resistance to HDACIs (43). Resistance to FK228 has been associated with upregulation of multiple drug resistance protein1 (MDR1) and P-glycoprotein (P-gp) that mediate FK228 efflux (56).

Reactive oxygen species in cancer research

Reactive oxygen species (ROS)

These are oxygen containing chemical species with reactive chemical properties generated inside the cell as the consequence of respiration and enzymatic activities. ROS include O_2^-derived free radicals such as superoxide anion radical (O_2^-) and the hydroxyl radical ($^{\cdot}OH$),

which contain an unpaired electron, and nonradical derivatives of O_2 such as hydrogen peroxide (H_2O_2) (57,58).

Mitochondria represent the major source of intracellular ROS. During oxidative phosphorylation, electrons are delivered through the respiratory chain, and a proton gradient is established across the inner mitochondrial membrane as energy source for ATP synthesis. One important biochemical event associated with this metabolic process is the production of superoxide. It is estimated that approximately 2% of the total mitochondrial O_2 consumption results in O_2^- production which is subsequently converted to hydrogen peroxide (58,59). Metabolism of O_2 to water is catalyzed by cytochrome c oxidase in the inner mitochondrial membrane and sequential addition of electrons to oxygen during electron transport generates various ROS (Figure 5). Some electrons may escape from the mitochondrial electron transport chain, such as from the reaction of O_2 with the ubisemiquinone (Q) site of complex III (Figure 5), and react with molecular oxygen to form superoxide. O_2^- can react with itself by spontaneous or enzymatic (e.g., superoxide dismutase, SOD) dismutation to form H_2O_2. H_2O_2 then reacts with reduced iron (FeII) to generate the reactive hydroxyl radical ($^{\bullet}OH$).

Apart from mitochondrial production ROS can also be synthesized by enzymes such as NADPH oxidases, also called as NOX proteins, synthesized by phagocytic cells to battle against bacterial infection (60).

Under normal physiological conditions production of intracellular ROS in kept in a state of redox homeostasis by cellular antioxidant defense system to prevent possible deleterious effect of ROS. Antioxidant system consists of enzymes as well as nonenzymatic antioxidants. Enzymes such as superoxide dismutase, glutathione peroxidase catalyze the conversion of O_2^- to

H_2O_2, which is then converted to water and O_2 by catalase (61). Nonenzymatic antioxidants, like vitamin E, vitamin C, β-carotene, glutathione, and coenzyme Q function to quench ROS (62). In addition, cells have secondary antioxidant defenses consist of protease systems specialized for the removal of oxidatively modified proteins as well as DNA repair or lipid repair enzymes. However, sometimes production of ROS exceeds the endogenous cellular capacity for their detoxification by antioxidant system and/or utilization leading to a nonhomeostatic state referred to as "oxidative stress" (60).

ROS in carcinogenesis

Growing evidence suggests that cancer cells in general are under increased oxidative stress compared to normal cells (63). This is mainly due to elevated ROS generation associated with active metabolism and oncogenic stimulation in cancer cells which in turn contributes to cancer progression. Oncogenes have been shown to cause increased ROS generation. Oncogenic H-Ras, for example, increases ROS generation which in turn mediate some of the biological effects of oncogenic Ras such as, mitogenesis in fibroblasts (64), the generation of genomic instability (65), and malignant transformation (66). Several studies have indicated that the Ras-induced membrane NADPH-oxidase complex plays an important role in producing ROS for Ras-induced transformation phenotypes (66-69). In addition, oncogenic Ras-increased ROS may cause DNA damage, contributing to Ras-induced mutagenesis in cells lacking the tumor suppressor p53 (70). The oncogene *c-myc* has also been shown to increase ROS generation, which induces DNA damage and mitigates p53 function leading to genetic instability (71).

Another possible mechanism for increased ROS production in cancer cells may involve malfunction of the mitochondrial respiratory chain. Metabolically active cancer cells require a high level of ATP supply to maintain their active biochemical functions associated with uncontrolled cell growth and proliferation. This energy demand places a further stress on the mitochondrial respiration chain, and is likely to contribute to increased ROS generation. In addition, any mutation in mitochondrial DNA (mtDNA) which codes for 13 components of the respiration complexes can adversely affect functioning of mitochondrial respiratory chain leading to excessive ROS generation. In fact, mtDNA mutations are frequently detected in cancer cells and have been shown to correlate with increased ROS contents (63,72).

ROS have broad range of responses inside the cell depending upon magnitude of level and duration of exposure. Recent studies have shown active involvement of ROS in the regulation of signal-transduction pathways (73) and during oncogenic signaling in cellular transformation and cancer (74,65). In general, low levels of ROS are mitogenic and promote cell proliferation, while intermediate levels cause transient or permanent cell cycle arrest and induce cell differentiation. Excessive production of ROS may inflict damage to various cellular components including DNA, protein, and lipid membranes and can induced cell apoptosis or necrosis (75).

ROS mediated nuclear DNA damage may results in genetic instability whereas damage to mitochondrial DNA will affect mitochondrial electron transport chain leading to further increase in ROS generation. Protein oxidation by ROS may affect redox equilibrium due to inhibition of enzymes involved such as catalases and peroxidases, which in turn impair the cells ability to clear ROS causing, further increase in oxidative stress. However the most important consequence

of ROS-mediated damage is lipid peroxidation, which refers to the addition of oxygen to unsaturated fatty acids to form organic hydroperoxides (ROOH). The oxidation of membrane phospholipids decreases the fluidity of the biological membranes and increases the membrane permeability. In mitochondria, where much of the ROS is generated, membrane damage by oxidation may cause release of cytochrome c and activate apoptotic cascades. Various studies have shown the role of reactive oxygen species in inducing apoptosis (76-78). However, in some cases massive cellular oxidation by high levels of ROS may lead to necrotic cell death instead of apoptosis or a combination of these two (63,79).

ROS generating agents in cancer research

As cancer cells are under increased ROS stress, they are more susceptible to further oxidative insults than normal cells, leading to cell death. Hence any agent that directly or indirectly causes ROS accumulation will preferentially kill cancer cells. This provides the basis for selective therapeutics against cancer. Increase in ROS stress to cause selective killing of cancer cells can be achieved by direct exposure of cells to ROS-generating agents or by inhibition of antioxidant system of the cell or by appropriate combination of the above.

Various agents have been shown to cause increased ROS generation leading to apoptosis of cancer cells such as, arsenic trioxide, anthracyclines and cisplatin (78,80,81). Some anticancer agents target the antioxidant enzyme of the cell leading to excessive accumulation of ROS. Estrogen derivative 2-ME, for example, was shown to inhibit SOD resulting in accumulation of cellular superoxide (O_2^-) and cell death (83). One effective strategy could be the use of appropriate combination of ROS-generating agents and inhibitors of antioxidant system leading

to severe oxidative stress and cell death. Combination of the ROS-generating agent ATO and SOD inhibitor 2-ME, for example, have been shown to cause ROS accumulation synergistically leading to effective killing of cancer cells (78).

HDACI as ROS generating agent

Recently HDACIs, a new class of selective anticancer drugs, have been shown to cause cell death by increasing ROS production. HDACIs such as, FK228, Varinostat, TSA and MS-275 causes accumulation of ROS in transformed cells upon treatment leading to apoptosis which can be prevented by use of free radical scavengers such as *N*-acetylcysteine (84,85,43). Mechanism involved in HDACI-induced ROS increase is not yet clear; few studies have suggested this increase in ROS is due to the inhibition of antioxidant system of the cell. HDACIs have been shown to deplete cellular glutathione (86). HDACIs have also been shown to up-regulate thioredoxin-binding protein-2, resulting in suppression of thioredoxin, which is a major intracellular scavenger of ROS, and leading to excessive accumulation of intracellular ROS (43).

Urinary Bladder Cancer

Incidence and etiology of bladder cancer

Urinary bladder cancer is one of the most common cancers and ranks fifth among all cancers in the Western world. It accounts for 336,000 new cases and 132,000 deaths annually worldwide (87). In US, it is the fourth and eighth most common malignancy in men and women, respectively, and the number of diagnosed cases is increasing annually (88). Cigarette smoking is the major risk factor, contributing to approximately 50% of all bladder cancers, followed by petrochemical and other industrial exposures (89).

Transitional cell or urothelial carcinoma is the most common type of bladder cancer, accounting for more than 90% all bladder cancers. Other types include adenocarcinomas, small cell carcinomas and squamous cell carcinomas. The urothelium lines the inner surfaces of almost the entire urinary tract, including the renal pelvis, ureter, bladder and proximal urethra. Since urothelium is the permeability barrier between urine and blood, it is constantly exposed to potential carcinogens. Although urothelium covers entire urinary tract, bladder urothelium is mostly affected by tumors, presumably owing to prolonged exposure to carcinogens.

Urothelial carcinomas are separated clinically into superficial tumors, also referred to as low-grade non-invasive papillary tumors, and muscle invasive tumors. Superficial tumors account for about 80% of urothelial carcinomas and are often multifocal and recurrent, with limited potential to become muscle-invasive. They originate from simple and nodular urothelial hyperplasia. Muscle invasive tumors on the other hand, derive from flat, high-grade carcinoma *in situ* (CIS) lesions and account for the rest 20% of urothelial carcinomas (87).

Full-blown urothelial carcinomas contain numerous genetic and epigenetic abnormalities, including chromosomal aberrations (e.g. aneusomies, deletions and amplifications), activation of oncogenes (e.g. H-*ras*), inactivation of tumor-suppressor genes (e.g. *p53,Rb*) and alterations in the tumor microenvironment (89).

Activation of the Ras signaling pathway

Accumulating evidence indicates that key components of this signaling pathway such as H-*ras* and upstream receptor tyrosine kinases (RTKs) are frequently activated in human urothelial carcinomas (Table 4).

H-ras: H-*ras* was the first human oncogene identified in urothelial carcinomas (Reddy et. al., 1982). H-*ras* activation in urinary carcinomas involves direct H-*ras* gene mutations (at codons 12, 13 and 61) as well as protein overexpression due to alternative splicing of the last intron of the H-*ras* gene (90). Recent studies indicate that H-*ras* mutations occur in 30–40% of urothelial carcinomas whereas overexpression of H-Ras is seen in over half of human urothelial carcinomas — a much higher frequency than that of H-*ras* mutations (Table 4) (87,91). The role of H-Ras activation in urothelial tumorigenesis has been verified with the help of transgenic mouse models. The targeted expression of an activated H-Ras in the urothelium of transgenic mice induced early-onset urothelial proliferation. In the transgenic mice, but not in wild-type controls, urothelial hyperplasia then evolved to low-grade non-invasive papillary tumors that resemble the human disease, indicating a pivotal role of H-Ras activation in urothelial carcinomas (92).

Receptor tyrosine kinases: In addition to activated H-Ras, several RTKs that function upstream of Ras are constitutively active in urothelial carcinomas leading to activation of Ras signaling pathway (Table 4). For example, mutations in the fibroblast growth factor receptor 3 (FGFR3) gene occur in about 70% of the low-grade non-invasive papillary tumors (93). Forced expression of FGFR3 mutants in NIH-3T3 cells resulted in cellular transformation and mitogen-activated protein kinase (MAPK) activation, resembling the transfection effects observed with activated H-Ras (94).

Targeting the RTK–Ras signalling pathway

Since RTK–Ras signalling pathway is widely involved in bladder cancer, components of this pathway can be exploited as therapeutic targets.

Targeting the RTK**.** Inhibitory antibodies against RTKs, particularly those target EGFR family proteins, have shown potent tumor-inhibitory activity in cultured cells and animal tumor models, and are being evaluated in clinical trials (95). Several small molecules have been identified based on *in vitro* screening assay, such as SU5402, SU6668, PD173074 and CHIR-258, that all inhibit FGFR3. Besides the small molecule approach, monoclonal antibodies raised against FGFR3 have been developed that show inhibitory effects on urothelial tumor cell-lines (96,87).

Targeting Ras protein. As described in the previous section (Targeting oncogenic Ras in human cancer) various strategies can be employed to counter oncogenic Ras in urothelial carcinomas. In addition, combination of farnesyl- and geranylgeranyl-transferase inhibitors, which exhibit high toxicity when used systemically, could be administered intravesically to treat bladder urothelial carcinomas, giving lower systemic toxicity**.** Treatment of oncogenic H-Ras-bearing urothelial tumors in animal models with Farnesyltransferase inhibitors (FTIs) has been found to significantly increase the tumor response to radiation (97).

HDACIs in bladder cancer

Since bladder cancer contains numerous epigenetic abnormalities in addition to various genetic defects, epigenetic modifiers such as HDACIs can be of great therapeutic importance. HDACIs can be used as monotherapy or in combination with existing therapies for bladder cancers such as surgical treatment or existing chemotherapeutic agents for bladder cancers, such

as methotrexate, vinblastine, doxorubicin or cisplatin (89). Several HDACIs have been evaluated recently for their therapeutic application in bladder cancer. The most important among them is a novel depsipeptide, FK228, which has been shown to be a potent chemotherapeutic agent for urothelial carcinoma *in vivo* with minimal undesirable side effects. It exhibited growth inhibitory effects on five different transitional cell carcinoma cell lines in a dose- and time-dependent manner (98,99). Recent studies have suggested that FK228 pretreatment increases the sensitivity of tumor cells to adenoviral gene therapy vectors (100,101). Besides FK228, other HDACIs, such as TSA and MS-275, have also been shown to block bladder cancer cell cycle *in vitro* and induce apoptosis (98,102). Belinostat, a novel histone deacetylase inhibitor has shown growth inhibitory effect on a number of bladder cancer cell lines (103). HDAC inhibition with sodium butyrate and TSA has been shown to increase the sensitivity of tumor necrosis factor-related apoptosis-inducing ligand-resistant bladder tumor cells (104).

LIST OF REFERENCES

1. Greider, C. W. 1998. Telomeres and senescence: the history, the experiment, the future. Curr.Biol. 8:R178-R181.
2. Bertram JS (2000) The molecular biology of cancer. Mol Aspects Med 21:167–223
3. Rak, J., J. L. Yu, G. Klement, and R. S. Kerbel. 2000. Oncogenes and angiogenesis: signaling three-dimensional tumor growth. J.Investig.Dermatol.Symp.Proc. 5:24-33.
4. Ravi, R., B. Mookerjee, Z. M. Bhujwalla, C. H. Sutter, D. Artemov, Q. Zeng, L. E. Dillehay, A. Madan, G. L. Semenza, and A. Bedi. 2000. Regulation of tumor angiogenesis by p53-induced degradation of hypoxia-inducible factor 1alpha. Genes Dev.14:34-44.
5. Reddy, E. P., Reynolds, R. K., Santos, E. & Barbacid, M. A point mutation is responsible for the acquisition of transforming properties by the T24 human bladder carcinoma oncogene. Nature 300, 149–152 (1982).
6. Minamoto, T., Mai, M., Ronai, Z., 2000. K-ras mutation: early detection in molecular diagnosis and risk assessment of colorectal, pancreas, and lung cancers-a review. Cancer Detect. Prev. 24, 1-12.
7. Bos JL. Ras oncogenes in human cancer: a review. Cancer Res 1989;49:4682–9.
8. Karnoub AE & Weinberg RA. Ras oncogenes: split personalities. Nature Reviews Molecular Cell Biology 9, 517-531 (July 2008)
9. Whyte DB, Kirschmeier P, Hockenberry TN, Nunez-Oliva I, James L, Catino JJ, Bishop WR, Pai JK. K- and N-Ras are geranylgeranylated in cells treated with farnesyl protein transferase inhibitors. J. Biol. Chem. 272, 14459–14464 (1997).

10. Hancock JF, Paterson H & Marshall CJA polybasic domain or palmitoylation is required in addition to the CAAX motif to localize p21ras to the plasma membrane. Cell 63, 133–139 (1990)

11. Campbell SL, Khosravi-Far R, Rossman KL, Clark GJ, Der CJ. Increasing complexity of Ras signaling. Oncogene 1998;17:1395–413.

12. Rajagopalan H, Bardelli A, Lengauer C, Kinzler KW, Vogelstein B, Velculescu VE. Tumorigenesis: RAF/RAS oncogenes and mismatch-repair status. Nature 418, 934 (2002).

13. M. Cully, H. You, A.J. Levine and T.W. Mak. Beyond PTEN mutations: the PI3K pathway as an integrator of multiple inputs during tumorigenesis, Nat. Rev., Cancer 6 (2006), pp. 184–192.

14. Hamad NM, Elconin JH, Karnoub AE, Bai W, Rich JN, Abraham RT, Der CJ, Counter CM. Distinct requirements for Ras oncogenesis in human versus mouse cells. Genes Dev. 16, 2045–2057 (2002).

15. Chien Y & White MA. RAL GTPases are linchpin modulators of human tumour-cell proliferation and survival. EMBO Rep. 4, 800–806 (2003).

16. Adjei AA. Blocking oncogenic Ras signaling for cancer therapy. J Natl Cancer Inst 2001;93:1062–74.

17. Kohl NE, Omer CA, Conner MW, Anthony NJ, Davide JP, deSolms SJ, Giuliani EA, Gomez RP, Graham SL, Hamilton K, Handt LK, Hartman GD, Koblan KS, Kral AM, Miller PJ, Mosser SD, O'Neill1 TJ, Rands E, Schaber MD, Gibbs JB & Oliff A.

Inhibition of farnesyltransferase induces regression of mammary and salivary carcinomas in ras transgenic mice. Nature Med. 1, 792–797 (1995).

18. D.B. Solit, L.A. Garraway, C.A. Pratilas, A. Sawai, G. Getz, A. Basso, Q. Ye, J.M. Lobo, Y. She, I. Osman, T.R. Golub, J. Sebolt-Leopold, W.R. Sellers and N. Rosen, BRAF mutation predicts sensitivity to MEK inhibition, Nature 439 (2006), pp. 358–362.

19. Hanahan, D. & Weinberg, R. A. The hallmarks of cancer. Cell 100, 57–70 (2000).

20. Fesik, SW. Promoting apoptosis as a strategy for cancer drug discovery. Nature Reviews Cancer 5, 876-885 (2005).

21. Degterev, A., M. Boyce, and J. Yuan. 2003. A decade of caspases. Oncogene 22:8543-8567.

22. Wyllie, A. H., J. F. Kerr, and A. R. Currie. 1980. Cell death: the significance of apoptosis. Int Rev.Cytol. 68:251-306.

23. Budihardjo, I., H. Oliver, M. Lutter, X. Luo, and X. Wang. 1999. Biochemical pathways of caspase activation during apoptosis. Annu.Rev.Cell Dev.Biol. 15:269-290.

24. Green, D. R. and G. Kroemer. 2004. The pathophysiology of mitochondrial cell death. Science 305:626-629.

25. Susin, S. A., H. K. Lorenzo, N. Zamzami, I. Marzo, B. E. Snow, G. M. Brothers, J. Mangion, E. Jacotot, P. Costantini, M. Loeffler, N. Larochette, D. R. Goodlett, R. Aebersold, D. P. Siderovski, J. M. Penninger, and G. Kroemer. 1999. Molecular characterization of mitochondrial apoptosis-inducing factor. Nature 397:441-446.

26. Hegde, R., S. M. Srinivasula, Z. Zhang, R. Wassell, R. Mukattash, L. Cilenti, G. DuBois, Y. Lazebnik, A. S. Zervos, T. Fernandes-Alnemri, and E. S. Alnemri. 2002. Identification

of Omi/HtrA2 as a mitochondrial apoptotic serine protease that disrupts inhibitor of apoptosis protein-caspase interaction. J Biol Chem 277:432-438.

27. Goldstein, J. C., N. J. Waterhouse, P. Juin, G. I. Evan, and D. R. Green. 2000. The coordinate release of cytochrome c during apoptosis is rapid, complete and kinetically invariant. Nat.Cell Biol 2:156-162.

28. Nagata, S. Apoptosis by death factor. Cell 88, 355–365 (1997).

29. Li H, Zhu H, Xu C, Yuan J. Cleavage of BID by Caspase 8 Mediates the Mitochondrial Damage in the Fas Pathway of Apoptosis.1998, Cell:94; 491–501.

30. Baell, J. B. & Huang, D. C. S. Prospects for targeting the Bcl-2 family of proteins to develop novel cytotoxic drugs. Biochem. Pharmacol. 64, 851–863 (2002).

31. Deveraux, Q. L., Takahashi, R., Salvesen, G. S. & Reed, J. C. X-linked IAP is a direct inhibitor of cell-death proteases. Nature 388, 300–304 (1997).

32. Du, C., Fang, M., Li, Y., Li, L. & Wang, X. Smac, a mitochondrial protein that promotes cytochrome c-dependent caspase activation by eliminating IAP inhibition. Cell 102, 33–42 (2000).

33. Verhagen AM, Ekert PG, Pakusch M, Silke J, Connolly LM, Reid GE, Moritz RL, Simpson RJ, Vaux DL. Identification of DIABLO, a mammalian protein that promotes apoptosis by binding to and antagonizing IAP proteins. Cell 102, 43–53 (2000).

34. Chene, P. Inhibiting the p53–MDM2 interaction: an important target for cancer therapy. Nature Rev. Cancer 3, 102–109 (2003).

35. Wu J, Grunstein M. 25 years after the nucleosome model: Chromatin modifications. Trends Biochem Sci 2000;25:612–623.

36. Luger K, Mader AW, Richmond RK, Sargent DF, Richmond TJ. Crystal structure of the nucleosome core particle at 2.8 A ° resolution. Nature 1997;389:251–260.

37. Jendwein T, Allis CD. Translating the histone code. Science 2001;293:1074–1080.

38. Spotswood HT, Turner BM. 2002. An increasingly complex code. J Clin Invest 110: 577-582.

39. Strahl, B. D. & Allis, C. D. The language of covalent histone modifications. Nature 403, 41–45 (2000).

40. Mai A, Massa S, Rotili D, Cerbara I, Valente S, Pezzi R et al. (2005). Histone deacetylation in epigenetics: an attractive target for anticancer therapy. Med Res Rev 25: 261–309.

41. Marmorstein R. Structure of histone acetyltransferases. J Mol Biol 2001;311:433–44.

42. Marks PA, Dokmanovic M. (2005). Histone deacetylase inhibitors: discovery and development as anticancer agents. Expert Opin Investig Drugs 14: 1497–1511.

43. Xu WS, Parmigiani RB, Marks PA. Histone deacetylase inhibitors: molecular mechanisms of action. Oncogene 2007;26:5541-52.

44. Dokmanovic M, Clarke C and Marks PA. Histone Deacetylase Inhibitors: Overview and Perspectives. Mol Cancer Res 2007;5:981-9.

45. Wilson AJ, Byun DS, Popova N, Murray LB, L'Italien K, Sowa Y, Arango D, Velcich A, Augenlicht LH, Mariadason JM. Histone deacetylase 3 (HDAC3) and other class I HDACs regulate colon cell maturation and p21 expression and are deregulated in human colon cancer. J Biol Chem 2006;281:13548–58.

46. Linggi BE, Brandt SJ, Sun ZW, Hiebert SW. Translating the histone code into leukemia. J Cell Biochem 2005;96:938–50.

47. Marks PA, Miller T, Richon VM. Histone deacetylases. Current Opin Pharmacol 2003;3:344-51.

48. Minucci S, Pelicci PG. (2006). Histone deacetylase inhibitors and the promise of epigenetic (and more) treatments for cancer. Nat Rev Cancer 6: 38–51.

49. Ueda H, Manda T, Matsumoto S, Mukumoto S, Nishigaki F, Kawamura I, Shimomura K (1994) FR901228, a novel antitumor bicyclic depsipeptide produced by Chromobacterium violaceum No. 968. III. Antitumor activities on experimental tumors in mice. J Antibiot (Tokyo) 47:315-323.

50. Vigushin DM. FR-901228 Fujisawa/National Cancer Institute (2002) Curr Opin Investig Drugs 3:1396-1402.

51. Furumai R, Matsuyama A, Kobashi N, Lee KH, Nishiyama M, Nakajima H, Takana A, Komatsu Y, Nishino N, Yoshida M, Horinouchi S (2002) FK228 (depsipeptide) as a natural prodrug that inhibits class I histone deacetylases. Cancer Res 62: 4916-4921

52. Bolden JE, Peart MJ, Johnstone RW (2006) Anticancer activities of histone deacetylase inhibitors. Nat Rev Drug Discov 5:769 -783

53. Konstantinopoulos PA, Vandoros GP, Papavassiliou AG (2006) FK228 (depsipeptide): a HDAC inhibitor with pleiotropic antitumor activities. Cancer Chemother Pharmacol 58:711-715.

54. Tsuji N, Kobayashi M, Nagashima K, Wakisaka Y, Koizumi K. A new antifungal antibiotic, trichostatin.J Antibiot 1976;29:1–6

55. Bali P, Pranpat M, Bradner J, Balasis M, Fiskus W, Guo F, Rocha K, Kumaraswamy S, Boyapalle S, Atadja P, Seto E, Bhalla K. Inhibition of histone deacetylase 6 acetylates and disrupts the chaperone function of heat shock protein 90: a novel basis for antileukemia activity of histone deacetylase inhibitors. J. Biol. Chem. 280, 26729–26734 (2005).

56. Glaser KB. (2006). Defining the role of gene regulation in resistance to HDAC inhibitors – mechanisms beyond P-glycoprotein. Leuk Res 30: 651–652.

57. Finkel T. Oxidant signals and oxidative stress. Curr Opin Cell Biol 15: 247–254, 2003.

58. Halliwell B and Gutteridge JMC. Free Radicals in Biology and Medicine. New York: Oxford University Press; 1999. pp. 1–350.

59. Fridovich, I., 1995. Superoxide radical and superoxide dismutases. Annu. Rev. Biochem. 64, pp. 97–112.

60. Ryter SW, Kim HP, Hoetzel A, Park JW, Nakahira K, Wang X, Choi AMK. Antioxidants & Redox Signaling. 2007, 9(1): 49-89.

61. Klaunig JE, Kamendulis LM. 2004. The role of oxidative stress in carcinogenesis. Annu Rev Pharmacol Toxicol 44: 239-267.

62. Clarkson PM, Thompson HS. 2000. Antioxidants: What role do they play in physical activity and health? Am J Clin Nutr 72: 637S-646S.

63. Pelicano, H., Carney, D., and Huang, P. (2004). ROS stress in cancer cells and therapeutic implications. Drug Resist. Updat. 7, 97–110.

64. Irani, K., Xia, Y., Zweier, J.L., Sollott, S.J., Der, C.J., Fearon, E.R.,Sundaresan, M., Finkel, T., and Goldschmidt-Clermont, P.J. (1997). Mitogenic signaling mediated by oxidants in Ras-transformed fibroblasts. Science 275, 1649–1652.

65. Woo, R.A., and Poon, R.Y. (2004). Activated oncogenes promote and cooperate with chromosomal instability for neoplastic transformation. Genes Dev. 18, 1317–1330.

66. Mitsushita J, Lambeth JD, Kamata T. The superoxide-generating oxidase Nox1 is functionally required for Ras oncogene transformation. Cancer Res 2004;64:3580-5.

67. Cho HJ, Jeong HG, Lee JS, Woo ER, Hyun JW, Chung MH, You HJ. Oncogenic H-Ras enhances DNA repair through the Ras/phosphatidylinositol 3-kinase/Rac1 pathway in NIH3T3 cells. Evidence for association with reactive oxygen species. J Biol Chem 2002;277:19358-66.

68. Santillo M, Mondola P, Serù R, Annella T, Cassano S, Ciullo I, Tecce MF, Iacomino G, Damiano S, Cuda G, Paternò R, Martignetti V, Mele E, Feliciello A, Avvedimento EV. Opposing functions of Ki- and Ha-Ras genes in the regulation of redox signals. Curr Biol 2001;11:614-9.

69. Liu R, Li B, Qiu M. Elevated superoxide production by active H-ras enhances human lung WI-38VA-13 cell proliferation, migration and resistance to TNF-alpha. Oncogene 2001;20:1486-96.

70. Kopnin PB, Agapova LS, Kopnin BP, Chumakov PM. Repression of sestrin family genes contributes to oncogenic Ras-induced reactive oxygen species up-regulation and genetic instability. Cancer Res 2007;67:4671-8.

71. Vafa, O., Wade, M., Kern, S., Beeche, M., Pandita, T.K., Hampton, G.M. and Wahl, G.M., 2002. c-Myc can induce DNA damage, increase reactive oxygen species, and mitigate p53 function: a mechanism for oncogene-induced genetic instability. Mol. Cell 9, pp. 1031–1044.

72. Carew, J.S., Zhou, Y., Albitar, M., Carew, J.D., Keating, M.J. and Huang, P., 2003. Mitochondrial DNA mutations in primary leukemia cells after chemotherapy: clinical significance and therapeutic implications. Leukemia 17, pp. 1437–1447.

73. Hancock, J.T., Desikan, R., and Neill, S.J. (2001). Role of reactive oxygen species in cell signalling pathways. Biochem. Soc. Trans. 29, 345–350.

74. Suh, Y.A., Arnold, R.S., Lassegue, B., Shi, J., Xu, X., Sorescu, D., Chung, A.B., Griendling, K.K., and Lambeth, J.D. (1999). Cell transformation by the superoxide-generating oxidase Mox1. Nature 401, 79–82.

75. Finkel T, Holbrook NJ. 2000. Oxidants, oxidative stress and the biology of ageing. Nature 408: 239-247.

76. Sastre, J., Pallardo, F.V. and Vina, J., 2000. Mitochondrial oxidative stress plays a key role in aging and apoptosis. IUBMB Life 49, pp. 427–435.

77. Carmody, R.J. and Cotter, T.G., 2001. Signalling apoptosis: a radical approach. Redox. Rep. 6, pp. 77–90.

78. Pelicano, H., Feng, L., Zhou, Y., Carew, J.S., Hileman, E.O., Plunkett, W., Keating, M.J. and Huang, P., 2003. Inhibition of mitochondrial respiration: a novel strategy to enhance drug-induced apoptosis in human leukemia cells by a reactive oxygen species-mediated mechanism. J. Biol. Chem. 278, pp. 37832–37839.

79. Kroemer, G., Dallaporta, B. and Resche-Rigon, M., 1998. The mitochondrial death/life regulator in apoptosis and necrosis. Annu. Rev. Physiol. 60, pp. 619–642.

80. Tsang, W.P., Chau, S.P., Kong, S.K., Fung, K.P. and Kwok, T.T., 2003. Reactive oxygen species mediate doxorubicin induced p53-independent apoptosis. Life Sci. 73, pp. 2047–2058.

81. Miyajima, A., Nakashima, J., Yoshioka, K., Tachibana, M., Tazaki, H. and Murai, M., 1997. Role of reactive oxygen species in cis-dichlorodiammineplatinum-induced cytotoxicity on bladder cancer cells. Br. J. Cancer. 76, pp. 206–210.

82. Yang JQ, Li S, Domann FE, Buettner GR, Oberley LW. Superoxide generation in v-Ha-ras-transduced human keratinocyte HaCaT cells. Mol Carcinog 1999;26:180-8.

83. Huang, P., Feng, L., Oldham, E.A., Keating, M.J. and Plunkett, W., 2000. Superoxide dismutase as a target for the selective killing of cancer cells. Nature 407, pp. 390–395.

84. Adachi M, Zhang Y, Zhao X, Minami T, Kawamura R, Hinoda Y, Imai K. Synergistic effect of histone deacetylase inhibitors FK228 and m-carboxycinnamic acid bis-hydroxamide with proteasome inhibitors PSI and PS-341 against gastrointestinal adenocarcinoma cells. Clin Cancer Res. 2004 Jun 1;10(11):3853-62.

85. Ruefli AA, Ausserlechner MJ, Bernhard D, Sutton VR, Tainton KM, Kofler R, Smyth MJ, Johnstone RW. (2001). The histone deacetylase inhibitor and chemotherapeutic agent suberoylanilide hydroxamic acid (SAHA) induces a cell-death pathway characterized by cleavage of Bid and production of reactive oxygen species. Proc Natl Acad Sci USA 98: 10833–10838.

86. Rikiishi H, Shinohara F, Sato T, Sato Y, Suzuki M, Echigo S. Chemosensitization of oral squamous cell carcinoma cells to cisplatin by histone deacetylase inhibitor, suberoylanilide hydroxamic acid. Int J Oncol 2007;30:1181-8.

87. Wu XR. Urothelial tumorigenesis: a tale of divergent pathways. Nature Reviews Cancer 5, 713-725 (September 2005)

88. American Cancer Society (online 2008) Cancer Facts & Figures 2008 [http://www.cancer.org/downloads/STT/2008CAFFfinalsecured.pdf]

89. Dinney CP, McConkey DJ, Millikan RE, Wu X, Bar-Eli M, Adam L, Kamat AM, Siefker-Radtke AO, Tuziak T, Sabichi AL, Grossman HB, Benedict WF, Czerniak B. Focus on bladder cancer. Cancer Cell 6, 111–116. (2004).

90. Czerniak B, Cohen GL, Etkind P, Deitch D, Simmons H, Herz F, Koss LG. Concurrent mutations of coding and regulatory sequences of the Ha-ras gene in urinary bladder carcinomas. Hum. Pathol. 23, 1199–1204 (1992).

91. Ye, D. W., Zheng, J. F., Qian, S. X. & Ma, Y. J. Correlation between the expression of oncogenes ras and c-erbB-2 and the biological behavior of bladder tumors. Urol. Res. 21, 39–43 (1993).

92. Zhang ZT, Pak J, Huang HY, Shapiro E, Sun TT, Pellicer A, Wu XR. Role of Ha-ras activation in superficial papillary pathway of urothelial tumor formation. Oncogene 20, 1973–1980 (2001).

93. Rieger-Christ KM, Mourtzinos A, Lee PJ, Zagha RM, Cain J, Silverman M, Libertino JA, Summerhayes IC. Identification of fibroblast growth factor receptor 3 mutations in urine

sediment DNA samples complements cytology in bladder tumor detection. Cancer 98, 737–744 (2003).

94. Kanai, M., Goke, M., Tsunekawa, S. & Podolsky, D. K. Signal transduction pathway of human fibroblast growth factor receptor 3. Identification of a novel 66-kDa phosphoprotein. J. Biol. Chem. 272, 6621–6628 (1997).

95. Bellmunt, J., Hussain, M. & Dinney, C. P. Novel approaches with targeted therapies in bladder cancer. Therapy of bladder cancer by blockade of the epidermal growth factor receptor family. Crit. Rev. Oncol. Hematol. 46 (Suppl.), S85–S104 (2003).

96. Rauchenberger R, Borges E, Thomassen-Wolf E, Rom E, Adar R, Yaniv Y, Malka M, Chumakov I, Kotzer S, Resnitzky D, Knappik A, Reiffert S, Prassler J, Jury K, Waldherr D, Bauer S, Kretzschmar T, Yayon A, Rothe C. Human combinatorial Fab library yielding specific and functional antibodies against the human fibroblast growth factor receptor 3. J. Biol. Chem. 278, 38194–38205 (2003).

97. Cohen-Jonathan E, Muschel RJ, Gillies McKenna W, Evans SM, Cerniglia G, Mick R, Kusewitt D, Sebti SM, Hamilton AD, Oliff A, Kohl N, Gibbs JB, Bernhard EJ. Farnesyltransferase inhibitors potentiate the antitumor effect of radiation on a human tumor xenograft expressing activated HRAS. Radiat. Res. 154, 125–132 (2000).

98. Karam JA, Fan J, Stanfield J, Richer E, Benaim EA, Frenkel E, Antich P, Sagalowsky AI, Mason RP, Hsieh JT. The use of histone deacetylase inhibitor FK228 and DNA hypomethylation agent 5-azacytidine in human bladder cancer therapy. Int J Cancer 2007;120:1795–802.

99. Fan J, Stanfield J, Guo Y, Karam JA, Frenkel E, Sun X, Hsieh JT. Effect of trans-2,3-dimethoxycinnamoyl azide on enhancing antitumor activity of romidepsin on human bladder cancer. Clin Cancer Res. 2008 Feb 15;14(4):1200-7.

100. Okegawa T, Nutahara K, Pong RC, Higashihara E, Hsieh JT. Enhanced transgene expression in urothelial cancer gene therapy with histone deacetylase inhibitor. J Urol. 2005 Aug;174(2):747-52.

101. Okegawa T, Sayne JR, Nutahara K, Pong RC, Saboorian H, Kabbani W, Higashihara E, Hsieh JT. A histone deacetylase inhibitor enhances adenoviral infection of renal cancer cells. J Urol. 2007 Mar;177(3):1148-56

102. Qu W, Kang YD, Zhou MS, Fu LL, Hua ZH, Wang LM. Experimental study on inhibitory effects of histone deacetylase inhibitor MS-275 and TSA on bladder cancer cells. Urol Oncol. 2009 Jan 30. [Epub ahead of print]

103. Buckley MT, Yoon J, Yee H, Chiriboga L, Liebes L, Ara G, Qian X, Bajorin DF, Sun TT, Wu XR, Osman I. The histone deacetylase inhibitor belinostat (PXD101) suppresses bladder cancer cell growth in vitro and in vivo. J Transl Med. 2007 Oct 12;5:49.

104. Earel JK Jr, VanOosten RL, Griffith TS. Histone deacetylase inhibitors modulate the sensitivity of tumor necrosis factor-related apoptosis-inducing ligand-resistant bladder tumor cells. Cancer Res. 2006 Jan 1;66(1):499-507

105. Fecteau KA, Mei J, WangHCR. Differential modulation of signaling pathways and apoptosis of ras-transformed cells by a depsipeptide FR901228. J Pharmacol Exp Ther 2002;300:890–9.

106. SongP, Wei J, Wang HCR. Distinct roles of the ERK pathway in modulatingap optosis of Ras-transformed and non-transformed cells induced by anticancer agent FR901228. FEBS Lett 2005;579:90–4.

APPENDIX

Table 1: Incidence of *ras* mutations in human cancer

TISSUE	H-Ras (%)	K-Ras (%)	N-Ras (%)
Adrenal gland	1	0	5
Biliary tract	0	32	1
Bone	2	1	0
Breast	1	5	1
Central nervous system	0	1	2
Cervix	9	8	1
Endometrium	1	14	0
Eye	0	4	1
Gastrointestinal tract	0	19	0
Haematopoietic and lymphoid tissue	0	5	12
Kidney	0	1	0
Large intestine	0	32	3
Liver	0	7	4
Lung	1	17	1
Oesophagus	1	4	0
Ovary	0	15	4
Pancreas	0	60	2
Prostate	6	8	1
Salivary gland	16	4	0
Skin	5	2	19
Small intestine	0	20	25
Stomach	4	6	2
Testis	0	5	4
Thymus	0	15	0
Thyroid	4	3	7
Upper aerodigestive tract	9	4	3
Urinary tract	30	4	3

Modified from Nature Reviews Molecular Cell Biology 9, 522

Table 2: Nonhistone protein substrates of HDACs

Function	Proteins
DNA binding transcriptional factors	p53, c-Myc, AML1, BCL-6, E2F1, E2F2, E2F3, GATA-1, GATA-2, GATA-3, GATA-4, Ying Yang 1 (YY1), NF-κB (RalA/p65), MEF2, CREB, HIF-1α, BETA2, POP-1, IRF-2, IRF-7, SRY, EKLF
Steroid receptor	Androgen receptor, estrogen receptor α, glucocorticoid receptor
Transcription coregulators	Rb, DEK, MSL-3, HMGI(Y)/HMGA1, CtBP2, PGC-1α
Signaling mediators	STAT3, Smad7, β-catenin, IRS-1
DNA repair enzyme	Ku70, WRN, TDG, NEIL2, FEN1
Nuclear import	Rch1, importin-α7
Chaperon proteins	HSP90
Structural protein	α-Tubulin
Inflammation mediators	HMGB1
Viral proteins	E1A, L-HDAg, S-HDAg, T antigen, HIV Tat

Modified from Oncogene 26:5542

Table 3: HDACI in clinical trials

Class	Compound	HDAC target	Potency (cells)	Stage of development
Hydroxamate	SAHA (Zolinza, vorinostat)	Classes I, II	μM	FDA approved for CTCL
	LBH589	Classes I, II	nM	Phase I
	PXD101	Classes I, II	μM	Phase II
	ITF2357	Classes I, II	nM	Phase I
	PCI-24781	Classes I, II	NA	Phase I
Cyclic peptide	FK228	HDAC1, 2	nM	Phase II
Benzamide	MS-275	HDAC1, 2, 3	μM	Phase II
	MGCD0103	Class I	NA	Phase II
Aliphatic acid	Phenylbutyrate	Classes I, IIa	Mm	Phase II
	Valproic acid	Classes I, IIa	mM	Phase II
	AN-9	NA	μM	Phase II
	Baceca	Classes I	NA	Phase II
	Savicol	NA	NA	Phase II
Abbreviations: CTCL, cutaneous T-cell lymphoma; FDA, Food and Drug Administration; HDACI, histone deacetylase inhibitors; NA, not available.				

Modified from Oncogene 26:5543

Table 4: Activation of Ras pathway in human bladder cancers

Gene	Mode of Activation	Frequency in tumors	Role in Tumorigenesis
H-ras	Mutation	30-40%	Genesis
H-ras	Over expression	50%	Genesis
FGFR3	Mutation	60-70%	Genesis
ERBB3	Over expression	ND	Genesis?
ERBB4	Over expression	ND	Genesis?
EGFR	Over expression	50%	Progression
ERBB2	Over expression	40-50%	Progression
EEBB2	Amplification	10%	Progression

EGFR: Epithelial Growth Factor Receptor; *FGFR3*: Fibroblast Growth Factor Receptor 3; *ERBB:* Erythroblastosis oncogene B*; ND:* not determined

Modified from Nature Reviews Cancer 5:717

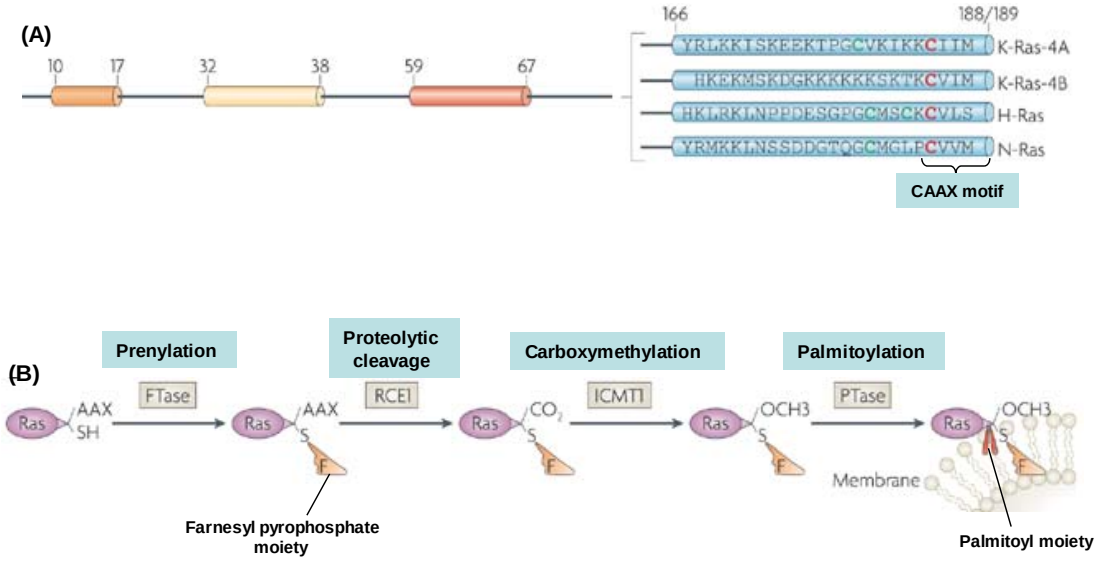

Modified from Nature Reviews Molecular Cell Biology 9, 523

Figure 1

Post-translational modifications of Ras proteins

(A) C-terminal sequences of Ras proteins

(B) C-terminal processing

See text for details

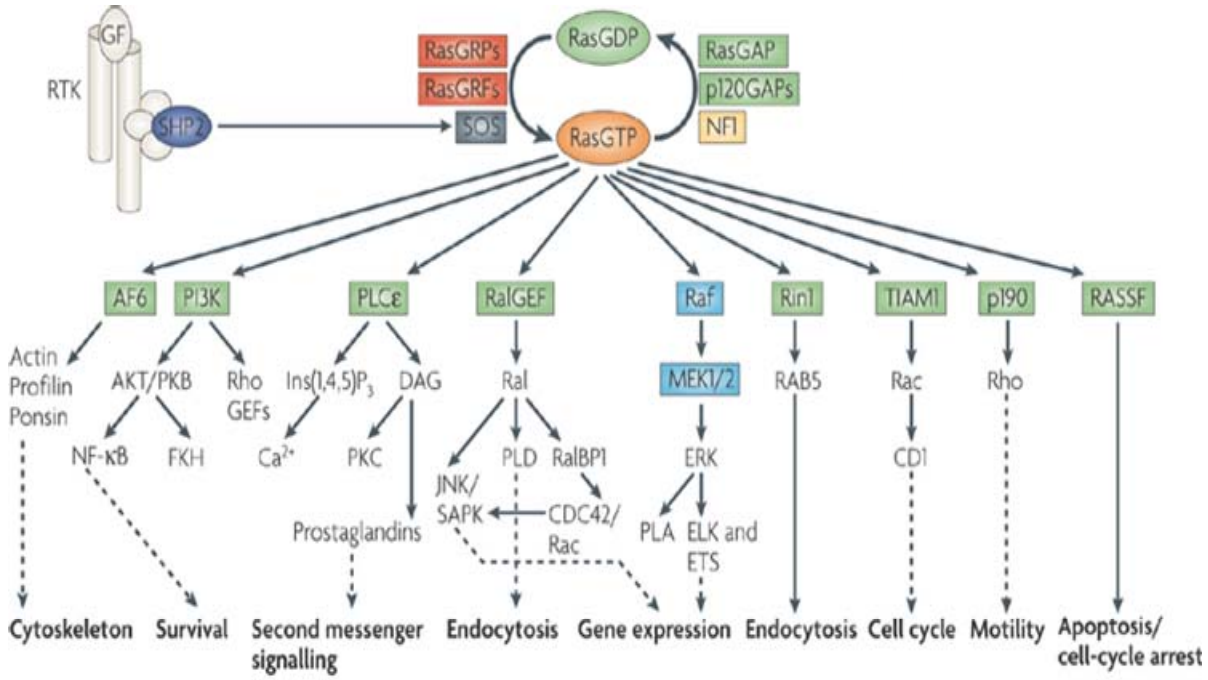

Modified from Nature Reviews Molecular Cell Biology 9, 526

Figure 2

Ras signaling networks

See text for details

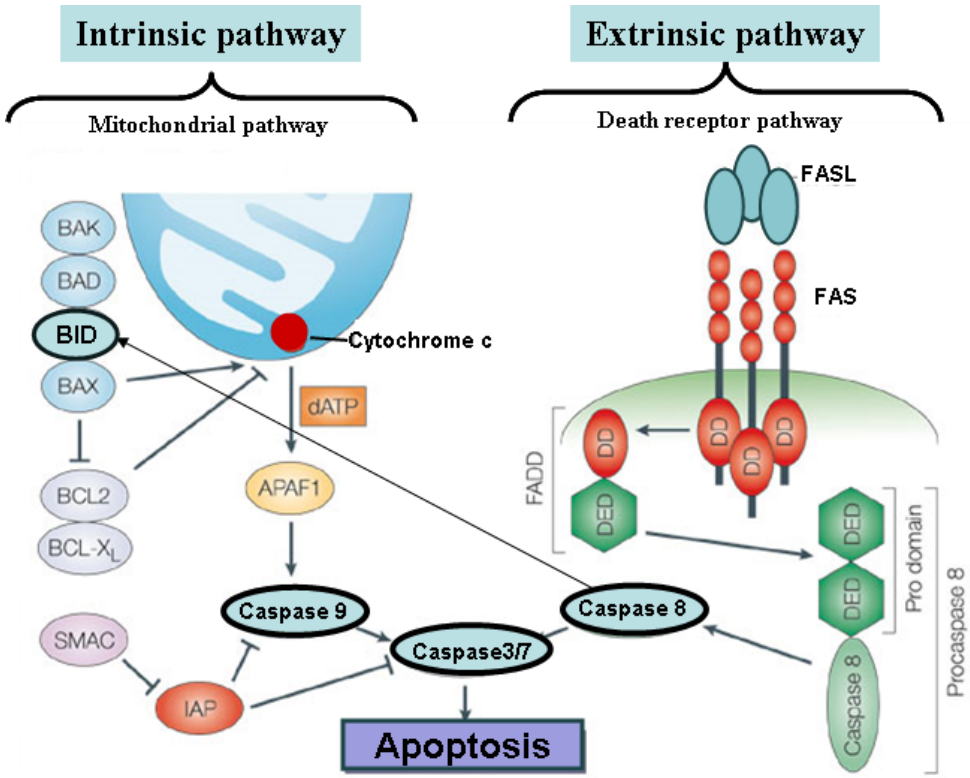

Modified from Nature Reviews Cancer 1, 878

Figure 3

General overview of apoptosis

See text for details

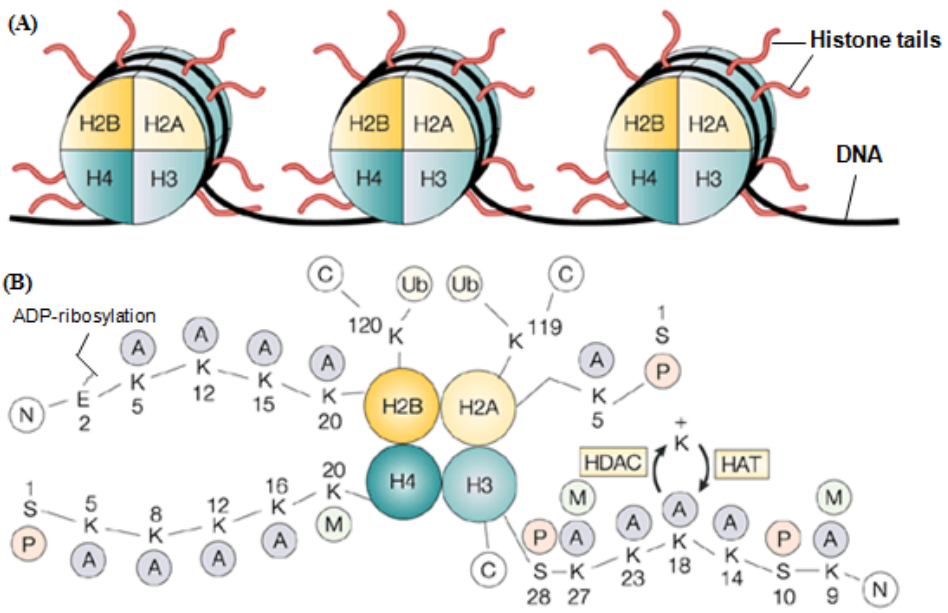

Modified from Nature Reviews Cancer 5, 195

Figure 4

Nucleosome and Chromatin remodelling

(A) The core nucleosome- DNA wraps around an octamer of histones

(B) Covalent modifications of amino-terminal tails of core histones. A, acetylation; C, carboxyl terminus; E, glutamic acid; K, lysine; M,methylation; N, aminoterminus; P, phosphorylation; S, serine; Ub, ubiquitination

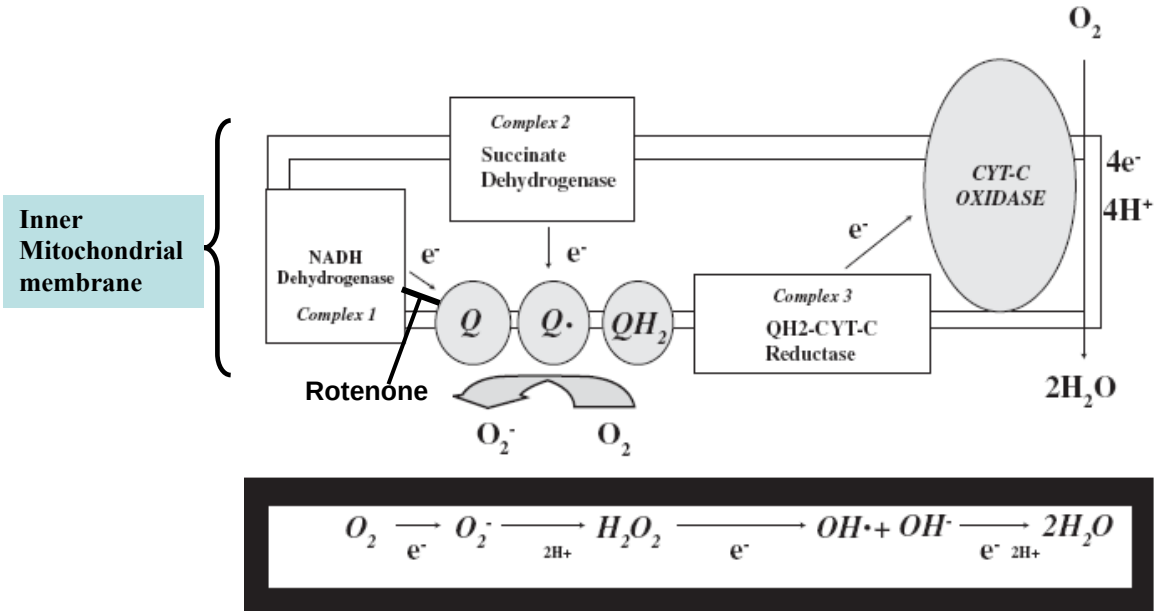

Figure 5

ROS generation during electron transport chain in the inner mitochondrial membrane

See text for details

PART –II

PRO-APOPTOTIC ABILITY OF ONCOGENIC H-RAS TO FACILITATE APOPTOSIS INDUCED BY HISTONE DEACETYLASE INHIBITORS IN HUMAN CANCER CELLS

Research described in this chapter is slightly modified version of an article that is published in 2007 in Molecular Cancer Thearpeutics by Shambhunath Choudhary and Hwa-Chain Robert Wang.

Choudhary S, Wang HCR. Proapoptotic ability of oncogenic H-Ras to facilitate apoptosis induced by histone deacetylase inhibitors in human cancer cells. *Mol Cancer Ther* 2007;6:1099-111. *Copyright © 2007 American Association for Cancer Research.*

In this paper "our" and "we" refers to me and co-authors. My contribution in the paper includes (1) Selection of the topic (2) Compiling and interpretation of the literature (3) Designing experiments (4) understanding the literature and interpretation of the results (5) providing comprehensive structure to the paper (6) Preparation of the graphs and figures (7) Writing and editing

Abstract

More than 35% of human urinary bladder cancers involve oncogenic H-Ras activation. In addition to tumorigenic ability, oncogenic H-Ras possesses a novel pro-apoptotic ability to facilitate the induction of apoptosis by histone deacetylase inhibitors (HDACIs). HDACIs are a new class of anticancer agents and are highly cytotoxic to transformed cells. To understand the connection between the selectivity of HDACIs on transformed cells and the pro-apoptotic ability of oncogenic H-Ras to facilitate HDACI-induced apoptosis, we introduced oncogenic H-Ras into urinary bladder J82 cancer cells to mimic an acquisition of the H-*ras* gene activation in tumor development. Expression of oncogenic H-Ras promoted J82 cells to acquire tumorigenic ability.

Meanwhile, oncogenic H-Ras increased susceptibility of J82 cells to HDACIs, including FR901228 and Trichostatin A (TSA), for inducing apoptosis. The caspase pathways, the B-Raf and extracellular signal regulatory kinase (ERK) pathway, $p21^{Cip1}$ and $p27^{Kip1}$, and core histone contents are regulated differently by FR901228 in oncogenic H-Ras-expressed J82 cells than their counterparts in parental J82 cells, contributing to the increased susceptibility to the induction of selective apoptosis. Our results lead us to a suggestion that HDACIs activate the pro-apoptotic ability of oncogenic H-Ras, indicating a potential therapeutic value of this new class of anticancer agents in the control of human urinary bladder cancer that has progressed to acquire oncogenic H-Ras.

Introduction

Activating mutations of *ras* genes are frequently found in human cancers (1-3). In fact, mutation in codon 12 of the H-*ras* gene is detected in more than 35% of patients with urinary bladder cancers (3). Expression of oncogenic Ras proteins results in cellular transformation and promotes tumorigenesis accompanied by an aberrantly regulated, complex signaling circuitry, such as constant activation of the extracellular signal regulatory kinase (ERK) pathway, which consists of Raf, Mek, and Erk, and the phosphatidylinositol 3-kinase (PI3-K) pathway, which consists of PI3-K, PDK, and Akt (4). In the quest to understand the roles of oncogenic Ras in tumorigenesis, delineating Ras-induced signaling pathways has helped reveal many potential targets for current therapeutic approaches focusing on inhibition of Ras protein synthesis and functions (5). It is important to identify anticancer agents and their molecular targets to selectively induce apoptosis of Ras-related cancer cells in order to increase the effectiveness of chemotherapy.

Histone deacetylase inhibitors (HDACIs), a new class of anticancer agents, have been shown to exhibit antimetastatic and antiangiogenic activities toward malignantly transformed cells in vitro and in vivo (6,7). HDACI molecules are structurally diverse and include depsipeptides such as FR901228 and hydoximates such as Trichostatin A (TSA) (6). We have shown the ability of FR901228, also named FK228 (NSC-630176) (8-10), to induce apoptosis of human breast cancer MCF7 and MDA-MB231 cells and to induce p21^{Cip1} expression in a p53-independent manner (11). We have also shown that FR901228 induces apoptosis in Ras-transformed mouse embryo fibroblast 10T1/2 cells, whereas it induces growth arrest of non-transformed counterpart cells in the G0/G1 phase of the cell cycle (12,13). Caspase-3 plays an

important role in FR901228-induced selective apoptosis of Ras-transformed 10T1/2 cells (12-14). In the non-transformed 10T1/2 cells, $p21^{Cip1}$ is induced by FR901228, but it is reduced in Ras-transformed cells (12). In addition, although the ERK pathway plays an anti-apoptotic role in parental 10T1/2 cells, it plays a pro-apoptotic role in FR901228-induced cell death of Ras-transformed cells (13). Raf-1 in the ERK pathway is particularly reduced by FR901228 in Ras-transformed 10T1/2 cells (12). The PI3-K pathway plays an anti-apoptotic role, whereas the stress-activated protein kinase p38 (p38/SAPK) pathway plays a pro-apoptotic role in FR901228-induced apoptosis of both Ras-transformed and parental 10T1/2 cells (13). Our studies indicate a pro-apoptotic role of oncogenic H-Ras in the FR901228-induced apoptosis in mouse cells. The novel pro-apoptotic ability of oncogenic H-Ras to increase cell susceptibility to selected anticancer agents, such as FR901228, should be seriously considered in developing anticancer therapeutics against Ras-related cancers. However, the values of the ERK, PI3-K, p38/SAPK, and caspase pathways, as well as Cdk inhibitors as therapeutic targets need to be validated in all types of human cancer cells subjected to FR901228 treatment.

Here, we present evidence that expression of oncogenic H-Ras resulted in increased susceptibility of human cancer J82 cells to both FR901228- and TSA-induced apoptosis. The J82 human urinary bladder transitional carcinoma cell line hosts wild-type *ras* and the inactive mutant *Rb* and *p53* genes with deletion of the *pTEN* gene (15,16). Expression of oncogenic H-Ras promoted J82cells to acquire tumorigenicity, mimicking an acquisition of H-*ras* gene activation in tumor development. Meanwhile, expression of oncogenic H-Ras facilitated the induction of apoptosis by FR901228, and reduced clonogenic resistance to FR901228. Our studies revealed both commonality and discrepancy in modulation of signaling pathways

associated with cell growth, survival, growth arrest, and apoptosis between oncogenic H-Ras-expressed and parental J82 cells. The discrepancies, which may contribute to the ability of FR901228 to selectively induce apoptosis in oncogenic H-Ras-expressed cells, should be considered in the selection of therapeutic targets for Ras-related human urinary bladder cancers.

Materials and Methods

Cell Cultures, Transfection, and Reagents

Human urinary bladder transitional carcinoma J82 and T24 cell lines (ATCC, Rockville, MD) and oncogenic H-Ras-expressed J82 cells were maintained in DMEM supplemented with 10% fetal bovine serum, 100 U/ml penicillin, and 100 μg/ml streptomycin at 37^{o}C. To generate oncogenic H-Ras-expressed J82 cells, we used a previously constructed pcDNA4/TO-E-H-*ras* plasmid (17), which carries the oncogenic H-*ras* (V12) gene. Cells in a 35 mm culture dish were transfected with 0.5 μg of pcDNA4/TO-E-H-*ras* plasmid DNA using PolyFect Transfection Reagent (Qiagen, Valencia, CA). After 48 h of transfection, cells were subcultured and selected in 100 μg/ml Zeocin (Invitrogen, Carlsbad, CA). Resistant cell clones were established as candidate J82-Ras cell lines. Stock aqueous solutions of FR901228 (obtained through a collaboration with Dr. KK Chan at the Ohio State University), TSA (ICN, Aurora, OH), U0126 (Cell Signaling, Beverly, MA), LY294002, SB203580, SP600125, and Ac-Asp-Glu-Val-Asp-CHO (Ac-DEVD-CHO) (Alexis, San Diego, CA) were prepared in DMSO and diluted in culture medium for assays.

Flow cytometry

Attached cells were trypsinized from cultures, rinsed with Ca^{++} and Mg^{++} free phosphate buffered saline, fixed in ethanol, and stained with propidium iodide for flow cytometric analysis, as performed previously (13). Analysis of DNA content and determination of the percentage of apoptotic cells and cells in each phase of the cell cycle were performed on Multicycle software (Phoenix Flow System, San Diego, CA).

Cell growth and survival rate assay

Cells were seeded in 12-well culture plates and treated with FR901228. Every 24 h, attached cells were trypsinized, washed, and then resuspended in culture medium containing 0.2% trypan blue to stain dead cells. Live cells were counted in a hemocytometer to determine relative cell growth and survival rate (12).

Cell growth inhibition assay

Inhibition of cell proliferation was determined by the inhibition of 5-bromo-2'-deoxyuridine (BrdU) incorporation into cellular DNA, using the BrdU cell proliferation ELISA kit (Roche, Indianapolis, IN). Five x 10^4 cells were seeded into each well of 96-well culture plates for 24 h. After treatment with FR901228, cells were labeled with BrdU for 12 h, fixed, incubated with peroxidase-conjugated BrdU-specific antibodies, and stained with peroxidase substrate. Quantification of BrdU-labeled cells was determined with an ELISA reader (Bio-Tek, Winooski, VT).

Cell viability assay

A Methyl Thiazolyl Tetrazolium (MTT) assay kit (ATCC, Manassas, VA) was used to measure cell viability in cultures. Five x 10^4 cells were seeded into each well of 96-well culture plates for 24 h. After treatments with HDACIs and/or inhibitors, cells were incubated with MTT Reagent for 4 h, followed by incubation with Detergent Reagent for 24 h. Reduced MTT reagent in cultures was quantified with an ELISA reader.

Clonogenic assay

Triplicates of 1 x 10^4 cells were seeded in 100 mm culture dishes for 24 h. After FR901228 treatment, cultures were rinsed and replaced with fresh medium. Growing colonies (>30 cells) were identified and counted under an anatomical microscope. Adherent colonies in untreated cultures were stained with crystal violet after 7 days, and FR901228-treated cultures were stained after 14 days.

Anchorage-independent cell growth assay

The base layer consisted of 2% low gelling SeaPlaque agarose (Sigma, St Louis, MO) in complete J82 culture medium. Soft agar consisting of 0.4% Sea Plaque agarose in a mixture (1:1) of complete J82 culture medium with 3 day-conditioned medium prepared from J82 culture, was mixed with $3x10^3$ cells and plated on top of the base layer in 60mm diameter culture dishes. Soft-agar cultures were maintained at 37^oC and observed microscopically for the appearance of colonies. Growing colonies were identified, and the number of colonies that reached 0.5 mm diameter by 14 days, was recorded.

Tumorigenic and histopathological studies

Cells were prepared with Matrigel basement membrane matrix (13.35 mg/ml; BD Biosciences), and $1x10^7$ cells in 100 μL were injected subcutaneously into flanks of 5-week old female athymic NCr-*nu/nu* mice (NCI, Frederick, MD). Four mice were used per group and maintained under pathogen-free conditions. Animals were monitored weekly until tumors were visible; then tumor growth was monitored every 3 days. Xenograft tumor tissues were immediately harvested after euthanasia by exposure to carbon dioxide. Tumor tissues were fixed in neutral buffered formalin and embedded in paraffin for histopathological evaluation of 5-μm hematoxylin and eosin (H&E) stained sections. Tumor tissues were also sliced into 1 mm^3 cubes and incubated with FR901228 in culture medium to detect activation of caspases using Western immunoblotting with specific antibodies. All animal procedures were approved by The University of Tennessee Animal Care and Use Committee and were in accordance with the NIH *Guide for the Care and Use of Laboratory Animals* (National Research Council, 1985).

Western Immunoblotting

To prepare cell lysates, cultured cells were lysed in a buffer (10 mM Tris-HCl, 150 mM NaCl, 1% Triton X-100, 5 mM EDTA, 10 mM sodium pyrophosphate, 10% glycerol, 0.1% Na_3VO_4, 50 mM NaF, pH 7.4) (12). Tumor tissues were sliced into 1 mm^3 cubes, incubated with FR901228 in culture medium, and lysed in the buffer above with 30 strokes of a loose-fitting Dounce homogenizer. Cell lysates (S20) were isolated from the supernatants after centrifugation

of crude cell or tissue lysates at 20,000 x g for 20 min. To prepare nuclear cell lysates containing core histones, cells were lysed in a hypotonic buffer (10 mM KH_2PO_4, 1 mM EDTA, 5 mM EGTA, 10 mM $MgCl_2$, 50 mM β-glycerolphosphate, 1 mM Na_3VO_4, 2 mM dithiothreitol, pH 7.2) with 30 strokes of a tight-fitting Dounce homogenizer (18). After centrifugation of crude lysates at 10,000 x g for 10 min, cell pellets containing nuclear histones were resuspended in lysis buffer and sonicated for 10 min as nuclear lysates (P10). Protein concentrations in cell lysates (S20) and nuclear lysates (P10) were measured using the BCA assay (Pierce, Rockford, IL). Equal amounts of cellular proteins were resolved by electrophoresis in either 10% or 14% SDS-polyacrylamide gels and transferred to nitrocellulose filters for Western immunoblotting, as previously described (12-14). Antibodies specific to Akt, Raf-1, Mek1/2, p38, JNK, acetylated H2A on Lys5, acetylated H2B on Lys12, H2B protein, acetylated H3 on Lys9, H3 protein, acetylated H4 on Lys8, procaspase-3, active caspase-3, active caspase-7, active caspase-8, full length and cleaved poly (ADP-ribose) polymerase (PARP; 89 kDa cleaved PARP and 116 kDa full length PARP), and β-Actin were purchased from Cell Signaling Technology (Beverly, MA). Specific antibodies to phosphorylated forms of Akt, Raf-1, B-Raf, Mek1/2, Erk1/2, p38, and JNK were also purchased from Cell Signaling Technology. Specific antibodies to H-Ras, B-Raf, Erk1/2, p53 (FL-393), $p27^{Kip1}$, and $p21^{Cip1}$ were purchased from Santa Cruz Biotechnology (Santa Cruz, CA). Antigen-antibody complexes on filters were detected by the SuperSignal chemiluminescence kit (Pierce, Rockford, IL).

Statistical Analysis

Statistical significance was analyzed by the Student's *t*-test. A p-value ≤ 0.05 was considered significant.

Results

Tumorigenicity of J82 cells was induced by oncogenic H-Ras

To determine the effects of oncogenic H-Ras on tumorigenic potential of human urinary bladder J82 cancer cells, cell clones were stably transfected with the expression plasmid vector pcDNA4/TO-E-H-*ras*. As shown in Fig. 1A, ectopic expression of oncogenic H-Ras in J82 cells resulted in a distinctive morphological change from a round, ruffled edge morphology (panel a) to an elongated, transformed morphology (panel b). Based on this change, the H-Ras expression level, and an enhanced cancerous ability of anchorage-independent growth in soft-agar (19), we developed a single-clonal J82-Ras cell line from selected cell clones. As shown in Fig. 1B-1, J82-Ras cells (lane 2) expressed a level of oncogenic H-Ras comparable to the counterpart level in the human bladder cancer T24 cell line (lane 3), which hosts the oncogenic H-*ras* mutant gene (20). Colony formation in soft-agar showed an average of 45 colonies developed from 3,000 J82 cells, and an average of 90 colonies developed from 3,000 J82-Ras cells (Fig. 1C). The cancerous ability of anchorage-independent growth in J82 cells was increased by oncogenic H-Ras. To conclude if J82-Ras cells had acquired tumorigenic ability, we inoculated J82-Ras and parental J82 cells into immunodeficient mice. Consistent with others' report (21), animals inoculated with parental J82 cells did not develop any xenograft tumors in 8 weeks. In contrast, nude mice inoculated with J82-Ras cells developed visible xenograft tumors in 15 days; tumors

developed to an average size of 0.3 cm diameter by 20 days and 1 cm by 30 days. Histopathological evaluation of J82-Ras-derived xenograft tumor tissues revealed neoplastic cells that invaded the adjacent skeletal muscle (Fig.1D, panel a) and a cohesive sheet of neoplastic cells characterized by ill-defined cytoplasmic borders, abundant slightly vacuolated eosinophilic cytoplasm, round to elongate nuclei, and multiple prominent nucleoli (panel b). Additionally, marked anisokaryosis (panel b) and anisocytosis as well as numerous binucleate and occasional multinucleate tumor giant cells were noted. The histopathological diagnosis confirmed that expression of oncogenic H-Ras induced the tumorigenic ability of J82 cells to produce poorly differentiated, xenograft adenocarcinoma in vivo.

Increased cell susceptibility to HDACIs by oncogenic H-Ras

To determine if expression of oncogenic H-Ras increased cell susceptibility to FR901228 for inducing cell death, we compared cell growth and survival rates of J82-Ras cells with parental J82 cells responding to FR901228 treatment. We detected that expression of oncogenic H-Ras did not result in any significant difference in the growth rate of J82-Ras cells versus parental J82 cells (Fig. 2A, 0 nM control lines). Treatment with 1 nM FR901228 reduced cell growth of both parental J82 and J82-Ras cells. Treatment with 5 nM FR901228 resulted in growth inhibition of both parental J82 and J82-Ras cells in 24 h. In contrast to a modestly reduced cell survival rate in parental J82 cultures, 5 nM FR901228 treatment significantly reduced cell survival in J82-Ras cultures by 48 h, indicating significantly higher cell death in J82-Ras cultures than in parental J82 cultures. Prolonged incubation with FR901228 at either 1 or 5 nM induced increased cell death in both parental J82 and J82-Ras cultures. We observed a

higher extent of apoptotic-like cell morphology with cell shrinkage and loss of cell contact induced by FR901228 treatment in J82-Ras cultures than in parental J82 cultures (data not shown). Although induction of apoptotic-like cell death by FR901228 was in a dose- and time-dependent manner, FR901228 at 5 nM induced a distinguishable, higher level of apoptosis in J82-Ras cultures than in parental J82 cells. Cell death by apoptosis in these cultures was verified by flow cytometry. As shown in Table 1, apoptotic cell population in attached cells was higher in J82-Ras cultures (increased from 2% to 7% and 24%) contrasted to parental J82 cultures (increased from 2% to 4% and 13%) after FR901228 treatment.

We used a clonogenic assay (22) to further determine whether the increased cell susceptibility to FR901228 by oncogenic H-Ras was attributed to a reduced resistance of oncogenic H-Ras-expressed J82 cells. As shown in Fig. 2B, approximately 600 clones (>30 cells/colony) developed from 1 x 10^4 untreated J82 and J82-Ras cells in 7 days (control). After 48 h of FR901228 treatment, we detected that approximately 25 clones had grown slowly and survived in J82 cultures (reached 30 cells/colony) by 14 days, and none survived in J82-Ras cultures (Fig. 2B, FR). Evidently, expression of oncogenic H-Ras in J82 cells increased susceptibility and reduced cell resistance to FR901228-induced apoptosis.

To expand our investigation of the pro-apoptotic role of oncogenic H-Ras in increasing cell susceptibility to HDACIs, we compared the susceptibility of J82 and J82-Ras to the induction of apoptosis by FR901228 and TSA, with the susceptibility to the human bladder cancer T24 cell line, which hosts the endogenous, oncogenic H-*ras* mutant gene (20). As shown in Fig. 2C, FR901228 treatment at either 5 or 25 nM reduced cell viability of J82-Ras and T24 cells to higher degrees than in J82 cells. Both J82-Ras and T24 cells also showed a higher

susceptibility than J82 cells to TSA-reduced cell viability in a dose-dependent manner (Fig. 2D). Interestingly, T24 cells showed a susceptibility similar to J82-Ras cells in response to either FR901228 or TSA treatment. Evidently, both FR901228 and TSA showed selectivity to induce cell death of oncogenic H-Ras-expressed human urinary bladder cancer J82 and T24 cells.

Differential regulation of caspase pathways by FR901228

To detect the apoptotic pathway induced by FR901128 in selective apoptosis of J82-Ras cells, we initially studied activation of executor caspase-3 by FR901228 in parental J82 and J82-Ras cells. We observed a higher level of procaspase-3 in J82-Ras cells than in parental J82 cells (Fig. 3A-1, lane 3 versus lane 1); FR901228 treatment increased the procaspase-3 protein level in parental J82 cells (lane 2 versus lane 1), but decreased procaspase-3 in J82-Ras cells (lane 4 versus lane 3). FR901228 treatment resulted in a higher level of active caspase-3 in J82-Ras cells (Fig. 3A-2, lane 4) than in parental J82 cells (lane 2). Studying the activation course of caspase-3 in FR901228-induced apoptosis revealed that FR901228 treatment did not induce detectable levels of active caspase-3 in J82 cells until 48 h (Fig. 3B-1, lane 3); in contrast, it induced an early caspase-3 activation in J82-Ras cells in 24 h (lane 5). Accelerated caspase-7 activation by FR901228 was also detected in J82-Ras cells (Fig. 3B-2, lanes 5 and 6) compared to parental J82 cells (lanes 2 and 3). Concomitantly, PARP, a downstream substrate of caspase-3 and -7 (23), was accordingly cleaved in parental J82 cells (Fig. 3B-3, lane 3) and J82-Ras cells (lanes 5 and 6). Expression of oncogenic H-Ras in J82 cells appears to accelerate FR901228-induced activation of caspase-3 and -7 and proteolysis of PARP.

To determine the upstream initiator caspases, which may contribute to the activation of caspase-3 and -7, we detected that active caspase-8 was induced by FR901228 in parental J82

cells by 48 hr (Fig. 3B-4, lane 3), and FR901228 treatment induced an early activation of caspase-8 in J82-Ras cells (lanes 5 and 6). Interestingly, caspase-9 was induced by FR901228 in J82-Ras cells (Fig. 3B-5, lanes 5 and 6) but was not induced in parental cells (lanes 1 to 3). Accordingly, the caspase-8 to caspase-3 and -7 pathway was induced by FR901228 in parental J82 cells. Both caspase-8 and -9 to caspase-3 and -7 pathways were induced by FR901228 in J82-Ras cells. The caspase-9 pathway appears to be potentiated by oncogenic H-Ras for activation in FR901228-induced selective apoptosis of J82-Ras cells.

To verify the role of caspase-3 and -7 in FR901228-induced cell death, J82 and J82-Ras cells were pretreated with the potent inhibitor Ac-DEVD-CHO to specifically inhibit caspase-3 and -7 (24), followed by FR901228 treatment. Pretreating cells with Ac-DEVD-CHO reduced FR901228-induced cleavage of PARP in both parental J82 (Fig. 3C-1, lane 4 versus lane 3) and J82-Ras (lane 8 versus lane 7) cells. Although treatment of cells with Ac-DEVD-CHO alone did not induce any detectable cleaved PARP (Fig. 3C-1, lanes 2 and 6), the treatment resulted in a modest reduction of cell viability (Fig. 3C-2). Pretreatment with Ac-DEVD-CHO did not significantly reverse the low degree of FR901228-reduced viability of J82 cells, but it significantly attenuated the FR901228-reduced viability of J82-Ras cells (Fig. 3C-2). We also used AEBSF-HCl (25), a serine protease inhibitor, in a similar study, but pretreatment with AEBSF-HCl did not enhance or suppress any FR901228-reduced cell viability (data not shown). These results indicate that caspase-3 and -7 played important roles in the FR901228-induced selective apoptosis of oncogenic H-Ras-expressed J82 cells. In addition, we treated xenograft tumor tissues of J82-Ras cells with FR901228 in vitro and detected active caspase-3, caspase-7, and cleaved PARP (Fig. 3D-1 to 3D-3, lanes 2 and 3); this result verified that the FR901228-

induced caspase activation also occurred in a three-dimensional tumor tissue-structural environment.

Regulation of Cdk inhibitors, p53, and histones by FR901228

FR901228 treatment induces growth arrest of human breast cancer MCF7 and MDA-MB231 cells in the G2/M phase of the cell cycle (11). However, FR901228 treatment growth-arrests mouse 10T1/2 cells and Ras-expressed 10T1/2 cells in the G0/G1 phase of the cell cycle (12,13). To study if growth arrest contributed to FR901228-induced growth inhibition of J82 and J82-Ras cells, we initially verified that cell proliferation in both parental J82 and J82-Ras cultures was suppressed by FR901228 treatment in 24 h (Fig. 4A). Subsequently, flow cytometric analysis revealed that FR901228 treatment of either J82 or J82-Ras cultures resulted in decreased cell populations in the G0/G1 phase, substantially decreased cell populations in the S phase, and significantly increased cell populations in the G2/M phase (Table 1). A higher population of J82-Ras cells than parental J82 cells ($p < 0.05$) accumulated in the G2/M phase after FR901228 treatment.

To pursue the involvement of Cdk inhibitors in FR901228-induced cell growth arrest, we detected that p21^{Cip1} was induced by FR901228 in J82 (Fig. 4B-1, lanes 2 and 3) and J82-Ras (lanes 5 and 6) cells. Adjusted by β-Actin levels (Fig. 4B-4), the induced p21^{Cip1} was reduced in J82-Ras cells undergoing apoptosis induced by FR901228 (lane 6). We also detected that p27^{Kip1} was increasingly induced by FR901228 in J82 (Fig. 4B-2, lanes 2 and 3) and J82-Ras (lanes 5 and 6) cells. Induction of p21^{Cip1} appears to correlate with induction of growth inhibition, and p27^{Kip1} induction appears to correlate with completion of cell growth arrest by

FR901228 in the G2/M phase of the cell cycle (Table 1). In addition, we detected that the mutant p53 was progressively reduced by FR901228 in J82 (Fig. 4B-3, lanes 2 and 3) and J82-Ras (lanes 5 and 6) cells. The reduction of the mutant p53 was correlated with FR901228-induced apoptosis.

Modification of core histones through acetylation has been reported to play a critical role in the growth arrest of cell proliferation (26,27). We detected that acetylation of core histones H2A on Lys5 (Fig. 4C-1), H2B on Lys12 (Fig. 4C-2), H3 on Lys9 (Fig. 4C-3), and H4 on Lys8 (Fig. 4C-4) was profoundly increased by FR901228 treatment in both parental J82 (lane 2) and J82-Ras (lane 5) cells by 24 h; however, acetylation was substantially reduced in cells treated with FR901228 for 48 h (lanes 3 and 6). The H2B protein level was reduced by FR901228 treatment in both parental J82 and J82-Ras cells (Fig. 4C-5, lanes 3 and 6). FR901228 progressively reduced the H3 protein level in J82-Ras cells undergoing apoptosis (Fig. 4C-6, lanes 5 and 6) than in parental J82 cells mainly undergoing growth arrest (lanes 2 and 3). However, we were unable to detect H2A and H4 protein with two commercially available specific antibodies. These results indicate a novel effect of oncogenic H-Ras on the reduction of histone contents induced by extended treatment with FR901228.

Roles of the ERK, PI3-K, and p38/SAPK pathways in FR901228-induced apoptosis

The ERK, PI3-K, and p38/SAPK pathways are modulated by FR901228 to play different roles in apoptosis of H-Ras-transformed and non-transformed mouse 10T1/2 cells (12,13). To investigate the role the ERK pathways may play in J82-Ras and parental J82 cells undergoing FR901228-induced selective apoptosis, we used U0126 to specifically inhibit Mek1/2 activity (13,14,28). As shown in Fig. 5A-1, treatments with U0126 alone for 48 h modestly reduced cell

viability in cultures of J82 and J82-Ras. Although U0126 treatment failed to affect FR901228-reduced viability in parental J82 cells, it enhanced FR901228-reduced viability of J82-Ras cells. Thus, expression of oncogenic H-Ras induced the survival role of the ERK pathway in J82-Ras cells responding to the FR901228-induced apoptosis. To identify targets in the ERK pathway for reducing cell viability, we studied FR901228-induced effects on activation-related phosphorylation and protein levels of ERK pathway kinases B-Raf, Raf-1, Mek1/2, and Erk1/2. We detected that protein levels of oncogenic H-Ras were not affected by FR901228 treatment (Fig. 5A-2). The overall phosphorylation level of B-Raf was elevated in J82-Ras cells (Fig. 5A-3, lane 4), compared to the counterpart phosphorylated kinase in parental J82 cells (lane 1). FR901228 treatment increased the overall phosphorylation of B-Raf in parental J82 cells (Fig. 5A-3, lanes 2 and 3), but reduced both the overall phosphorylation and cognate protein levels of B-Raf in J82-Ras cells (Fig. 5A-3 and 5A-4, lanes 5 and 6). Although B-Raf protein levels may vary slightly between experiments, in general, they were unchanged in parental J82 cells treated with FR901228. Adjusted by the cognate protein level of B-Raf, the specific phosphorylation level of B-Raf (p/B-Raf) was elevated by FR901228 treatment in both parental J82 and J82-Ras cells. Adjusted with β-Actin levels (Fig. 5A-11), FR901228 treatment resulted in significant reduction of B-Raf protein in J82-Ras cells. B-Raf protein appears to be a distinct target for FR901228-induced reduction in J82-Ras cells, but not in parental J82 cells.

Expression of oncogenic H-Ras also elevated the overall activation-related phosphorylation level of Raf-1 in J82-Ras compared to parental J82 cells (Fig. 5A-5, lane 4 versus lane 1). FR901228 treatment resulted in reduction of the overall phosphorylation and protein levels of Raf-1 in both J82 and J82-Ras cells (Fig. 5A-5 and 5A-6, lanes 2, 3, 5, and 6);

based on the cognate Raf-1 protein level, the specific phosphorylation level of Raf-1 (p/Raf-1) was slightly increased in parental J82 cells and reduced in J82-Ras cells. Adjusted with β-Actin levels, FR901228 treatment resulted in significant reduction of Raf-1 protein (Raf-1/Actin) in both parental J82 and J82-Ras cells. Thus, Raf-1 protein appears to be a common target for FR901228-induced reduction in J82 and J82-Ras cells.

To further investigate the ERK downstream pathway from Raf regulated in FR901128-treated cells, we detected that phosphorylation levels of Mek1/2 (Fig. 5A-7) and Erk1/2 (Fig. 5A-9) were not noticeably increased in J82-Ras cells (lane 4 versus lane 1). Although treatment of J82-Ras cells with FR901228 suppressed the overall phosphorylation and protein levels of B-Raf (Fig. 5A-3 and 5A-4, lanes 5 and 6) and Raf-1 (Fig. 5A-5 and -5A-6), it increased phosphorylation of Mek1/2 (Fig. 5A-7) and Erk1/2 (Fig. 5A-9). In contrast, FR901228 treatment did not induce any noticeable change in phosphorylation of Mek1/2 and Erk1/2 in parental J82 cells (Fig. 5A-7 and 5A-9, lanes 2 and 3). Increased phosphorylation/activation of Mek1/2 and Erk1/2 appears to correlate with increased specific phosphorylation of B-Raf in J82-Ras cells. Expression of oncogenic H-Ras in J82 cells appears to potentiate the ERK downstream kinases for activation in response to FR901228 treatment.

While investigating the PI3-K, the p38/SAPK, and the JNK/SAPK pathways involved in FR901228-induced cell death, we detected that expression of oncogenic H-Ras in J82 cells (lanes 4 versus 1) did not increase the phosphorylation of Akt (Fig. 5B-1) and p38 (Fig. 5B-3), but changed the phosphorylation profiles of JNK (Fig. 5B-5). FR901228 treatment did not result in any significant change in the overall phosphorylation of Akt in either J82 (Fig. 5B-1 and 5B-2, lanes 2 and 3) or J82-Ras (lanes 5 and 6) cells. Interestingly, FR901228 treatment profoundly

reduced phosphorylation of p38 in parental J82 cells (Fig. 5B-3, lanes 2 and 3), but it did not result in any change in phosphorylation of p38 in J82-Ras cells (lanes 5 and 6). Thus, expression of oncogenic H-Ras prevented p38 from dephosphorylation induced by FR901228. On the other hand, FR901228 treatment profoundly reduced phosphorylation of JNK but not cognate protein in parental J82 cells (Fig. 5B-5 and -6, lanes 2 and 3) and in J82-Ras cells (lane 6). In pursuing the role the PI3-K, the p38/SAPK, and the JNK/SAPK pathways may play in FR901228-induced cell death, we detected that treatments with LY294002, which specifically inhibits PI3-K activity (13,29), alone modestly reduced cell viability in cultures of J82 and J82-Ras, but it failed to result in any significant change in the FR901228-reduced viability (Fig. 5C-1). The PI3-K pathway was unlikely to play a role in the FR901228-induced growth inhibition or apoptosis of J82 and J82-Ras cells. After using SB203580, which specifically inhibits p38 activity (13,30), to block the p38/SAPK pathway, we detected that SB203580 treatment attenuated FR901228-reduced viability in J82-Ras cells, but not in parental J82 cells (Fig. 5C-2). Therefore, the p38/SAPK pathway appears to be differentially maintained by oncogenic H-Ras and to play a pro-apoptotic role in FR901228-induced apoptosis of J82-Ras cells. Using SP600125, which specifically inhibits JNK activity (31,32), to block the JNK/SAPK pathway, we detected that J82-Ras cells were less susceptible to SP600125 treatment than parental J82 cells, and SP600125 treatment additionally enhanced FR901228-reduced viability in parental J82 cells, but not in J82-Ras cells (Fig. 5C-3). The JNK/SAPK pathway appears to play a survival role in parental J82 cells. Although expression of oncogenic H-Ras induced phosphorylation of both p54 and p48 JNK and induced resistance to SP600125, suppression of the JNK/SAPK pathway by FR901228 treatment may still contribute to the induction of cell death in J82-Ras cells.

Discussion

Understanding the pro-apoptotic ability of oncogenic H-Ras to enhance the cytotoxicity of anticancer agents in order to induce selective apoptosis provides cellular and molecular bases for developing therapeutic strategies to target Ras-related human cancers. In our previous studies (12-14), we showed that expression of oncogenic H-Ras in mouse 10T1/2 cells increases susceptibility to FR901228 but not the potent apoptosis inducer staurosporine, for inducing selective apoptosis. In this report, we present evidence to verify selectivity of HDACIs to target human bladder cancer cells associated with oncogenic H-Ras expression, as summarized in Fig.6.

The human urinary bladder carcinoma J82 cell line hosts wild-type *ras* genes, and is not tumorigenic to immune-deficient mice (15,16,21). In our studies, introduction of the oncogenic H-*ras* gene into J82 cells promoted cells to acquire the tumorigenic ability to develop xenograft tumors in immune-deficient mice; however, it was also accompanied by the novel pro-apoptotic property for FR901228 and TSA to induce selective apoptosis. The human urinary bladder carcinoma T24 cell line, in which oncogenic H-Ras is endogenously expressed (20), showed a comparable level of susceptibility with J82-Ras cells to both FR901228 and TSA for inducing cell death. However, expression of oncogenic H-Ras in J82 cells did not increase susceptibility to other agents, including U0126, LY294002, SB203580, SP600125, and Ac-DEVD-CHO, which is consistent with our results from studying mouse fibroblasts (13). The pro-apoptotic ability of oncogenic H-Ras that facilitates agents to induce cell death is HDACI-specific, but is not a cell type-specific property. HDACIs may activate the pro-apoptotic potential of oncogenic H-Ras. In addition, expression of the oncogenic v-*src* gene in 10T1/2 cells resulted in cellular

transformation but did not increase cell susceptibility to FR901228 for inducing apoptosis (result not shown). Whether the selectivity of HDACIs to induce cell death of oncogenic H-Ras-expressed cells is applicable to other oncogene-expressed cells needs to be broadly investigated.

Caspase pathways were differentially induced by FR901228 between oncogenic H-Ras-expressed and parental J82 cells. Previously, we reported that caspase-3 plays an important role in FR901228-induced selective apoptosis of Ras-transformed 10T1/2 cells (12-14). Here, we detected that FR901228 not only induced accelerated caspase-3 activity but also caspase-7 in the selective apoptosis of oncogenic H-Ras-expressed J82 cells as compared to parental J82 cells. Inhibition of caspase-3 and -7 alleviated FR901228-reduced cell viability, which clearly verified the contributing role of these caspases in the induction of apoptosis by FR901228. Investigating their upstream caspase pathways, we detected that both the caspase-8 and caspase-9 pathways were activated in oncogenic H-Ras-expressed J82 cells, but only the caspase-8 pathway was induced in parental counterpart J82 cells after FR901228 treatment. Other studies have shown that FR901228 treatment induces the extrinsic Fas pathway-dependent activation of caspase-8 and -3 in human osteosarcoma and leukemia cells (33,34), and induces the intrinsic mitochondrial pathway-dependent activation of caspase-9 and -3, but not caspase-8, in lung cancer cells (35). Either the extrinsic caspase-8 or the intrinsic caspase-9 initiator pathway is reportedly sufficient to activate its downstream executioners, caspase-3 and -7 (36). Whether the additional activation of caspase-9 in J82-Ras cells, but not in parental J82 cells, plays an enhancing role in the accelerated induction of selective apoptosis in J82-Ras needs to be clarified.

Expression of oncogenic H-Ras in J82 cells resulted in an increased cell population in the

G2/M phase of the cell cycle in response to FR901228-induced cell growth arrest. Studies of Cdk inhibitors revealed distinct regulation of p21^{Cip1} and p27^{Kip1} in the course of FR901228-induced cell growth arrest of J82 cells. High levels of p21^{Cip1} were initially induced in 24 h and subsequently reduced by 48 h in both parental J82 and J82-Ras cells, whereas the p27^{Kip1} level was continuously increased in the course of FR901228 treatment. Increased expression of p27^{Kip1} has been postulated to play a role in complete suppression of human cancer cell growth (37). In fact, FR901228 induced growth inhibition of both parental J82 and J82-Ras cells in 24 h. Accordingly, an early induction of p21^{Cip1} plus a progressive induction of p27^{Kip1} may be required to growth-arrest J82 and J82-Ras cells. Both p21^{Cip1} and p27^{Kip1} have been postulated to play multiple roles in the regulation of apoptosis, protein assembly, and gene transcription in addition to inhibitors of the cell cycle (38). The significance of the distinctive, sequential regulation of p21^{Cip1} and p27^{Kip1} in FR901228-induced cell growth arrest and apoptosis remains to be determined. On the other hand, it is interesting that in J82-Ras cells, a lower level of p21^{Cip1} and a higher level of p27^{Kip1} were induced compared to parental J82 cells undergoing FR901228-induced growth arrest. We reported previously that FR901228 treatment induces p21^{Cip1} expression in non-transformed 10T1/2 cultures in which cells are mainly arrested in the G0/G1 phase of the cell cycle; in contrast, FR901228 treatment reduces the basal level of p21^{Cip1} in Ras-transformed 10T1/2 cultures in which significant apoptosis is induced (12). We did not detect any induction of p27^{Kip1} in either non-transformed or Ras-transformed 10T1/2 cultures after FR901228 treatment (data not shown). Sandor et al. observed that human colon cancer HCT116-derived cell clones lacking p21^{Cip1} are not arrested in the G1 phase, but are arrested in the G2/M phase of the cell cycle following FR901228 treatment; they

suggested that p21*Cip1* is required for FR901228-induced G1 arrest, and G2/M arrest in the absence of p21*Cip1* is associated with increased cell death induced by FR901228 (39). In addition, expression of p21*Cip1* is induced by FR901228 in a p53-independent manner, but expression of p21*Cip1* has been suggested to play a role in degrading mutant p53 in FR901228-treated cells (40). J82 cells host the mutant *p53* gene (15), and the mutant p53 protein was progressively and substantially reduced in J82 and J82-Ras cells undergoing FR901228-induced growth arrest followed by apoptosis. It has been suggested that FR901228 induces a novel p53-related feedback activity that results in depletion of mutant p53 protein in association with increased cytotoxicity of FR901228 to tumor cells (40,41). Accordingly, enhanced reduction of p21*Cip1* and depletion of mutant p53 conceivably contribute to FR901228-induced selective apoptosis of oncogenic H-Ras-expressed J82 cells.

It was expected that FR901228 treatment induced profound acetylation of core histones H2A, H2B, H3, and H4 in both J82 and J82-Ras cells. However, it was unexpected that acetylated histones and their protein contents were subsequently reduced in cells undergoing FR901228-induced growth inhibition or apoptosis. Particularly, reduction of H3 content by FR901228 appears to be accelerated by expression of oncogenic H-Ras in J82 cells in association with enhanced cell death. Modification of core histones through acetylation has been reported to play a critical role in the growth arrest of cell proliferation (26,27). It is possible that oncogenic H-Ras-induced modification of histones in conjunction with apoptosis-related chromosomal DNA fragmentation contribute to the enhanced histone reduction in J82-Ras cells undergoing FR901228-induced cell death. However, the mechanism for reducing histone content and the role of reduced histones in FR901228-induced apoptosis remain to be clarified.

The ERK pathway was targeted by FR901228 treatment in both parental and oncogenic H-Ras-expressed J82 cells. FR901228 treatment resulted in substantial reduction of Raf-1 protein in both parental J82 and J82-Ras cells, a result consistent to the outcome of substantially reduced Raf-1 protein in FR901228-treated mouse 10T1/2 cells (12). It has been suggested that FR901228 treatment results in destabilization of Raf-1 protein due to dissociation from Hsp90 (42,43). Possibly, the association between Raf-1 and Hsp90 is a target for FR901228 to reduce Raf-1 protein in J82 and 10T1/2 cells, regardless of Ras activation. On the other hand, expression of oncogenic H-Ras increased phosphorylation/activation of B-Raf. It has been suggested that Ras-activated B-Raf, but not inactive B-Raf, is subjected to regulation by Hsp90, and inhibition of Hsp90 activity destabilizes activated B-Raf for degradation (44). Therefore, activated B-Raf may become susceptible to the Hsp90-involved degradation induced by FR901228 treatment in J82-Ras cells. Raf family members have been reportedly involved in cell survival (45). In contrast to a maintained, unchanged B-Raf level and a reduced Raf-1 level in parental J82 cells, reduction of both Raf-1 and B-Raf conceivably contributed to the increased susceptibility of J82-Ras cells to FR901228-induced apoptosis.

FR901228 treatment stimulated the survival role of the ERK pathway in J82-Ras cells, but not in parental J82 cells. Although expression of oncogenic H-Ras in J82 cells increased phosphorylation of both B-Raf and Raf-1, it did not lead to significant phosphorylation of downstream kinases Mek1/2 and Erk1/2 until FR901228 treatment. FR901228 treatment resulted in reduction of both overall phosphorylated B-Raf and B-Raf protein in J82-Ras cells; however, the specific phosphorylation of B-Raf was highly increased. Possibly, the FR901228-increased specific phosphorylation contributed to the increased specific kinase activity of B-Raf,

leading to the induction of downstream kinases Mek1/2 and Erk1/2 in J82-Ras cells. In contrast, Mek1/2 and Erk1/2 were not activated by FR901228 in parental J82 cells. Consequently, blockage of the ERK pathway by inhibition of Mek1/2 activation resulted in enhanced cell death in FR901228-treated J82-Ras cells, but not in parental J82 cells. Thus, the downstream ERK pathway plays an anti-apoptotic role in FR901228-induced apoptosis of J82-Ras cells. Accordingly, suppression of the downstream ERK pathway enhanced the FR901228-induced selective apoptosis of J82-Ras cells.

The PI3-K pathway, in addition to the ERK pathway, was also unconventionally regulated in J82 cells. Akt is downstream from PI3-K and pTEN, and its activation is positively regulated by PI3-K and negatively regulated by pTEN (46). Previously, we showed that expression of oncogenic H-Ras in 10T1/2 cells induces the PI3-K pathway to activate Akt, and blockage of PI3-K activity enhances FR901228-induced apoptosis in both non-transformed and Ras-transformed 10T1/2 cells (13). Clearly, the PI3-K pathway plays an anti-apoptotic role in FR901228-induced cell death of mouse cells. Here, expression of oncogenic H-Ras in J82 cells, in which the *pTEN* gene is deleted (16), did not increase phosphorylation of Akt. Suppression of PI3-K activity did not change FR901228-reduced cell viability. Thus, the PI3-K pathway is unlikely to play a role in FR901228-induced cell death of either J82 or J82-Ras cells. On the other hand, the p38/SAPK pathway was also not induced by oncogenic H-Ras in J82 cells. However, in contrast to a suppression of the p38/SAPK pathway induced by FR901228 in parental J82 cells, FR901228 did not suppress the p38/SAPK pathway in J82-Ras cells. Inhibition of p38 activity attenuated the FR901228-reduced cell viability in J82-Ras cells, but not in parental J82 cells, indicating that a pro-apoptotic role of the p38/SAPK pathway was induced

in J82-Ras cells responding to FR901228-induced apoptosis. On the other hand, inhibition of JNK activity enhanced the FR901228-reduced cell viability in parental J82 cells, but not in J82-Ras cells, indicating a survival role of the JNK/SAPK pathway in parental J82 cells responding to FR901228-induced apoptosis. Possibly, expression of oncogenic H-Ras in J82 cells had suppressed the survival JNK activity; FR901228 treatment further reduced JNK phosphorylation as a contributing factor to the resulting cell death. These unconventionally regulated pathways may indicate an outcome from multiple mutations occurring in human cancers.

Current Ras-targeted anticancer approaches mainly focus on inhibition of Ras protein synthesis, interference with Ras processing to functional sites, or blockage of downstream Ras effectors, approaches based on understanding the roles of oncogenic Ras in tumorigenesis (5). Growing evidence indicates transformed cells are much more sensitive than normal cells to growth-inhibitory and apoptotic effects of HDACIs (6,47). Other evidence has shown that anticancer agents, including 5-fluorouracil (48), etoposide VP16 (49), cisplatin (50), lovastatin (51), and arsenic (52) selectively induce apoptosis of oncogenic H-Ras-expressed cells. Our studies verified the pro-apoptotic activity of oncogenic H-Ras that facilitated HDACIs to induce cell death of human urinary bladder cancer J82 cells. Our results suggest a potential value of HDACIs in treating human cancers involving activation of H-Ras. However, whether human cancers involving H-Ras overexpression are potential targets for HDACI therapy needs to be studied. Although the precise role of H-Ras activation in urinary bladder tumorigenesis remains controversial, clinical and basic studies have suggested that activation of H-Ras accompanied by inactivation of tumor suppressor p53 play important roles in tumorigenesis to high-grade invasive urothelial tumors (53,54). Our previous studies showed that expression of oncogenic H-

Ras alone in mouse embryo fibroblasts induces cellular transformation and tumorigenicity in immune-deficient mice, and increases cell susceptibility to FR901228 for inducing apoptosis (12-14). Our current report indicates that expression of oncogenic H-Ras in bladder tumor J82 cells, which host mutant *p53, Rb*, and *pTEN* genes, promotes tumorigenesis and increases cell susceptibility to HDACIs for inducing apoptosis. Possibly, HDACI therapy may be applicable to human cancers that acquire oncogenic H-Ras mutation at various stages of tumorigenesis, but that possibility needs to be verified clinically. FR901228 has been shown to exhibit strong activities inhibiting Class I HDAC-1 and HDAC-2, mild activity inhibiting Class II HDAC-4, and weak activity inhibiting Class II HDAC-6, assayed *in vitro* (55). Some studies have suggested that Class I HDACs are important in the regulation of proliferation and survival in cancer cells (56-58). Selective inhibition of Class I HDACs by FR901228 conceivably contributes to its selectivity in control of cancer cells. In addition, a recent report showed that ectopic expression of oncogenic H-Ras elevates reactive oxygen species (ROS) in ovarian epithelial cells (59). Two HDACIs, SAHA and MS-275, have been shown to cause an accumulation of ROS in transformed cells but not in normal cells (60). Whether expression of oncogenic H-Ras and FR901228 treatment additively increased ROS in the selective induction of apoptosis of J82-Ras cells needs to be clarified. Multiple mutations occur within human cancer cells; consequently affected signaling pathways are unconventionally regulated. It is important that the values of individual molecular targets need to be considered in individual cases for designing therapeutic protocols using HDACIs in combination with other agents to treat human urinary bladder cancers involving H-Ras activation.

LIST OF REFERENCES

1. Bos JL. Ras oncogenes in human cancer: a review. Cancer Res 1989; 49:4682–9.
2. Bertram JS. The molecular biology of cancer. Mol Aspects Med 2000; 21:167–223.
3. Buyru N, Tigli H, Ozcan F, Dalay N. Ras oncogene mutations in urine sediments of patients with bladder cancer. J Biochem Mol Biol 2003;36: 399–402.
4. Campbell SL, Khosravi-Far R, Rossman KL, Clark GJ, Der CJ. Increasing complexity of Ras signaling. Oncogene 1998;17:1395–413.
5. Adjei AA. Blocking oncogenic Ras signaling for cancer therapy. J Natl Cancer Inst 2001;93:1062–74.
6. Marks PA, Miller T, Richon VM. Histone deacetylases. Curr Opin Pharmacol 2003;3:344–51.
7. Dokmanovic M, Marks PA. Prospects: histone deacetylase inhibitors. J Cell Biochem 2005;96:293–304.
8. Ueda H, Nakajima H, Hori Y, et al. FR901228, a novel antitumor bicyclic depsipeptide produced by Chromobacterium violaceum No. 968. I. Taxonomy, fermentation, isolation, physico-chemical and biological properties, and antitumor activity. J Antibiot (Tokyo) 1994;47:301–10.
9. Ueda H, Manda T, Matsumoto S, et al. FR901228, a novel antitumor bicyclic depsipeptide produced by Chromobacterium violaceum No. 968. III. Antitumor activities on experimental tumors in mice. J Antibiot (Tokyo) 1994;47:315–23.
10. Vigushin DM. FR-901228 Fujisawa/National Cancer Institute. Curr Opin InvestigDrug s 2002;3:1396–402.

11. Rajgolikar G, Chan KK, Wang HCR. Effects of a novel antitumor depsipeptide FR901228 on human breast cancer cells. Breast Cancer Res Treat 1998;51:29–38.
12. Fecteau KA, Mei J, WangHCR. Differential modulation of signaling pathways and apoptosis of ras-transformed cells by a depsipeptide FR901228. J Pharmacol Exp Ther 2002;300:890–9.
13. SongP, Wei J, Wang HCR. Distinct roles of the ERK pathway in modulatingap optosis of Ras-transformed and non-transformed cells induced by anticancer agent FR901228. FEBS Lett 2005;579:90–4.
14. SongP, Wei J, Plummer H, Wang HCR. Potentiated caspase-3 in Ras-transformed 10T1/2 cells. Biochem Biophys Res Commun 2004; 322:557–64.
15. ChengYT, Li YL, Wu JD, et al. Overexpression of MDM-2 mRNA and mutation of the p53 tumor suppressor gene in bladder carcinoma cell lines. Mol Carcinog1995;13:173 – 81.
16. WangDS , Rieger-Christ K, Latini JM, et al. Molecular analysis of PTEN and MXI1 in primary bladder carcinoma. Int J Cancer 2000;88: 620–5.
17. SongP, Wang HCR. Efficient identification of tetR-expressing cell lines for tetracycline regulated gene expression. Electron J Biotechnol 2004;7:210–3.
18. WangHCR, Fecteau KA. Detection of a novel quiescence-dependent protein kinase. J Biol Chem 2000;275:25850–7.
19. Hanahan D, WeinbergRA. The hallmarks of cancer. Cell 2000;100: 57–70.

20. Taparowsky E, Suard Y, Fasano O, Shimizu K, Goldfarb M, Wigler M. Activation of the T24 bladder carcinoma transformingg ene is linked to a single amino acid change. Nature 1982;300:762–5.
21. Marshall CJ, Franks LM, Carbonell AW. Markers of neoplastic transformation in epithelial cell lines derived from human carcinomas. J Natl Cancer Inst 1977;58:1743–51.
22. FangY, Linardic CM, Richardson DA, Cai W, Behforouz M, Abraham RT. Characterization of the cytotoxic activities of novel analogues of the antitumor agent, lavendamycin. Mol Cancer Ther 2003;2:517–26.
23. Slee EA, Adrain C, Martin SJ. Executioner caspase-3, -6, and -7 perform distinct, non-redundant roles duringthe demolition phase of apoptosis. J Biol Chem 2001;276:7320–6.
24. Talanian RV, Quinlan C, Trautz S, et al. Substrate specificities of caspase family proteases. J Biol Chem 1997;272:9677–82.
25. de Bruin EC, Meersma D, de Wilde J, et al. A serine protease is involved in the initiation of DNA damage-induced apoptosis. Cell Death Differ 2003;10:1204–12.
26. Grewal SS, Moazed D. Heterochromatin and epigenetic control of gene expression. Science 2003;301:798–802.
27. Taddei A, Roche D, Bickmore WA, Almouzni G. The effects of histone deacetylase inhibitors on heterochromatin: implications for anticancer therapy. EMBO Rep 2005;6:520–4.
28. Favata MF, Horiuchi KY, Manos EJ, et al. Identification of a novel inhibitor of mitogen activated protein kinase. J Biol Chem 1998;273: 18623–32.

29. ShengH, Shao J, DuBois RN. Akt/PKB activity is required for Ha-Rasmediated transformation of intestinal epithelial cells. J Biol Chem 2001; 276:14498–504.
30. Somwar R, Koterski S, Sweeney G, et al. A dominant-negative p38 MAPK mutant and novel selective inhibitors of p38 MAPK reduce insulinstimulated glucose uptake in 3T3-L1 adipocytes without affecting GLUT4 translocation. J Biol Chem 2002;277:50386–95.
31. Bennett BL, Sasaki DT, Murray BW, et al. SP600125, an anthrapyrazolone inhibitor of Jun N-terminal kinase. Proc Natl Acad Sci U S A 2001; 98:13681–6.
32. Watanabe J, Nishiyama H, Matsui Y, et al. Dicoumarol potentiates cisplatin-induced apoptosis mediated by c-Jun N-terminal kinase in p53 wild-type urogenital cancer cell lines. Oncogene 2006;25:2500–8.
33. Aron JL, Parthun MR, Marcucci G, et al. Depsipeptide (FR901228) induces histone acetylation and inhibition of histone deacetylase in chronic lymphocytic leukemia cells concurrent with activation of caspase 8- mediated apoptosis and down-regulation of c-FLIP protein. Blood 2003; 102:652–8.
34. Imai T, Adachi S, Nishijo K, et al. FR901228 induces tumor regression associated with induction of Fas ligand and activation of Fas signaling in human osteosarcoma cells. Oncogene 2003;22:9231–42.
35. Doi S, Soda H, Oka M, et al. The histone deacetylase inhibitor FR901228 induces caspase dependent apoptosis via the mitochondrial pathway in small cell lungcancer cells. Mol Cancer Ther 2004;3: 1397–402.
36. Boatright KM, Salvesen GS. Mechanisms of caspase activation. Curr Opin Cell Biol 2003;15:725–31.

37. Hoshino R, Tanimura S, Watanabe K, Kataoka T, Kohno M. Blockade of the extracellular signal-regulated kinase pathway induces marked G1 cell cycle arrest and apoptosis in tumor cells in which the pathway is constitutively activated. J Biol Chem 2001;276:2686–92.
38. Coqueret O. New roles of p21 and p27 cell cycle inhibitors: a function for each cell compartment? Trends Cell Biol 2003;13:65–70.
39. Sandor V, Senderowicz A, Mertins S, et al. P21-dependent G1 arrest with downregulation of cyclin D1 and upregulation of cyclin E by the histone deacetylase inhibitor FR901228. Br J Cancer 2000;83: 817–25.
40. Blagosklonny MV, Trostel S, Kayastha G, et al. Depletion of mutant p53 and cytotoxicity of histone deacetylase inhibitors. Cancer Res 2005; 65:7386–92.
41. Kitazono M, Bates S, Fok P, Fojo T, Blagosklonny MV. The histone deacetylase inhibitor FR901228 (depsipeptide) restores expression and function of pseudo-null p53. Cancer Biol Ther 2002;1:665–8.
42. Schulte TW, Blagosklonny MV, Ingui C, Neckers L. Disruption of the Raf-1-Hsp90 molecular complex results in destabilization of Raf-1 and loss of Raf-1-Ras association. J Biol Chem 1995;270:24585–8.
43. Yu X, Guo ZS, Marcu MG, et al. Modulation of p53, ErbB1, ErbB2, and Raf-1 expression in lungcancer cells by depsipeptide FR901228. J Natl Cancer Inst 2002;94:504–13.
44. da Rocha Dias S, Friedlos F, Light Y, Springer C, Workman P, Marais R. Activated B-RAF is an Hsp90 client protein that is targeted by the anticancer drug17- allylamino-17 demethoxygeldanamycin. Cancer Res 2005;65:10686–91.

45. Hagemann C, Rapp UR. Isotype-specific functions of Raf kinases. Exp Cell Res 1999;253:34–46.

46. SongG, OuyangG, Bao S. The activation of Akt/PKB signaling pathway and cell survival. J Cell Mol Med 2005;9:59–71.

47. Espino PS, Drobic B, Dunn KL, Davie JR. Histone modifications as a platform for cancer therapy. J Cell Biochem 2005;94:1088–102.

48. TsengYS, TzengCC, Chiu AW, et al. Ha-ras overexpression mediated cell apoptosis in the presence of 5-fluorouracil. Exp Cell Res 2003;288: 403–14.

49. Chen G, Shu J, Stacey DW. Oncogenic transformation potentiates apoptosis, S-phase arrest and stress-kinase activation by etoposide. Oncogene 1997;15:1643–51.

50. Viktorsson K, Heiden T, Molin M, Akusjarvi G, Linder S, Shoshan MC. Increased apoptosis and increased clonogenic survival of 12V-H-ras transformed rat fibroblasts in response to cisplatin. Apoptosis 2000;5: 355–67.

51. ChangMY, Jan MS, Won SJ, Liu HS. Ha-ras Val12 oncogene increases susceptibility of NIH/3T3 cells to lovastatin. Biochem Biophys Res Commun 1998;248:62–8.

52. Puccetti E, Beissert T, Guller S, et al. Leukemia-associated translocation products able to activate RAS modify PML and render cells sensitive to arsenic-induced apoptosis. Oncogene 2003;22:6900–8.

53. Wu XR. Urothelial tumorigenesis: a tale of divergent pathways. Nat Rev Cancer 2005;5:713–25.

54. Oxford G, Theodorescu D. The role of Ras superfamily proteins in bladder cancer progression. J Urol 2003;170:1987–93.

55. Furumai R, Matsuyama A, Kobashi N, et al. FR901228 (depsipeptide) as a natural prodrugthat inhibits class I histone deacetylases. Cancer Res 2002;62:4916–21.

56. Glaser KB, Li J, Staver MJ, et al. Role of class I and class II histone deacetylases in carcinoma cells usingsi RNA. Biochem Biophys Res Commun 2003;310:529–36.

57. Bolden JE, Peart MJ, Johnstone RW. Anticancer activities of histone deacetylase inhibitors. Nat Rev DrugDi scov 2006;5:769–83.

58. Trachootham D, Zhou Y, ZhangH , et al. Selective killingof oncogenically transformed cells through a ROS-mediated mechanism by h-phenylethyl isothiocyanate. Cancer Cell 2006;10:241–52.

59. Ungerstedt JS, Sowa Y, Xu W-S, et al. Role of thioredoxin in the response of normal and transformed cells to histone deacetylase inhibitors. Proc Natl Acad Sci U S A 2005;102:673–8. Molecular Cancer Therapeutics 1111 Mol Cancer

APPENDIX

Table

Table 1. Flow cytometric analysis of FR901228-treated cells

	J82			J82-Ras		
Treatment (h):	**0**	**24**	**48**	**0**	**24**	**48**
Apoptotic (%):	2±1	4±2	13±7	2±1	7±3	24±7
Live (%):						
G0/G1:	52±2	51±6	45±10	53±4	46±12	32±11
S:	22±1	5±1	4±1	22±1	5±1	6±1
G2/M:	26±3	44±3	51±3***a***	25±2	48±12	61±4***b***

J82 and J82-Ras cultures were treated with 5 nM FR901228 for 0, 24, and 48 h. Anchored cells were trypsinized from cultures, and cell populations were analyzed by flow cytometry to detect apoptotic cell population and live cells in each phase of the cell cycle. Each value represents a mean of results from two independent experiments ± standard deviation. The Student's *t*-test was used to analyze statistical significance of ***b*** versus ***a*** ($p < 0.05$).

Figure 1. Tumorigenicity of J82 cells induced by oncogenic H-Ras. **(A)** Morphological features of J82 (panel a) and J82-Ras (panel b) cells in cultures. **(B-1 and B-2)** Lysates of growing J82, J82-Ras, and T24 cells were analyzed with Western immunoblotting using specific antibodies to detect levels of H-Ras and β-Actin. **(C)** Triplicates of 3 x 10^3 J82 and J82-Ras cells were seeded in soft-agar in 60 mm diameter culture dishes. By 14 days, cell colony formation (≥0.5 mm diameter) was counted microscopically and averaged ± standard deviation. **(D)** H&E stained histologic sections revealed cohesive sheets of neoplastic cells with anaplastic features of J82-Ras-derived xenograft tumor tissues. White arrows indicate J82-Ras xenograft tumor cells invaded adjacent host mouse skeletal muscle, and asterisks indicate skeletal myofibers (panel **a**). Black arrows indicate anisokaryosis and multiple prominent nucleoli (panel **b**). Scale bars are shown at 200 and 50 μm in panel **a** and **b**, respectively.

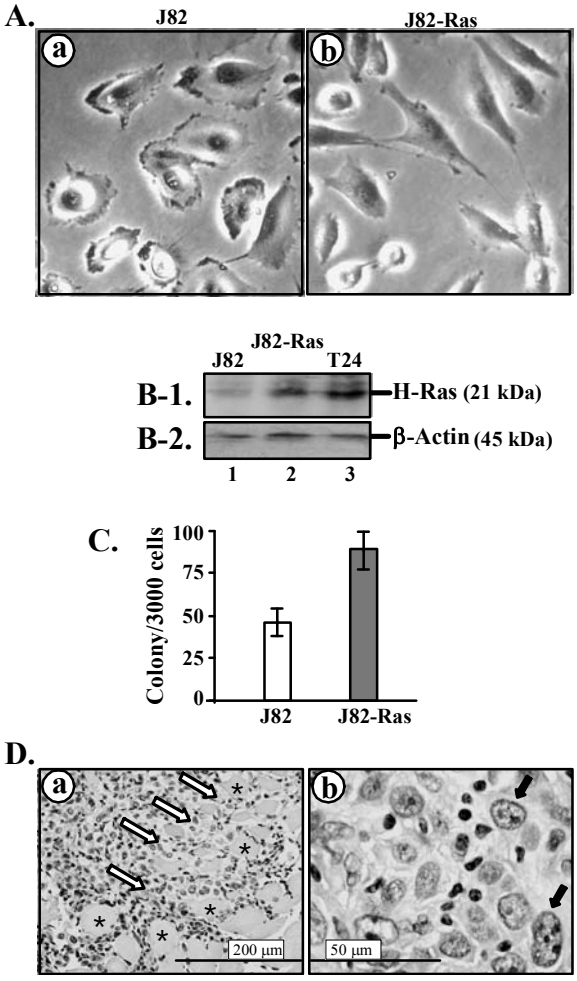
A.
J82
J82-Ras
a
b
J82-Ras
J82
T24
B-1.
H-Ras (21 kDa)
B-2.
β-Actin (45 kDa)
1
2
3
C.
Colony/3000 cells
100
75
50
25
0
J82
J82-Ras
D.
a
b
200 μm
50 μm

Figure 2. Increased cell susceptibility to HDACIs by oncogenic H-Ras. (A) J82 and J82-Ras cells were treated with 0, 0.2, 1, and 5 nM FR901228 (FR) for 0, 24, and 48 h. Every 24 h, live cells were counted in a hemocytometer. Relative cell growth and survival rates in cultures were normalized by the number of live cells determined at 0 hour, set as 100%. Each value represents a mean of triplicates, and error bars represent standard deviation. **(B)** Triplicates of 1 x 10^4 J82 and J82-Ras cells were seeded in 100 mm diameter culture dishes. After 24 h, the cells were treated with 5 nM FR901228 for 48 h. Then, cultures were replaced with fresh medium. By 7 days, control untreated cultures were stained with crystal violet. By 14 days, FR901228-treated cultures were stained with crystal violet. Cell colonies (> 30 cells) were counted microscopically and averaged ± standard deviation. **(C and D)** J82, J82-Ras, and T24 cells were treated with 0, 1, 5, and 25 nM FR901228 for 36 h or TSA at 0, 1, 5, and 25 nM for 48 h. Quantification of cell viability in these cultures was determined with an MTT assay kit. Relative cell viability was normalized by the value determined in untreated cells, set as 100%. Each value represents a mean of tetraplicates, and error bars represent standard deviation.

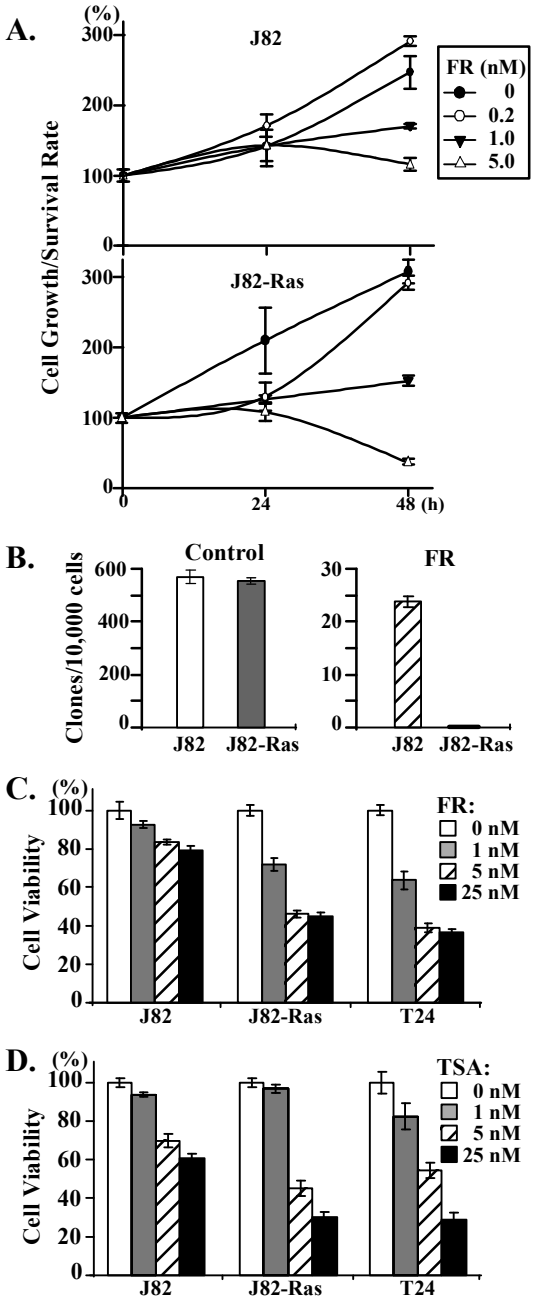
A.
(%)
J82
FR (nM)
0
0.2
1.0
5.0
Cell Growth/Survival Rate
J82-Ras
0
24
48 (h)
B.
Control
FR
Clones/10,000 cells
J82
J82-Ras
C.
(%)
FR:
0 nM
1 nM
5 nM
25 nM
Cell Viability
J82
J82-Ras
T24
D.
(%)
TSA:
0 nM
1 nM
5 nM
25 nM
Cell Viability
J82
J82-Ras
T24

Figure 3. FR901228-induced apoptotic caspase pathway facilitated by oncogenic H-Ras. (A-1 and A-2) J82 and J82-Ras cells were treated with 0 and 5 nM FR901228 for 48 h. **(B-1 to B-6)** J82 and J82-Ras cells were treated with 5 nM FR901228 for 0 (lanes 1 and 4), 24 (lanes 2 and 5), and 48 (lanes 3 and 6) h. **(C-1 and C-2)** J82 and J82-Ras cells were pretreated with 100 μM of the caspase-3 and -7 inhibitor Ac-DEVD-CHO (CI) for 6 h. Then, J82 and J82-Ras cultures were treated with 5 nM FR901228 for 48 h. Cell lysates were prepared from these cultures and analyzed by Western immunoblotting using specific antibodies to detect levels of procaspase-3 **(A-1)**, active caspase-3 **(A-2 and B-1),** active caspase-7 **(B-2)**, full length and cleaved PARP **(B-3)**, active caspase-8 **(B-4),** active caspase-9 **(B-5),** β-Actin **(B-6),** and cleaved PARP **(C-1).** Levels of cleaved caspase-9 **(B-5)** and β-Actin **(B-6)** were quantified by densitometry. The relative protein levels of caspase-9 (C-9/Actin) were calculated by normalizing the levels of caspase-9 with the levels of β-Actin, and then were normalized by the level in untreated J82 cells (lane 1), set as 1 (X, arbitrary unit). **(C-2)** Quantification of cell viability was determined with an MTT assay kit. Relative cell viability was normalized by the value determined in untreated cells, set as 100%. Each value represents a mean of tetraplicates, and error bars represent standard deviation. **(D-1 to D-4)** Xenograft tumor tissues of J82-Ras cells were sliced to 1 mm^3 cubes and incubated with 0, 5, and 25 nM FR901228 for 48 h. Lysates were analyzed by Western immunoblotting using specific antibodies to detect levels of active caspase-3, active caspase-7, full length and cleaved PARP, and β-Actin. Asterisk indicates the full length PARP.

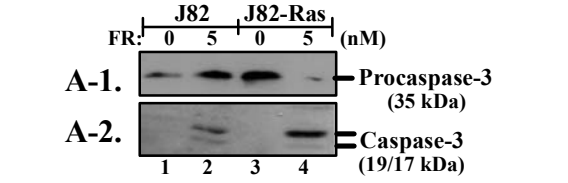
J82
J82-Ras
FR: 0 5 0 5 (nM)
A-1.
Procaspase-3
(35 kDa)
A-2.
Caspase-3
(19/17 kDa)
1 2 3 4

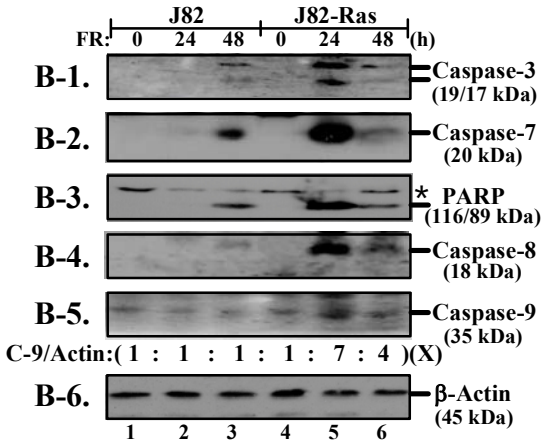
J82
J82-Ras
FR: 0 24 48 0 24 48 (h)
B-1.
Caspase-3
(19/17 kDa)
B-2.
Caspase-7
(20 kDa)
B-3.
* PARP
(116/89 kDa)
B-4.
Caspase-8
(18 kDa)
B-5.
Caspase-9
(35 kDa)
C-9/Actin:(1 : 1 : 1 : 1 : 7 : 4)(X)
B-6.
β-Actin
(45 kDa)
1 2 3 4 5 6

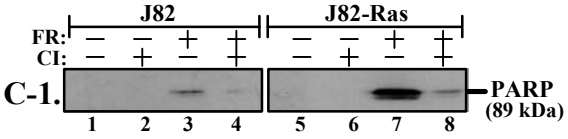
J82
J82-Ras
FR: – – + + – – + +
CI: – + – + – + – +
C-1.
PARP
(89 kDa)
1 2 3 4 5 6 7 8

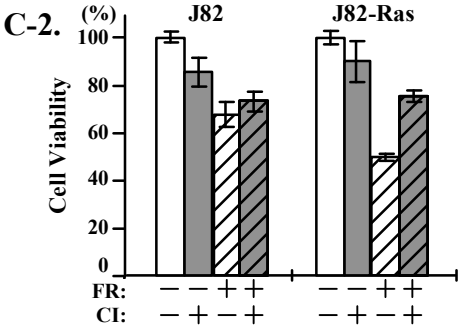
C-2.
(%)
J82
J82-Ras
Cell Viability
100
80
60
40
20
0
FR: – – + + – – + +
CI: – + – + – + – +

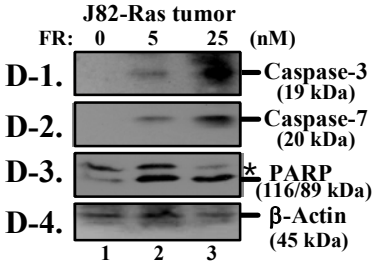
J82-Ras tumor
FR: 0 5 25 (nM)
D-1.
Caspase-3
(19 kDa)
D-2.
Caspase-7
(20 kDa)
D-3.
* PARP
(116/89 kDa)
D-4.
β-Actin
(45 kDa)
1 2 3

Figure 4. Regulation of CDK inhibitors, mutant p53, and histones in FR901228-treated cells. (A) J82 and J82-Ras cells were treated with 5 nM FR901228 for 24 h. Inhibition of cell growth by FR901228 was determined by the blockage of BrdU incorporation into cellular DNA. Quantification of BrdU-labeled cells was determined with an ELISA reader. Relative cell growth rate was normalized by the value of BrdU detected in untreated cells, set as 100%. Each value represents a mean of tetraplicates, and error bars represent standard deviation. **(B-1 to B-4 and C-1 to C-6)** J82 and J82-Ras cultures were treated with 5 nM FR901228 for 0 (lanes 1 and 4), 24 (lanes 2 and 5), and 48 (lanes 3 and 6) h. Western immunoblotting with specific antibodies was used to detect $p21^{Cip1}$, $p27^{Kip1}$, p53, and β-Actin in cell lysates (**B-1 to B-4**), and acetylated H2A, acetylated H2B, acetylated H3, acetylated H4, total H2B protein, and total H3 protein in nuclear lysates**(C-1 to C-6)**.

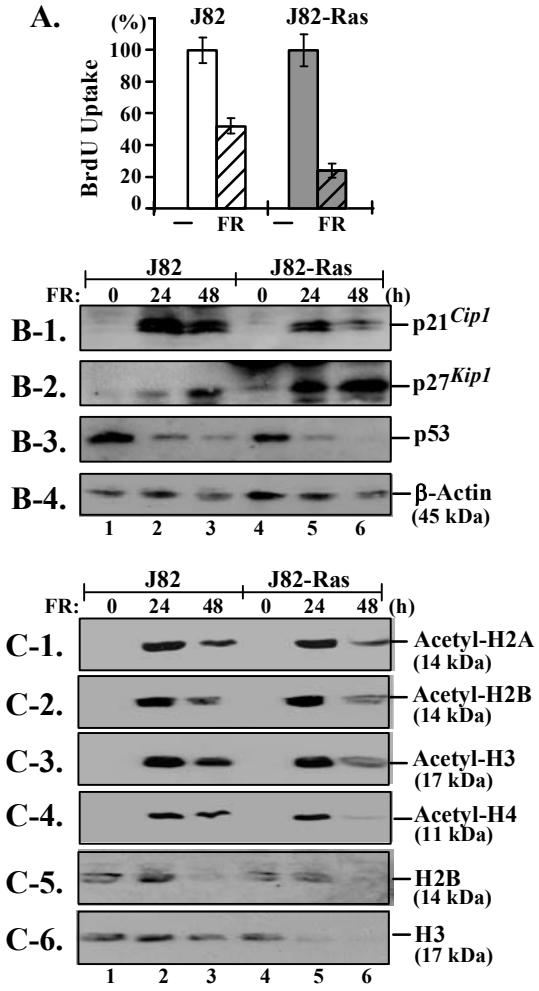
A.
(%)
J82
J82-Ras
BrdU Uptake
100
80
60
40
20
0
—
FR
—
FR
J82
J82-Ras
FR: 0 24 48 0 24 48 (h)
B-1.
p21Cip1
B-2.
p27Kip1
B-3.
p53
B-4.
β-Actin
(45 kDa)
1 2 3 4 5 6
J82
J82-Ras
FR: 0 24 48 0 24 48 (h)
C-1.
Acetyl-H2A
(14 kDa)
C-2.
Acetyl-H2B
(14 kDa)
C-3.
Acetyl-H3
(17 kDa)
C-4.
Acetyl-H4
(11 kDa)
C-5.
H2B
(14 kDa)
C-6.
H3
(17 kDa)
1 2 3 4 5 6

Figure 5. Roles of the ERK, PI3-K, p38/SAPK, and JNK/SAPK pathways in FR901228-induced apoptosis. (A-1, C-1, C-2, and C-3) J82 and J82-Ras cultures were treated with 5 nM FR901228 in the presence and absence of 20 μM U0126 (U0), 1 μM LY294002 (LY), 1 μM SB203580 (SB), or 30 μM SP600125 for 36 h. Quantification of cell viability in these cultures was determined with an MTT assay kit. Relative cell viability was normalized by the value determined in untreated cells, set as 100%. Each value represents a mean of tetraplicates, and error bars represent standard deviation. The Student's *t*-test was used to analyze statistical significance of ***b*** versus ***a*** ($p < 0.01$), ***d*** versus ***c*** ($p < 0.01$), and ***f*** versus ***e*** ($p < 0.01$). **(A-2 to A-11, and B-1 to B-7)** J82 and J82-Ras cultures were treated with 5 nM FR901228 for 0 (lanes 1 and 4), 24 (lanes 2 and 5), and 48 (lanes 3 and 6) h. Cell lysates were analyzed with Western immunoblotting using specific antibodies to detect levels of H-Ras, phosphorylated B-Raf (p-B-Raf), total B-Raf protein, phosphorylated Raf-1 (p-Raf-1), total Raf-1 protein, phosphorylated Mek1/2 (p-Mek1/2), total Mek1/2 proteins, phosphorylated Erk1/2 (p-Erk1/2), total Erk1/2 proteins, β-Actin**,** phosphorylated Akt (p-Akt), total Akt protein**,** phosphorylated p38 (p-p38), total p38 protein, phosphorylated JNK (p-JNK), total JNK protein, and β-Actin. Levels of p-B-Raf, B-Raf, p-Raf-1, Raf-1, and β-Actin were quantified by densitometry. The relative levels of specific phosphorylation of B-Raf (p/B-Raf) and Raf-1 (p/Raf-1) were calculated by normalizing the levels of p-B-Raf (A-3) and p-Raf-1 (A-5) with the levels of their cognate proteins (A-4 and A-6), and then were normalized by the level in parental J82 cells (lane 1), set as 1 (X, arbitrary unit). The relative protein levels of B-Raf (B-Raf/Actin) and Raf-1 (Raf-1/Actin) were calculated by normalizing the levels of B-Raf (A-4) and Raf-1 (A-6) with the levels of β-Actin

(A-11), and then were normalized by the level in untreated J82 cells (lane 1) and J82-Ras (lane 4), set as 1 (X, arbitrary unit).

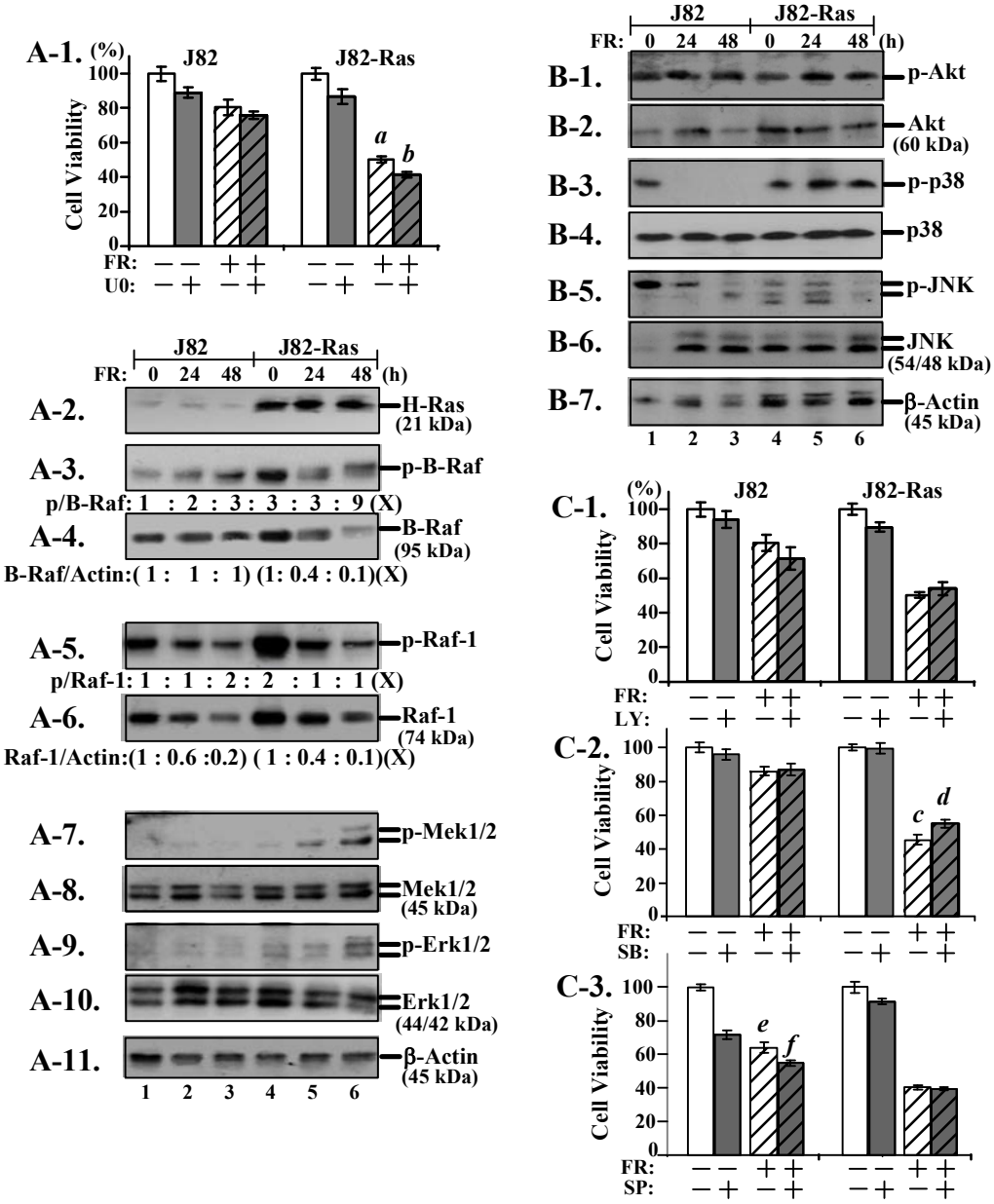

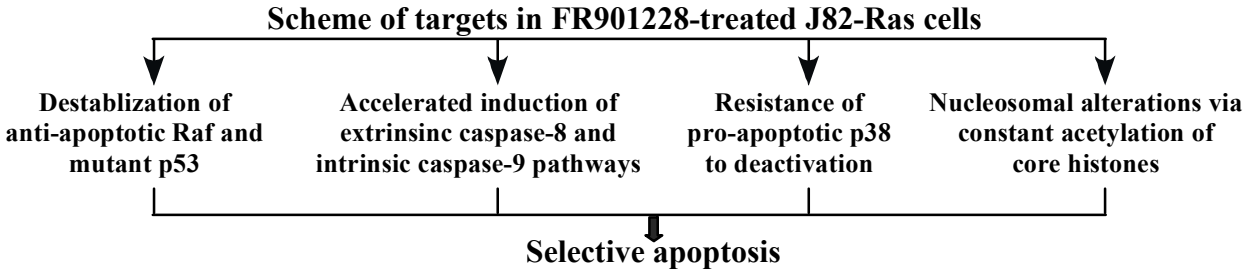

Figure 6. Proposed targets by FR901228 to induce selective apoptosis of H-Ras–expressed cells.

PART –III

PRO-APOPTOTIC ACTIVITY OF ONCOGENIC H-RAS FOR HISTONE DEACETYLASE INHIBITOR TO INDUCE APOPTOSIS OF HUMAN CANCER HT29 CELLS

This chapter is a slight modification of the research paper published in 2007 in Journal of Cancer Research and Clinical Oncology by Shambhunath Choudhary and Hwa-Chain Robert Wang.

Choudhary S, Wang HCR. Pro-apoptotic activity of oncogenic H-Ras for histone deacetylase inhibitor to induce apoptosis of human cancer HT29 cells. J Cancer Res Clin Oncol 2007;133:725-39.

In this paper "our" and "we" refers to me and co-authors. My contribution in the paper includes (1)Selection of the topic (2) Compiling and interpretation of the literature (3) Designing experiments (4)understanding the literature and interpretation of the results (5) providing comprehensive structure to the paper (6) Preparation of the graphs and figures (7) Writing and editing

Abstract

Purpose To verify the pro-apoptotic activity of oncogenic H-Ras in the increased susceptibility of human cancer cells to histone deacetylase inhibitor (HDACI).

Methods The pro-apoptotic activity of oncogenic H-Ras(V12) was verified by its ability to increase susceptibility of human colorectal adenocarcinoma HT29 cells to HDACI for inducing apoptosis and growth inhibition, assayed by various methods. The mode of action of HDACI FR901228 was studied by its ability to modulate protein phosphorylation, acetylation, and expression levels in various signaling pathways, measured by Western blot analysis.

Results Activation of caspase-3, -7, and -8, and serine protease by FR901228 was facilitated by oncogenic H-Ras to induce apoptosis. Expression of H-Ras(V12) changed the intrinsic

modulation of Raf in cells responding to FR901228 treatment. Both $p21^{Cip1}$ and $p27^{Kip1}$ were induced in FR901228-treated cells arrested in either the G0/G1 or G2/M phase of the cell cycle. Deacetylation of FR901228-induced acetylation of core histones was accelerated by H-Ras(V12) in cells undergoing apoptosis.

Conclusion Expression of H-Ras(V12) increased susceptibility of HT29 cells to HDACI FR901228 and Trichostatin A for inducing apoptosis. The pro-apoptotic activity of H-Ras(V12) responding to HDACI indicates a potential value of this new class of anticancer agents in treating Ras-related human cancers.

Keywords: Pro-apoptosis, Ras, HDACI, Depsipeptide, Signaling pathway

Introduction

Evidence has shown pro-apoptotic activity of oncogenic H-Ras in the increased cell susceptibility to anticancer agents, including 5-fluorouracil (1), etoposide VP16 (2), cisplatin (3), lovastatin (4) and arsenic (5). We have shown the pro-apoptotic activity of oncogenic H-Ras(V12) that allows HDACI FR901228 to induce selective apoptosis of mouse embryo fibroblast 10T1/2 cells (6, 7,8). However, the pro-apoptotic ability of H-Ras(V12) to increase the susceptibility of human cells to HDACI for inducing apoptosis has not yet been studied. It is important to verify the pro-apoptotic activity of oncogenic H-Ras in human cells that allows HDACI to induce selective cell death; the result will indicate if a potential value of HDACI can be recognized for treating human cancers related to Ras activation.

Oncogenic Ras is widely involved in human cancers (9). Expression of oncogenic Ras proteins results in cellular transformation and promotes tumorigenesis accompanied by an aberrantly regulated, complex signaling circuitry, including constant activation of the extracellular signal regulatory kinase (ERK) and phosphatidylinositol 3-kinase (PI3-K) pathways (10,11). Constant activation of the ERK pathway (which consists of Raf, Mek, and Erk) and the PI3-K pathway (which consists of PI3-K, PDK, and Akt) contributes to cellular transformation and suppression of apoptosis (10). In addition, expression of oncogenic H-Ras(V12) induces CBP/p300 degradation in NIH3T3 cells (12). The CBP and p300 co-activators exhibit both histone and non-histone protein acetylase activities (13). Thus, constant activation of Ras proteins not only result in significant changes in protein phosphorylation but also in protein acetylation. We have shown that FR901228 induces apoptosis in H-Ras(V12)-transformed 10T1/2 cells, whereas it induces growth arrest of non-transformed counterpart cells in the G0/G1

phase of the cell cycle (6,8). Thus, FR901228 exhibits a selectivity to induce apoptosis of Ras-transformed 10T1/2 cells. FR901228, also named FK228, (NSC-630176), is a bicyclic depsipeptide isolated from cultures of *Chromobacterium violaceum* (14-17). FR901228 is a pro-drug and has a stable molecular hydrophobic structure that facilitates its entry through cell membrane into cells. Its internal disulfide bond can be reduced by intracellular glutathione to form two free sulfhydryl groups that are active to chelate the zinc in the HDAC active site (18). Increased intracellular glutathione is associated with multidrug resistance; therefore, FR901228 is potentially effective for treating tumor cells with glutathione-mediated drug resistance. HDACI contains a structurally diverse group of molecules that include hydroxamates such as Trichostatin A (TSA), aliphatic acids such as phenyl butyrate, benzamides such as MS-275, and electrophilic ketones such as trifluoromethyl ketones in addition to depsipeptides (19). Growing evidence indicates transformed cells are much more sensitive than normal cells to the growth-inhibitory and apoptotic effects of HDACI (19-21). Hence, it is important to understand if expression of oncogenic H-Ras in human cancer cells will increase susceptibility to HDACI for inducing cell death.

We have shown that caspase-3 plays an important role in FR901228-induced selective apoptosis of Ras-transformed 10T1/2 cells (6-8). FR901228 also induces p21^{Cip1} expression in non-transformed 10T1/2 cells growth-arrested by FR901228 in the G0/G1 phase of the cell cycle, but it reduces p21^{Cip1} levels in Ras-transformed 10T1/2 cells undergoing FR901228-induced apoptosis (6). Raf-1 is particularly reduced in Ras-transformed 10T1/2 cultures undergoing FR901228-induced apoptosis (6). Interestingly, we detected that the ERK pathway plays an anti-apoptotic role in parental 10T1/2 cells, but it plays a pro-apoptotic role in

FR901228-induced apoptosis of H-Ras(V12)-expressed 10T1/2 cells (8). The PI3-K pathway plays an anti-apoptotic role in both H-Ras(V12)-expressed and parental 10T1/2 cells (8). However, the question of whether oncogenic-H-Ras may exhibit pro-apoptotic activity that will allow FR901228 to induce selective apoptosis of human cancer cells remains unanswered. Concomitantly, the roles of the ERK and PI3-K pathways as well as caspase and Cdk inhibitors in human cells also need to be verified for delineating signaling pathways involved in FR901228-induced apoptosis and growth arrest.

In this communication, we present new evidence that expression of H-Ras(V12) resulted in increased susceptibility of human cancer HT29 cells to both HDACI FR901228- and TSA-induced apoptosis. The HT29 human colorectal adenocarcinoma cell line hosts wild-type *ras*, active mutant B-*raf*, wild-type *raf-1*, and the inactive mutant *p53* genes (22). Accordingly, the ERK signaling pathway, including Mek and Erk, downstream from active B-Raf is activated. Therefore, expression of H-Ras(V12) in HT29 cells was expected to reveal activities other than the induction of the ERK pathway to facilitate or attenuate FR901228-induced apoptosis. Surprisingly, expression of H-Ras(V12) in HT29 cells did not protect the activated ERK pathway from suppression by FR901228 treatment. FR901228 treatment differentially modulated Raf-1 phosphorylation in H-Ras(V12)-expressed cells from its counterpart in parental HT29 cells. Expression of H-Ras(V12) facilitated the induction of the apoptotic pathway by FR901228. Regarding the regulation of signaling pathways associated with cell growth, survival, growth arrest, and apoptosis, our studies revealed both commonalities and discrepancies between H-Ras(V12)-expressed cells and parental HT29 cells that may contribute to the pro-apoptotic activity of H-Ras(V12) that allows FR901228 to selectively induce apoptosis.

Materials and methods

Cell cultures, transfection, and reagents

HT29 (ATCC, Rockville, MD) and its derived cell lines, a human colon adenocarcinoma cell line SW480 (obtained through a collaboration with Dr S. Baek at The University of Tennessee), as well as a human urinary bladder cancer J82 cell line (ATCC) were maintained in Dulbecco's modified Eagle medium (DMEM) supplemented with 10% fetal bovine serum, 100 U/ml penicillin, and 100 μg/ml streptomycin. 10T1/2-TR-H-*ras* cells were maintained in Basal Medium Eagle medium supplemented with 10% fetal bovine serum, 100 U/ml penicillin, and 100 μg/ml streptomycin (6-8,23). These cultures were incubated at 37°C and routinely subcultured every 2 to 3 days. To generate H-Ras(V12)-expressed HT29 cells, cells in a 35 mm culture dish were transfected with 0.5 μg of pcDNA4/TO-E-H-*ras* plasmid DNA, which carries the H-Ras(V12) gene (23), using PolyFect Transfection Reagent (Qiagen, Valencia, CA). After 48 h of transfection, cells were subcultured and selected in 100 μg/ml Zeocin (Invitrogen, Carlsbad, CA). Resistant cell clones were established to HT29-Ras cell lines. Stock aqueous solutions of FR901228 (obtained through a collaboration with Dr. KK Chan at the Ohio State University), TSA (ICN, Aurora, OH), U0126 (Cell Signaling, Beverly, MA), and Ac-Asp-Glu-Val-Asp-CHO (Ac-DEVD-CHO) (Alexis, San Diego, CA) were prepared in DMSO and diluted in culture medium for assays. The 4-(2-Aminoethyl)benzenesulfonylfluoride-HCl (AEBSF-HCl) (Acros, Fair Lawn, NJ) was prepared in H_2O and diluted in the culture medium for assays. Recombinant human TRAIL/Apo2L, FasL, and TNF-α (PeproTech, Rocky Hill, NJ) were prepared in distilled water and diluted in culture medium for assays.

Cell growth and survival Assay

Cells were seeded in 12-well culture plates. Every 24 h after treatments with FR901228 and TSA, cells were trypsinized, washed, and then resuspended in culture medium containing 0.2% trypan blue for 2 min to stain dead cells. Live cells were counted in a hemocytometer to determine relative cell growth and survival rate (6,7).

Cell proliferation inhibition assay

Inhibition of cell proliferation was determined by the inhibition of 5-bromo-2'-deoxyuridine (BrdU) incorporation into cellular DNA (7), using the BrdU cell proliferation ELISA kit (Roche, Indianapolis, IN). Five x 10^4 cells were seeded into each well of 96-well culture plates for 24 h. After treatment with FR901228, cells were labeled with BrdU for 12 h, fixed, incubated with peroxidase-conjugated BrdU-specific antibodies, and stained with peroxidase substrate. Quantification of BrdU-labeled cells was determined with an ELISA reader (Bio-Tek, Winooski, VT).

Apoptotic-like cell death assay

Apoptotic-like cell death in cultures was quantified using a Cell Death Detection ELISA kit (Roche, Indianapolis, IN) (8). After FR901228 treatments, cell lysates were incubated with anti-histone antibodies. Fragmented DNA in the complexes of nucleosomes with histone was detected with peroxidase-conjugated anti-DNA antibody and stained with peroxidase substrate 2,2'-azino-bis-(3-ethylbenzthiazoline-6-sulfonic acid). Quantification of cell death was determined with an ELISA reader.

Cell viability assay

A Methyl Thiazolyl Tetrazolium (MTT) assay kit (ATCC, Manassas, VA) was used to measure cell survivability in cultures. Five x 10^4 cells were seeded into each well of 96-well culture plates for 24 h. After treatments with HDACI and inhibitors to caspases, serine protease, or kinases, cells were incubated with MTT Reagent for 4 h, followed by incubation with Detergent Reagent for 24 h. Reduced MTT reagent in cultures was quantified with an ELISA reader.

Flow cytometric analysis of cell growth arrest and cell death

Cells were trypsinized from cultures, rinsed with Ca^{++} and Mg^{++} free phosphate buffered saline, fixed in ethanol, and stained with propidium iodide (6,8,23). Subsequently, flow cytometric analysis was performed on the Coulter EPICS Elite Cytometer (Hialeah, FL) by using a 15 milliwatt air-cooled argon laser to produce 488 nm light. Fluorescent light emission was collected with a 610LPDC filter. Analysis of DNA content and determination of the percentage of cells in each phase of the cell cycle were performed on Multicycle software (Phoenix Flow System, San Diego, CA).

An Annexin-V-FITC Apoptosis Detection Kit with propidium iodide (BD Biosciences, San Jose, CA) was also used to detect cell death by flow cytometry. In brief, FR901228-treated cells were trypsinized from cultures, rinsed with phosphate buffered saline, and stained with annexin-V-FITC and propidium iodide. Flow cytometric analysis was performed on the Coulter EPICS Elite Cytometer (Hialeah, FL). FITC and propidium iodide fluorescent light emission were collected with 550 nm and 645 nm band pass filters, respectively, and analyzed using

Multicycle software (Phoenix Flow System, San Diego, CA).

Western immunoblotting

To prepare cell lysates containing Ras, Rap1, Akt, B-Raf, Raf-1, Mek1/2, Erk1/2, Fas, FasL, caspase-3, caspase-7, caspase-8, poly (ADP-ribose) polymerase (PARP), Bad, p53, $p21^{Cip1}$, $p27^{Kip1}$, and β-Actin, cells were lysed in a buffer (10 mM Tris-HCl, 150 mM NaCl, 1% Triton X-100, 5 mM EDTA, 10 mM sodium pyrophosphate, 10% glycerol, 0.1% Na_3VO_4, 50 mM NaF, pH 7.4) (6). Cell lysates (S20) were isolated from the supernatants after centrifugation of crude lysates at 20,000 x g for 20 min. To prepare cell lysates containing nuclear core histones, cells were lysed in a hypotonic buffer (10 mM KH_2PO_4, 1 mM EDTA, 5 mM EGTA, 10 mM $MgCl_2$, 50 mM β-glycerolphosphate, 1 mM Na_3VO_4, 2 mM dithiothreitol, pH 7.2) with 30 strokes of a tight-fitting Dounce homogenizer. After centrifugation of crude lysates at 10,000 x g for 10 min, cell pellets (P10) containing nuclear histones were resuspended in lysis buffer and sonicated for 10 min as nuclear lysates. Protein concentrations in cell lysates (S20) and nuclear lysates (P10) were measured using the BCA assay (Pierce, Rockford, IL). Equal amounts of cellular proteins were resolved by electrophoresis in either 10% or 14% SDS-polyacrylamide gels and transferred to nitrocellulose filters for Western immunoblotting, as previously described (6,7,8). Antibodies specific to Akt, Raf-1, Mek1/2, Bad, acetylated H2B on Lys12, H2B protein, acetylated H3 on Lys9, H3 protein, active caspase-3, active caspase-7, active caspase-8, PARP, and β-Actin; and specific antibodies to phosphorylated forms of Akt, Raf-1, B-Raf, Mek1/2, Erk1/2, and Bad (Ser112) were purchased from Cell Signaling Technology (Beverly, MA). Specific antibodies to H-Ras, Rap1, B-Raf, Erk1/2, Fas, FasL, p53, $p27^{Kip1}$, and $p21^{Cip1}$ were

purchased from Santa Cruz Biotechnology (Santa Cruz, CA). Antigen-antibody complexes on filters were detected by the SuperSignal chemiluminescence kit (Pierce, Rockford, IL).

Statistical analysis

Statistical significance was analyzed by the Student's *t*-test. A p-value ≤ 0.05 was considered significant.

Results

Increased susceptibility of HT29 cells to FR901228 by oncogenic H-Ras

To determine whether expression of oncogenic H-Ras in human cancer cells may facilitate FR901228-induced apoptosis, HT29 cells were stably transfected with the expression plasmid vector pcDNA4/TO-E-H-*ras,* which carries the oncogenic H-*ras(V12)* gene (23). Two H-*ras(V12)*-transfected HT29 cell lines, HT29-Ras-1 and -2, were established based on their distinct H-Ras expression levels (Fig. 1a). H-Ras protein was expressed by approximately 4- and 9-fold in HT29-Ras-1 and HT29-Ras-2 cells, respectively, as compared to its endogenous counterpart protein in parental HT29 cells. Expression of H-Ras(V12) did not result in any noticeable difference in cell growth rate (Fig. 1b, HT29-Ras-1 and HT29-Ras-2, 0 nM control lines) or visible difference in cell morphology (data not shown) compared to parental HT29 cells. To detect any change in susceptibility of HT29-Ras-1 and HT29-Ras-2 cells to FR901228 for inducing cell death, cultures were treated with FR901228 at various concentrations for 48 h. As

shown in Fig. 1b, treatment of parental HT29 and HT29-Ras-1 cells with 1 nM FR901228 resulted in growth inhibition in 24 h and 48 h. In contrast, treatment of HT29-Ras-2 cells with 1 nM FR901228 induced growth inhibition in 24 h and significant cell death in 48 h. Treatment with 5 nM FR901228 resulted in growth inhibition of all these cultures in 24 h, and it induced modest cell death in parental HT29 and HT29-Ras-1 cultures and profound cell death of HT29-Ras-2 cells by 48 h. Induction of cell death by FR901229 was in a dose- and time-dependent manner. FR901228 induced cell death of HT29-Ras-2 cells at a discriminating concentration of 1 nM, whereas this concentration mainly induced growth inhibition of parental HT29 and HT29-Ras-1 cells in 48 h. A threshold of oncogenic H-Ras expression appeared to be involved in the increased susceptibility of HT29 cells to FR901228 for inducing cell death.

Flow cytometric analysis of apoptosis and cell growth arrest by FR901228

To further analyze FR901228-induced growth inhibition and cell death, we used flow cytometry to detect populations of cells undergoing apoptosis and growth arrest in the cultures of HT29 and HT29-Ras-2 cells. As indicated in Table 1, treatment with FR901228 at 1 nM for 48 h induced a modest population of apoptotic cells in parental HT29 cultures (increased from <1% to 4%), in contrast to a significantly increased population of apoptotic cells in HT29-Ras-2 cultures (increased from <1% to 20%). We also used an Annexin-V-FITC Apoptosis Detection Kit with propidium iodide (BD Biosciences, San Jose, CA) to detect phosphatidylserine externalization in cell population undergoing cell death by flow cytometry. As shown in Fig. 1c, FR901228 treatment resulted in higher populations of cells that were undergoing cell death (3% and 9.3%) and apoptotic cells (7% and 29%) in HT29-Ras cultures than their counterpart cell population in

parental HT29 cultures (1.8 and 3%; 2% and 8%) by 24 and 36 h. Cell population in HT29-Ras-2 cultures was induced by FR901228 to increasingly undergo apoptosis to a higher level than the apoptotic cell level induced in parental HT29 cultures. Apparently, expression of H-Ras(V12) in HT29 cells facilitated the induction of apoptosis by FR901228.

Analysis of the live cell population throughout the cell cycle showed an increased population in the G0/G1 phase and a substantially reduced population in the S phase in cultures of parental HT29 cells after FR901228 treatment for 24 h (Table 1). In contrast, FR901228 treatment of HT29-Ras-2 cells resulted in a substantially reduced population in the S phase and an increased cell population in the G2/M phase. Thus, expression of H-Ras(V12) in HT29 cells appeared to change their susceptibility to FR901228 for growth arrest from the G0/G1 to G2/M phase of the cell cycle.

Apoptotic pathways induced by FR901228

To further verify that the FR901228 induced apoptosis of HT29 cells, we measured the level of fragmented DNA in the complexes of nucleosomes with histones induced by FR901228 in cultures of HT29 and HT29-Ras-2 cells. As shown in Fig. 2a, the FR901228-induced apoptotic DNA fragmentation was profoundly higher in HT29-Ras-2 cultures than in parental HT29 cultures. Studying the involved caspases in the FR901228-induced apoptosis, we detected that higher levels of active caspase-3 were induced in HT29-Ras-2 cells (Fig. 2b, lanes 5 and 6) than in parental counterpart HT29 cells (lanes 2 and 3) by 48 h in a dose-dependent manner. In addition, higher levels of active caspase-3 (Fig. 2c-1), active caspase-7 (Fig. 2c-2), and proteolytically modified, downstream substrate PARP (Fig. 2c-3), were induced in HT29-Ras-2

cells (lanes 5 and 6) than in parental HT29 cells (lanes 2 and 3) in a time-dependent manner. To determine the upstream caspases, which may contribute to the activation of caspase-3 and caspse-7, we detected that active caspase-8 was induced to higher levels in HT29-Ras-2 cells (Fig. 2c-4, lanes 5 and 6) than in parental HT29 cells (lanes 2 and 3). However, we did not detect any differential induction of caspase-9 in these cells (data not shown). Accordingly, the caspase-8 to caspase-3 and -7 pathway was induced by FR901228 treatment in HT29 cells. Induction of caspase-3, caspase-7, and caspase-8 activation by FR901228 was enhanced by expression of H-Ras(V12) in HT29 cells.

To determine the role of caspase-3 and -7 activation in FR901228-induced cell death, HT29 and HT29-Ras-2 cells were pre-treated with the potent caspase-3 and -7 inhibitor, Ac-DEVD-CHO (8,24), followed by FR901228 treatment for 48 h. As shown in Fig. 2d, treatment of cells with Ac-DEVD-CHO alone resulted in a modest reduction of cell viability in both HT29 and HT29-Ras-2 cultures. A modest reduction of cell viability was also detected in parental HT29 cultures treated with FR901228 alone, and the Ac-DEVD-CHO pretreatment did not result in a significant reversal of the FR901228-reduced cell viability. In contrast, FR901228 treatment resulted in a profound reduction of cell viability in HT29-Ras-2 cultures, and the Ac-DEVD-CHO pretreatment attenuated the FR901228-reduced cell viability. Accordingly, the role of caspase-3 and -7 activation was evident in oncogenic Ras-expressed HT29 cells undergoing FR901228-induced apoptosis, but was not clear in parental HT29 cells under FR901228 treatment.

To investigate other proteases involved in FR901228-induced cell death, we pre-treated cells with AEBSF-HCl (24), a serine protease inhibitor. Treatment with AEBSF-HCl alone

induced a modest reduction of cell viability in both HT29 and HT29-Ras-2 cultures (Fig. 2d). Pre-treatment with AEBSF-HCl did not reverse FR901228-reduced cell viability in parental HT29 cultures, but it alleviated FR901228-reduced cell viability in HT29-Ras-2 cultures. Again, the role of serine protease activation was evident in H-Ras(V12)-expressed HT29 cells undergoing FR901228-induced apoptosis, but was not clear in parental HT29 cells under FR901228 treatment. These results taken together indicate that caspase-3, caspase-7, and serine protease(s) were differentially induced by FR901228 to play roles in inducing apoptosis of HT29-Ras-2 cells.

To pursue the involvement of death receptor family in FR901228-induced differential cell death of HT29-Ras-2 cells, we studied the activity of TRAIL and FasL, and TNFα in FR901228-induced cell death. As shown in Fig. 3a, 3b, and 3c**,** expression of oncogenic H-Ras(V12) increased cell susceptibility to TRAIL and FasL, but not TNFα, for inducing cell death. Co-treatment with either TRAIL or FasL profoundly enhanced FR901228-induced cell death of both HT29 and HT29-Ras-2 cells, regardless of H-Ras(V12) expression (Fig. 3a and 3b). Although expression o f H-Ras(V12) did not increase cell susceptibility to TNFα, co-treatment with TNFα also enhanced FR901228-induced cell death modestly in HT29 cells and significantly in HT29-Ras-2 cell (Fig. 3c). Accordingly, these results indicate that H-Ras(V12) expression played a role in differentially potentiating TRAIL and FasL pathways in cells for FR901228-induced cell death; therefore, activation of the death receptor family pathways by their ligands predominantly promoted the ability of FR901228 to induce cell death. We also detected that the expression levels of FasL and Fas were differentially increased by FR901228 treatment in HT29 and HT29-Ras-2 cells. As shown in Fig. 3d-1, Fas expression was induced by

FR901228 to a higher level in HT29-Ras-2 cells by 24 h (lane 5) than in HT29 cells (lane 2). FR901228-induced expression of FasL was maintained to a higher level in HT29-Ras-2 cells by 48 h (Fig. 3d-2, lane 5) than in HT29 cells (lane 2). These results indicate that H-Ras(V12) expression played a role in differentially potentiating both FasL and Fas for FR901228-induced expression.

Induction of Cdk inhibitors in cell growth arrest by FR901228

To investigate FR901228-induced cell growth inhibition, we verified the ability of FR901228 to inhibit cell proliferation by detecting the inhibition of BrdU uptake into cells. As shown in Fig. 4a, cell proliferation in both parental HT29 and HT29-Ras-2 cultures was suppressed by FR901228 treatment in 24 h. To pursue the involvement of Cdk inhibitors in FR901228-induced cell growth inhibition, we detected the induction of p21^{Cip1} and p27^{Kip1} in FR901228-treated cells. As shown in Fig. 4b, p21^{Cip1} expression was induced by FR901228 in HT29 (lanes 2 and 3) and HT29-Ras-2 (lanes 5 and 6) cultures. The level of p21^{Cip1} was induced in growth-inhibited HT29 cells by FR901228 in 24 h (lane 2) and unchanged by 48 h (lane 3). The level of p21^{Cip1} was induced in HT29-Ras-2 cells by FR901228 in 24 h (lane 5), but reduced by 48 h (lane 6) when cells underwent significant apoptosis. The mutant p53 was also reduced in HT29 (Fig. 4c, lane 3) and HT29-Ras-2 (lane 6) cells after FR901228 treatment for 48 h. Interestingly, another Cdk inhibitor, p27^{Kip1}, was not induced until 48 h after FR901228 treatment of HT29 (Fig. 4d, lane 3) and HT29-Ras-2 (lane 6) cells. It appeared that p21^{Cip1} expression was correlated with an early growth arrest, and p27^{Kip1} expression was correlated with either a complete growth arrest or induction of apoptosis by FR901228 in both HT29 and HT29-Ras-2

cells.

Target in the ERK pathway by FR901228

To investigate the role the ERK pathway may play in HT29 and HT29-Ras-2 cells undergoing FR901228 treatment, we used kinase inhibitor U0126 to specifically suppress Mek1/2 activity (7,8,26). As shown in Fig. 5a, treatments with U0126 alone for 48 h modestly reduced cell viability in cultures of HT29 and HT29-Ras-2. However, U0126 treatment significantly decreased the FR901228-reduced viability of parental HT29 cells. The significantly reduced cell viability by FR901228 in HT29-Ras-2 cultures was additionally decreased by U0126 treatment. Thus, the ERK pathway played a survival role in both HT29 and HT29-Ras-2 cells responding to the FR901228 treatment.

To detect if the ERK pathway was targeted by FR901228 to reduce cell viability, we studied FR901228-induced effects on activation-related phosphorylation and protein levels of ERK pathway kinases B-Raf, Raf-1, Mek1/2, and Erk1/2. Equal amounts of cellular proteins isolated from treated and control cultures were analyzed by Western immunoblotting with specific antibodies. We detected that the overall phosphorylation level of B-Raf was elevated in HT29-Ras-2 cells (Fig, 5b-1, lane 4), compared to its counterpart kinase in parental HT29 cells (lane 1). FR901228 treatment reduced the overall phosphorylation and cognate protein levels of B-Raf in HT29-Ras-2 cells (Fig, 5b-1, 5b-2, lanes 5 and 6) in contrast to the unchanged counterpart levels in parental HT29 cells (lanes 2 and 3). Based on the cognate protein level of B-Raf, the specific phosphorylation level of B-Raf (p/B-Raf) was elevated in HT29-Ras-2 cells (approximately 2-fold), compared to its counterpart in parental HT29 cells. FR901228 treatment

reversed the increased, specific phosphorylation level of B-Raf in HT29-Ras-2 cells to a level maintained in parental HT29 cells.

Expression of H-Ras(V12) modestly elevated the overall activation-related phosphorylation level and protein level of Raf-1 in HT29 cells (Fig, 5c-1, 5c-2, lane 4 versus lane 1); accordingly, its specific phosphorylation was unchanged. FR901228 treatment resulted in a profound reduction of the protein level of Raf-1 in both HT29 and HT29-Ras-2 cells (Fig, 5c-2, lanes 2, 3, 5, and 6); however, the overall phosphorylation level of Raf-1 was not accordingly reduced in either parental HT29 or HT29-Ras-2 cells (Fig, 5c-1). Adjusted with β-Actin levels (Fig. 5d), we detected that Raf-1 protein was reduced by FR901228 to lower levels in parental HT29 cells (Raf-1/Actin, reduced from 1X to 0.3 and 0.1X) (Fig. 5c-2, lanes 2 and 3) than in HT29-Ras-2 cells (reduced from 2.9 X to 0.8 and 0.4 X) (lanes 5 and 6), but the reduction rate of Raf-1 protein in HT29 cells was similar to the rate in HT29-Ras-2 cells (approximately reduced 1X to 0.3 and 0.1X). Based on the cognate protein levels of Raf-1, the specific phosphorylation level of Raf-1 (p/Raf-1) was highly elevated to approximately 13-fold (Fig, 5c-1 and 4c-2, lane 3) in parental HT29 cells, but only elevated approximately 2-fold in HT29-Ras-2 cells (lane 6). It appeared that an intrinsic mechanism was involved in increasing the specific phosphorylation of Raf-1 in order to maintain the overall level of activation/phosphorylation in both HT29 and HT29-Ras-2 cells in response to FR901228-reduced Raf-1 protein. Raf-1 protein was a target in FR901228-treated cells. It has been suggested that FR901228-induced upregulation of Rap1 plays a role in suppression of the Ras-Raf-Erk kinase signaling pathway (27). We also detected increased expression of Rap1 induced by FR901228 in both HT29 and HT29-Ras-2 cells, and a higher level of Rap1 was induced by FR901228 in HT29 cells (Fig. 5e,

lanes 2 and 3)than in HT29-Ras-2 cells (lanes 5 and 6). The increased levels of Rap1 may play a role in regulating Raf-1 and B-Raf in both HT29 and HT29-Ras-2 cells.

HT29 cells host the active mutant B-*raf* gene (22). The downstream kinases Mek1/2 and Erk1/2 were highly phosphorylated/activated in HT29 cells (Fig, 5f-1, 5g-1, lane 1), compared to their counterpart kinases in human urinary bladder carcinoma J82 cells in which the ERK pathway is not constitutively active (lane 7). FR901228 treatment reduced the activation-related phosphorylation of both Mek1/2 and Erk1/2 in both HT29 (Fig, 5f-1, 5g-1, lanes 2 and 3) and HT29-Ras-2 (lanes 5 and 6) cells. Protein levels of Mek1/2 and Erk1/2 were not significantly changed by FR901228 treatment in either HT29 or HT29-Ras-2 cells (Fig, 5f-2, 5g-2). Reduced phosphorylation of Mek1/2 and Erk1/2 appeared to correlate with the reduced Raf-1 protein, regardless of the maintained overall phosphorylation of Raf-1 in FR901228-treated cells.

While investigating the role the PI3-K pathway plays in FR901228-induced apoptosis of HT29 and HT29-Ras-2 cells, we observed that protein phosphorylation of Akt was not detectable in HT29 and HT29-Ras-2 cells (Fig. 5h-1, lanes 1 to 6), as compared to its counterpart kinase in J82 cells (lane 7). Expression of H-Ras(V12) in HT29 cells failed to conventionally activate the PI3-K pathway (lane 4). Although the PI3-K pathway is a known downstream pathway of Ras (10), the dissociation of the PI3-K pathway from Ras in HT29 cells remains to be clarified. To clarify a target role the PI3-K pathway may play in HT29 and HT29-Ras-2 cells treated with FR901228, we used kinase inhibitor LY294002 to specifically suppress PI3-K activity (20, 28). We detected that LY294002 treatment did not enhance or decrease any FR901228-reduced cell viability in either HT29 or HT29-Ras-2 cultures (data not shown). Thus, the PI3-K pathway was unlikely to play any target role for FR901228 in the induction of apoptosis in either HT29 or

HT29-Ras-2 cells.

To further investigate the effect of the suppressed ERK pathway on the cross-talk to apoptotic pathway, we investigated regulation of Bcl-2 family members in FR901228-treated cells. We detected that the overall phosphorylation level of Bad on Ser112 was lower in HT29-Ras-2 cells (Fig. 5i-1, lane 4) than in parental HT29 cells (lane 1). FR901228 treatment increased the overall phosphorylation of Bad in both parental (Fig. 5i-1, lanes 2 and 3) and HT29-Ras-2 (lanes 5 and 6) cells, but the induced overall phosphorylation levels were noticeably lower in HT29-Ras-2 cells than in parental HT29 cells. Adjusted by their cognate protein levels (Fig. 5i-2), the specific phosphorylation of Bad was significantly lower in HT29-Ras-2 cells (p/Bad, lanes 4 to 6, approximately 0.5- to 0.9-fold) than its counterpart level in parental HT29 cells (lanes 1 to 3, 1- to 2.9-fold). Increased phosphorylation of Bad on Ser112 by Raf-1 has been reported to deactivate Bad (29-31). FR901228-increased phosphorylation of Bad is likely to be attributed to the increased specific phosphorylation/activation of Raf-1.

We also studied the role of JNK/SAPK and p38/SAPK in FR901228-induced cell death. Blockage of JNK and p38 by their specific inhibitors, SP600125 (32) and SB203580 (33), did not result in any detectable changes in FR901228-induced cell death (data not shown). Therefore, these SAPK pathways may not be involved in FR901228-induced cell death of HT29 and HT29-Ras-2 cells.

Acetylation of core histones induced by FR901228

While verifying the effect of FR901228 on modulating histone acetylation in equal amounts of nuclear proteins isolated from HT29 and HT29-Ras-2 cells, we detected that acetylation of core

histones H2B on Lys-12 (Fig. 6a-1) and H3 on Lys-9 (Fig. 6b-1) was substantially induced by FR901228 treatment in both HT29 (lane 2) and HT29-Ras-2 (lane 5) cells by 24 h. However, histone acetylation was reduced in cells treated with FR901228 for 48 h (lanes 3 and 6). Acetylated histones (Fig. 6a-1, 6b-1) and their cognate protein levels (Fig. 6a-2, 6b-2) were reduced by FR901228 treatment to lower levels in HT29-Ras-2 undergoing apoptosis (lane 6) than their counterparts in parental HT29 cells mainly undergoing growth arrest (lane 3). Reduction of H2B and H3 contents by extended FR901228 treatment appeared to be enhanced by expression of H-Ras(V12) in cells undergoing apoptosis.

Pro-apoptotic susceptibility of oncogenic Ras to HDACI

To further investigation of oncogenic Ras in cell susceptibility to HDACI, we included a human colon adenocarcinoma cell line SW480 that carries oncogenic K-*ras4B* gene and wild-type *raf* genes (34) in our studies. HT29, HT29-Ras-2, and SW480 cells were treated with FR901228 and a FR901228-unrelated HDACI, TSA, followed by determining cell viability in treated cultures. As shown in Fig. 7a, FR901228 treatment of HT29-Ras-2 cells at concentrations of 1, 5, and 25 nM and FR901228 treatment of SW480 cells at concentrations of 5 and 25 nM reduced viability to higher degrees than the reduced viability in counterpart HT29 cells. TSA treatment at concentrations of 25 and 100 nM reduced viability of both HT29-Ras-2 and SW480 cells to higher degrees than the reduced viability of parental counterpart HT29 cells (Fig. 7b). Apparently, the increased susceptibility to HDACI by oncogenic Ras in human colorectal adenocarcinoma cells is not cell line-limited and is also not limited to depsipeptide FR901228, but also includes TSA.

To verify that increased cell susceptibility to TSA by expression of oncogenic Ras is not limited to human colorectal adenocarcinoma cells, we tested whether TSA was able to selectively induce cell death in Ras-transformed 10T1/2 cells. 10T1/2-TR-H-*ras* cultures, in which ectopic expression of H-Ras(V12) is controlled by tetracycline (7, 8, 23), were treated with TSA at a discriminating concentration of 5 nM for 72 h in the absence and presence of tetracycline induction. As shown in Fig. 7c, TSA treatment of 10T1/2-TR-H-*ras* cultures, in which oncogenic Ras was not induced, resulted in reduction of the relative cell growth rate in 24 h and inhibition of cell growth by 72 h. In contrast, TSA treatment of 10T1/2-TR-H-*ras* cultures, in which expression of oncogenic Ras was induced by tetracycline, reduced the relative cell growth rate in 24 h, inhibited cell growth in 48 h, and induced cell death by 72 h. The selectivity of TSA to induce cell growth inhibition and cell death of Ras-expressed cells is not a cell type-specific event.

Discussion

Investigation of the pro-apoptotic activity of H-Ras(V12) in human cancer cells that allows HDACI to induce apoptosis provides cellular bases for developing therapeutic strategies to target Ras-related human cancers. Previously, we reported that expression of H-Ras(V12) in mouse 10T1/2 cells increases susceptibility to FR901228, but not the potent apoptosis inducer staurosporine (6-8). In contrast, expression of the oncogenic v-*src* gene in 10T1/2 cells showed no pro-apoptotic activity in FR901228-induced apoptosis (result not shown). In this report, we present evidence that expression of H-Ras(V12) in human cancer HT29 cells resulted in increased susceptibility to cell death induced after treatment with FR901228 and a structurally

unrelated HDACI, TSA. We also verified TSA's ability to selectively induce cell death of H-Ras(V12)-expressed 10T1/2 cells. In addition, expression of H-Ras(V12) in either HT29 or 10T1/2 cells did not result in increased cell susceptibility to other agents, including U0126, LY294002, Ac-DEVD-CHO, and AEBSF-HCl. Therefore, the pro-apoptotic activity of H-Ras(V12) that allows agents to induce cell death is an HDACI-specific, but is not a cell type-specific property. Although the selectivity of HDACI to induce cell death of H-Ras(V12)-expressed cells may not be applicable to other Ras-unrelated oncogene-expressed cells, it may be applicable to other Ras family, such as K-Ras, as evident with a high susceptibility of SW480 cell line, which hosts the oncogenic K-*ras* gene, to both FR901228 and TSA for inducing cell death.

Both an enhanced induction of caspase-3 and caspase-7 activation and an induced serine protease activity evidently play important roles in the increased cell susceptibility to FR901228 for inducing cell death of oncogenic-H-Ras-expressed cells. Previously, we reported that expression of H-Ras(V12) in mouse 10T1/2 cells not only increases procaspase-3 expression level, but also facilitates FR901228-induced activation of caspase-3 for inducing cell death (7). Although the procaspase-3 protein level was not noticeably increased by expression of H-Ras(V12) in HT29 cells, activation of caspase-3 by FR901228 was enhanced in HT29-Ras-2 cells for inducing apoptosis. In addition to caspase-3 and caspase-7 activation, serine protease activity was detected in HT29-Ras-2 cells, but not in parental HT29 cells, was also likely to play a role in the induction of apoptosis by FR901228. Thus, caspase-3, caspase-7, and serine protease were differentially induced by FR901228 in H-Ras(V12)-expressed HT29 cells to play roles in FR901228-induced selective apoptosis. Both the extrinsic caspase-8 and the intrinsic

caspase-9 initiator pathways have been postulated to activate the executioner caspase-3 and caspase-7 (35). Studies have shown that FR901228 treatment induces a Fas pathway-dependent activation of caspase-8 and caspase-3 in human osteosarcoma and leukemia cells (36-38), and induces mitochondrial pathway-dependent activation of caspase-9 and caspase-3, but not caspase-8, in lung cancer cells (39). Our study indicated the extrinsic caspase-8 initiator caspase pathway, but not the intrinsic caspase-9 pathway, was induced by FR901228 in both HT29 and HT29-Ras-2 cells. Activation of caspase-3 and caspase-7 by FR901228 in HT29 cells appears to be independent from caspase-9 activity.

In pursuing the involvement of the death receptor family pathways in FR901228-induced cell death of HT29 and HT29-Ras-2 cells, we detected that H-Ras(V12) expression played a role in differentially potentiating TRAIL- and FasL-induced death receptor pathways for FR901228-induced cell death. Activation of the death receptor pathways by TRAIL and FasL predominantly promoted the ability of FR901228 to induce cell death of both HT29 and HT29-Ras-2 cells. It has been reported that HDACI enhances the susceptibility of brain tumor cells to TRAIL-induced cell death (40), and TRAIL-induced activation of caspase-8 is enhanced by expression of oncogenic H-Ras (41). FR901228 treatment induces FasL expression, leading to activation of caspase-8 and -3 in human osteosarcoma cells (38). We detected that FR901228 treatment not only increased expression level of FasL, but also Fas in HT29 and HT29-Ras-2 cells; higher levels of FasL and Fas were induced by FR901228 in HT29-Ras-2 cells than in HT29 cells. In addition, we detected that activation of TNFα-induced death receptor pathway promoted the ability of FR901228 to induce cell death in HT29-Ras-2 cells. Oncogenic H-Ras-expression induces susceptibility of 10T1/2 cells to TNFα-induced apoptosis (42). Apparently,

these death receptor family pathways were potentiated by H-Ras(V12) expression to facilitate FR901228-induced cell death in HT29-Ras-2 cells.

Profound acetylation of core histones H2B and H3 was expected in HT29 and HT29-Ras-2 cells treated with FR901228. Unexpectedly, within equal amounts of isolated nuclear proteins, we detected that acetylated histones and their protein contents were reduced in cells undergoing growth inhibition or apoptosis. Particularly, reduction of H2B and H3 contents by FR901228 appears to be accelerated by expression of H-Ras(V12) in HT29 cells in association with an enhanced cell death. It is possible that H-Ras(V12)-induced modification of core histones in conjunction with apoptosis-related chromosomal DNA fragmentation contribute to the enhanced histone reduction in HT29-Ras-2 cells undergoing FR901228-induced cell death. Modification of core histones through acetylation has been reported to play a critical role in the growth arrest of cell proliferation (43, 44). However, the mechanism for reducing histone content and the role of reduced histones in FR901228-induced apoptosis remain to be clarified.

Investigation of Cdk inhibitors involved in FR901228-induced cell growth arrest revealed that p21^{Cip1} was initially and p27^{Kip1} was subsequently induced by FR901228 treatment in both oncogenic Ras-expressed and parental HT29 cells. Up-regulation of p27^{Kip1} has been postulated to play a role in complete growth suppression of human cancer cells, in which the constitutively activated ERK pathway is suppressed (45). The ERK pathway is constantly activated in parental HT29 cells. FR901228 treatment of HT29 and HT29-Ras-2 cells suppressed the ERK pathway. Accordingly, subsequent to p21^{Cip1} expression, p27^{Kip1} expression may contribute to a complete growth inhibition of HT29 and HT29-Ras-2 cells by FR901228. FR901228 treatment induces p21^{Cip1} expression, but not p27^{Kip1} (data not shown),

in non-transformed 10T1/2 cultures in which cells are mainly arrested in the G0/G1 phase of the cell cycle; in contrast, FR901228 treatment reduces the basal level of p21^{Cip1} in Ras-transformed 10T1/2 cultures in which significant apoptosis is induced (6). Sandor et al. observed that human colon cancer HCT116-derived cell clones lacking p21^{Cip1} are not arrested in the G1 phase, but are arrested in the G2/M phase of the cell cycle following FR901228 treatment; they suggested that p21^{Cip1} is required for FR901228-induced G1 arrest, and G2/M arrest in the absence of p21^{Cip1} is associated with increased cell death induced by FR901228 (46). We observed that expression of H-Ras(V12) in HT29 cells changed the susceptibility to FR901228 for growth-arresting cells from the G0/G1 to G2/M phase of the cell cycle. Possibly, decreased p21^{Cip1} protein content in HT29-Ras cells plays a role in the increased susceptibility to FR901228-induced apoptosis. Both p21^{Cip1} and p27^{Kip1} have been postulated to play multiple roles in the regulation of apoptosis, protein assembly, and gene transcription in addition to inhibitors of the cell cycle (47). The roles of sequential expression of p21^{Cip1} and p27^{Kip1} as well as down-regulation of p21^{Cip1} in FR901228-induced cell growth arrest and apoptosis remain to be clarified.

The ERK pathway was targeted and suppressed by FR901228 treatment in both parental and H-Ras(V12)-expressed HT29 cells. Blocking the ERK pathway resulted in an enhancement of FR901228-induced apoptosis; thus, the ERK pathway plays an anti-apoptotic role in FR901228-induced apoptosis of both parental and H-Ras(V12)-expressed HT29 cells. FR901228 treatment resulted in substantial reduction of Raf-1 protein in both parental HT29 and HT29-Ras-2 cells, a result consistent to the outcome of substantially reduced Raf-1 protein in FR901228-treated mouse 10T1/2 cells (6). It has been suggested that FR901228 treatment

results in destabilization of Raf-1 protein due to dissociation from Hsp90 (48, 49). Possibly, the association between Raf-1 and Hsp90 is a target for FR901228 to reduce Raf-1 protein in HT29 and 10T1/2 cells, regardless of Ras activation. Recently, it has been suggested that FR901228-induced upregulation of Rap1 plays a role in suppression of the Ras-Raf-Erk kinase signaling pathway (27). We detected an increased level of Rap1 induced by FR901228 in both HT29 and HT29-Ras-2 cells. FR901228-increased Rap1 expression may play a role in regulating Raf-1 and B-Raf in both HT29 and HT29-Ras-2 cells; however, the effect of H-Ras(V12) expression on the role of Rap1 in FR901228-induced cell death remains to be determined. Based on the reduced cognate Raf-1 protein levels in FR901228-treated cells, the specific phosphorylation of Raf-1 was highly increased by FR901228 in parental HT29 cells and was modestly increased in HT29-Ras-2 cells. It appears that a novel mechanism is involved in increasing the specific phosphorylation/activation of Raf-1 in order to maintain the overall level of phosphorylated Raf-1. The specific phosphorylation of Raf-1 may contribute to its specific kinase activity in phosphorylating Bad on Ser112 and suppressing the apoptotic activity of Bad (29-31). It is highly possible that suppression of Bad contributes to suppression of the mitochondrial caspase-9-inovolved pathway in FR901228-treated cells. Whether the less phosphorylated/inhibited Bad in H-Ras(V12)-expressed HT29 cells than in parental HT29 cells plays a role in the selective apoptosis induced by FR901228 remains to be clarified. On the other hand, phosphorylation levels of Mek1/2 and Erk1/2 were profoundly suppressed by FR901228 in both parental HT29 and HT29-Ras-2 cells. Apparently, maintenance of the overall phosphorylation and the increases in specific phosphorylation of Raf-1 may not be sufficient to prevent the downstream Mek1/2 and Erk1/2 from down-regulation by FR901228 treatment. Possibly, the protein level of Raf-1

plays an important role in maintaining the activity of Mek1/2 and Erk1/2. A question of whether the reduction of the Raf-1 protein level by FR901228 treatment is sufficient to block signals for phosphorylation/activation of downstream Mek1/2 and Erk1/2 needs to be addressed. In addition, although differential modulation in phosphorylation and protein levels of B-Raf and Raf-1 by FR901228 treatment was detectable in between HT29 and HT29-Ras-2 cells, phosphorylation of the downstream Mek1/2 and Erk1/2 was down-regulated in both HT29 and HT29-Ras-2 cells. The role FR901228-induced differential modulation of B-Raf and Raf-1, which may involve induction of pro-apoptotic pathways such as Mst2 (50), may play in selective induction of cell death HT29-Ras-2 cells remains to be clarified.

The HT29 cell line hosts the active B-*raf* mutant gene (22), and contains constantly activated downstream Mek1/2 and Erk1/2. Expression of H-Ras(V12) in HT29 cells appears to slightly enhance the ERK pathway. Possibly, an intrinsic, feedback signaling circuit is involved in the constant regulation of the constitutively B-Raf-activated ERK pathway in HT29 cells. The HT29 cell line also hosts the inactive *p53* mutant gene (22). FR901228 treatment resulted in reduction of mutant p53 in both parental and H-Ras(V12)-expressed HT29 cells. Apparently, FR901228's ability to induce cell death is not dependent on p53 function. In addition, Akt phosphorylation was not detectable in HT29 cells; and expression of oncogenic H-Ras failed to induce phosphorylation of Akt. The PI3-K pathway appears to be aberrantly inhibited in HT29 cells and plays no role in FR901228-induced cell death. In general, mutation of either the *ras* gene or the B-*raf* gene may be sufficient for human cancer development (51, 52). Our studies using HT29 cells as hosts to express oncogenic H-Ras revealed that H-Ras(V12) may possess an additional, pro-apoptotic activity affecting oncogenic B-Raf in response to HDACI-induced

selective cell death.

Current Ras-targeted anticancer approaches mainly focus on inhibition of Ras protein synthesis, interference with Ras processing to functional sites, or blockage of downstream Ras effectors, approaches based on understanding the roles of oncogenic Ras in tumorigenesis (51). However, agents targeting the pro-apoptotic activity of oncogenic Ras are still overlooked. Our studies verified the pro-apoptotic activity of oncogenic H-Ras that allows HDACI to induce cell death of human cancer HT29 cells. Our results indicate the ability of HDACI to discriminate between oncogenic H-Ras-expressed and counterpart human cells, and suggest a potential value of HDACI in treating Ras-related human cancers. The values of the ERK and PI3-K pathways, the death receptor family pathways, caspase-3, caspase-7, and caspase-8, and Cdk inhibitors as molecular targets need to be considered individually for designing therapeutic protocols using HDACI in combination with other agents to assure the effectiveness of target therapies for treat human cancer involving Ras or Raf activation.

LIST OF REFERENCES

1. Tseng YS, Tzeng CC, Chiu AW, Lin CH, Won SJ, Wu IC, Liu HS (2003) Ha-ras overexpression mediated cell apoptosis in the presence of 5-fluorouracil. Exp Cell Res 288:403-414.
2. Chen G, Shu J, Stacey DW (1997) Oncogenic transformation potentiates apoptosis, S-phase arrest and stress-kinase activation by etoposide. Oncogene 15:1643-1651.
3. Viktorsson K, Heiden T, Molin M, Akusjarvi G, Linder S , Shoshan MC (2000) Increased apoptosis and increased clonogenic survival of 12V-H-ras transformed rat fibroblasts in response to cisplatin. Apoptosis 5:355-367.
4. Chang MY, Jan MS, Won SJ, Liu HS (1998) Ha-rasVal12 oncogene increases susceptibility of NIH/3T3 cells to lovastatin. Biochem Biophy Res Commun 248:62-68.
5. Puccetti E, Beissert T, Guller S, Li JE, Hoelzer D, Ottmann OG, Ruthardt M (2003) Leukemia-associated translocation products able to activate RAS modify PML and render cells sensitive to arsenic-induced apoptosis. Oncogene 2:6900-6908.
6. Fecteau KA, Mei J, Wang HCR (2002) Differential modulation of signaling pathways and apoptosis of ras-transformed cells by a depsipeptide FR901228. J Pharmacol Exp Ther 300:890-899.
7. Song P, Wei J, Plummer H, Wang HCR (2004) Potentiated caspase-3 in Ras-transfromed 10T1/2 cells. Biochem Biophys Res Commun 322:557-564.
8. Song P, Wei J, Wang HCR (2005) Distinct roles of the ERK pathway in modulating apoptosis of Ras-transformed and non-transformed cells induced by anticancer agent FR901228. FEBS Lett 579:90-94.
9. Bertram JS (2000) The molecular biology of cancer. Mol Aspects Med 21:167-223.

10. Campbell SL, Khosravi-Far R, Rossman KL, Clark GJ, Der CJ (1998) Increasing complexity of Ras signaling. Oncogene 17:1395-1413.
11. Mendelsohn J, Howley PM, Israel MA , Liotta LA (ed). The molecular basis of cancer (2nd Ed). W.B. Saunders Company, Philadelphia, PA, 2001.
12. Sanchez-Molina S, Oliva JL, Garcia-Vargas S, Valls E, Rojas JM, Martinez-Balbas MA (2006) The histone acetyltransferases CBP/p300 are degraded in NIH 3T3 cells by activation of Ras signalling pathway. Biochem J 398:215-224.
13. Yuan LW, Giordano A (2002) Acetyltransferase machinery conserved in p300/CBP-family proteins. Oncogene 21:2253-2260.
14. Ueda H, Nakajima H, Hori Y, Fujita T, Nishimura M, Goto T, Okuhara M (1994a) FR901228, a novel antitumor bicyclic depsipeptide produced by Chromobacterium violaceum No. 968. I. Taxonomy, fermentation, isolation, physico-chemical and biological properties, and antitumor activity. J Antibiot (Tokyo) 47:301-310.
15. Ueda H, Manda T, Matsumoto S, Mukumoto S, Nishigaki F, Kawamura I, Shimomura K (1994b) FR901228, a novel antitumor bicyclic depsipeptide produced by Chromobacterium violaceum No. 968. III. Antitumor activities on experimental tumors in mice. J Antibiot (Tokyo) 47:315-323.
16. Vigushin DM. FR-901228 Fujisawa/National Cancer Institute (2002) Curr Opin Investig Drugs 3:1396-1402.
17. Piekarz R, Bates S (2004) A review of depsipeptide and other histone deacetylase inhibitors in clinical trials. Curr Pharm Des 10:2289-2298.

18. Konstantinopoulos PA, Vandoros GP, Papavassiliou AG (2006) FK228 (depsipeptide): a HDAC inhibitor with pleiotropic antitumor activities. Cancer Chemother Pharmacol 58:711-715.

19. Marks PA, Miller T, Richon VM. Histone deacetylases (2003) Curr Opin Pharamacol 3:344-351.

20. Espino PS, Drobic B, Dunn KL, Davie JR (2005) Histone modifications as a platform for cancer therapy. J Cell Biochem 94:1088-1102.

21. Dokmanovic M, Marks PA (2005) Prospects: histone deacetylase inhibitors. J Cell Biochem 96:293-304.

22. Huang F, Hsu S, Yan Z, Winawer S, Friedman E (1994) The capacity for growth stimulation by TGF beta 1 seen only in advanced colon cancers cannot be ascribed to mutations in APC,DCC, p53 or ras. Oncogene 9:3701-3706.

23. Song P, Wang HCR (2004) Efficient identification of tetR-expressing cell lines for tetracyline-regulated gene expression. Electron J Biotechnol 7:210-213.

24. Talanian RV, Quinlan C, Trautz S, Hackett MC, Mankovich JA, Banach D, Ghayur T**,** Brady KD, Wong WW (1997) Substrate specificities of caspase family proteases. J Biol Chem 272:9677-9682.

25. de Bruin EC, Meersma D, de Wilde J, den Otter I, Schipper EM, Medema JP, Peltenburg LTC (2003) A serine protease is involved in the initiation of DNA damage-induced apoptosis. Cell Death Diff 10:1204-1212.

26. Favata MF, Horiuchi KY, Manos EJ, Daulerio AJ, Stradley DA, Feeser WS, Van-Dyk DE, Pitts WJ, Earl RA, Hobbs F, Copeland RA, Magolda RL, Scherle PA, Trzaskosl JM

27. Kobayashi Y, Ohtsuki M, Murakami T, Kobayashi T, Sutheesophon K, Kitayama H, Kano Y, Kusano E, Nakagawa H, Furukawa Y (2006) Histone deacetylase inhibitor FK228 suppresses the Ras-MAP kinase signaling pathway by upregulating Rap1 and induces apoptosis in malignant melanoma. Oncogene 25:512-524.
28. Sheng H, Shao J, DuBois RN (2001) Akt/PKB activity is required for Ha-Ras-mediated transformation of intestinal epithelial cells. J Biol Chem 276:14498-14504.
29. Wang HG, Rapp UR, Reed JC (1996) Bcl-2 targets the protein kinase Raf-1 to mitochondria. Cell 87:629-638.
30. Troppmair J, Rapp UR (2003) Raf and the road to cell survival: a tale of bad spells, ring bearers and detours. Biochem Pharmacol 66:1341-1345.
31. Chang F, Steelman LS, Shelton JG, Lee JT, Navolanic PM, Blalock WL, Franklin R, McCubrey JA (2003) Regulation of cell cycle progression and apoptosis by the Ras/Raf/MEK/ERK pathway. Int J Oncol 22:469-480.
32. Bennett BL, Sasaki DT, Murray BW, O'Leary EC, Sakata ST, Xu W, Leisten JC, Motiwala A, Pierce S, Satoh Y, Bhagwat SS, Manning AM, Anderson DW (2001) SP600125, an anthrapyrazolone inhibitor of Jun N-terminal kinase. Proc Natl Acad Sci USA 98:13681-13686.
33. Somwar R, Koterski S, Sweeney G, Sciotti R, Djuric S, Berg C, Trevillyan J, Scherer PE, Rondinone CM, Klip A (2002) A dominant-negative p38 MAPK mutant and novel

selective inhibitors of p38 MAPK reduce insulin-stimulated glucose uptake in 3T3-L1 adipocytes without affecting GLUT4 translocation. J Biol Chem 277:50386-50395.

34. Daniel JC, Peter HS, John PM, Joel SH, Ursula E, Arthur DL, David VG (1983) Activation of Ki-*ras*2 gene in human colon and lung carcinomas by two different point mutations. Nature 304:507-513.
35. Boatright KM, Salvesen GS (2003) Mechanisms of caspase activation. Curr Opin Cell Biol 15:725-731.
36. Watanabe K, Okamoto K, Yonehara S (2005) Sensitization of osteosarcoma cells to death receptor-mediated apoptosis by HDAC inhibitors through downregulation of cellular FLIP. Cell Death Differ 12:10-18.
37. Aron JL, Parthun MR, Marcucci G, Kitada S, Mone AP, Davis ME, Shen T, Murphy T, Wickham J, Kanakry C, Lucas DM, Reed JC, Grever MR, Byrd JC (2003) Depsipeptide (FR901228) induces histone acetylation and inhibition of histone deacetylase in chronic lymphocytic leukemia cells concurrent with activation of caspase 8-mediated apoptosis and down-regulation of c-FLIP protein. Blood 102:652-658.
38. Imai T, Adachi S, Nishijo K, Ohgushi M, Okada M,Yasumi T, Watanabe K, Nishikomori R, Nakayama T, Yonehara S, Toguchida J, Nakahata T (2003) FR901228 induces tumor regression associated with induction of Fas ligand and activation of Fas signaling in human osteosarcoma cells. Oncogene 22:9231-9242.
39. Doi S, Soda H, Oka M, Tsurutani J, Kitazaki T, Nakamura Y, Fukuda M, Yamada Y, Kamihira S, Kohno S (2004) The histone deacetylase inhibitor FR901228 induces caspase-dependent apoptosis via the mitochondrial pathway in small cell lung cancer

cells. Mol Cancer Ther 3:1397-1402.

40. Sonnemann J, Kumar KS, Heesch S, Muller C, Hartwig C, Maass M, Bader P, Beck JF (2006) Histone deacetylase inhibitors induce cell death and enhance the susceptibility to ionizing radiation, etoposide, and TRAIL in medulloblastoma cells. Int J Oncol 28:755-766.
41. Nesterov A, Nikrad M, Johnson T, Kraft AS (2004) Oncogenic Ras sensitizes normal human cells to tumor necrosis factor-α-related apoptosis-inducing ligand-induced apoptosis. Cancer Res 64:3922-3927.
42. Trent JC II, McConkey DJ, Loughlin SM, Harbison MT, Fernandez A, Ananthaswamy HN (1996) Ras signaling in tumor necrosis factor-induced apoptosis. EMBO J 15:4497-4505.
43. Grewal SS, Moazed D (2003) Heterochromatin and epigenetic control of gene expression. Science 301:798-802.
44. Taddei A, Roche D, Bickmore WA, Almouzni G (2005) The effects of histone deacetylase inhibitors on heterochromatin: implications for anticancer therapy? EMBO Rep 6:520-524.
45. Hoshino R, Tanimura S, Watanabe K, Kataoka T, Kohno M (2001) Blockade of the extracellular singal-regulated kinase pathway induces marked G1 cell cycle arrest and apoptosis in tumor cells in which the pathway is constitutively activated. J Biol Chem 276:2686-2692.

46. Sandor V, Senderowicz A, Mertins S, SackettD, Sausville E, Blagosklonny MV, Bates SE (2000) P21-dependent G1 arrest with downregulation of cyclin D1 and upregulation of cyclin E by the histone deacetylase inhibitor FR901228. Br J Cancer 83:817-825.
47. Coqueret O (2000) New roles fo p21 and p27 cell cycle inhibitors: a function for each cell compartment? Trends Cell Biol 13:65-70.
48. Schulte TW, Blagosklonny MV, Ingui C, Neckers L (1995) Disruption of the Raf-1-Hsp90 molecular complex results in destabilization of Raf-1 and loss of Raf-1-Ras association. J Biol Chem 270:24585-24588.
49. Yu X, Guo ZS, Marcu MG, Neckers L, Nguyen DM, Chen GA, Schrump DS (2002) Modulation of p53, ErbB1, ErbB2, and Raf-1 expression in lung cancer cells by depsipeptide FR901228. J Natl Cancer Inst 94:504-513.
50. O'Neill E, Rushworth L, Baccarini M, Kolch W (2004) Role of the kinase MST2 in suppression of apoptosis by the proto-oncogene product Raf1. Science 306:2267-2270.
51. Adjei AA (2001) Blocking oncogenic Ras signaling for cancer therapy. J Natl Cancer Inst 93:1062-1074.
52. Sridhar SS, Hedley D, Siu LL (2005) Raf kinase as a target for anticancer therapeutics. Mol Cancer Ther 4:677-685.

APPENDIX

Table

Table 1. Flow cytometric analysis of FR901228-treated cells

	HT29			HT29-Ras		
Treatment:	**0 hr**	**24 hr**	**48 hr**	**0 hr**	**24 hr**	**48 hr**
Apoptotic (%):	<1	1	4±1	<1	4±2	20±2
Live (%):						
G0/G1:	60±8	72±4	75±2***a***	59±6	57±11	57±6***b***
S:	17±2	3±1	4±1	12±3	3±1	5±2
G2/M:	23±7	25±3	21±1***c***	29±10	40±13	38±3***d***

HT29 and HT29-Ras cultures were treated with 1 nM FR901228 for 0, 24, and 48 hours. Anchored cells were trypsinized from cultures, and cell populations were analyzed by flow cytometry to detect apoptotic cell population and live cells in each phase of the cell cycle. Each value represents a mean of results from two independent experiments ± standard deviation. Student's *t*-test was used to analyze statistical significance of ***b*** versus ***a*** ($p < 0.01$) and ***d*** versus ***c*** ($p < 0.001$).

Fig. 1 Increased cell susceptibility to FR901228 by oncogenic H-Ras. (**a**) Expression levels of H-Ras and β-Actin in HT29, HT29-Ras-1, and HT29-Ras-2 cells were determined by Western immunoblotting with antibodies specific to H-Ras and β-Actin. Detected levels of H-Ras and β-Actin on radiograms were quantified by densitometry. The levels of H-Ras were normalized by the cognate levels of β-Actin, and then the relative levels of H-Ras in HT29-Ras-1 and -2 cells were normalized by the level of endogenous H-Ras determined in parental HT29 cells, set as 1 (X, arbitrary unit), as shown in parentheses. (**b**) HT29, HT29-Ras-1, and HT29-Ras-2 cells were treated with 0, 0.2, 1, and 5 nM FR901228 (FR) for 0, 24, and 48 h. Relative cell growth and survival rates in cultures were normalized by the number of live cells determined at 0 h, set as 100%. Each value represents a mean of triplicates, and error bars represent standard deviation. The Student's *t*-test was used to analyze statistical significance of ***ii*** versus ***i*** ($p < 0.001$). (**c**) HT29-Ras-2 and HT29 cells were treated with 1 nM FR901228 for 0, 12, 24, and 36 h. Then, cell death in the population of attached cells was assessed by flow cytometry with an Annexin-V-FITC Apoptosis Detection Kit with propidium iodide.

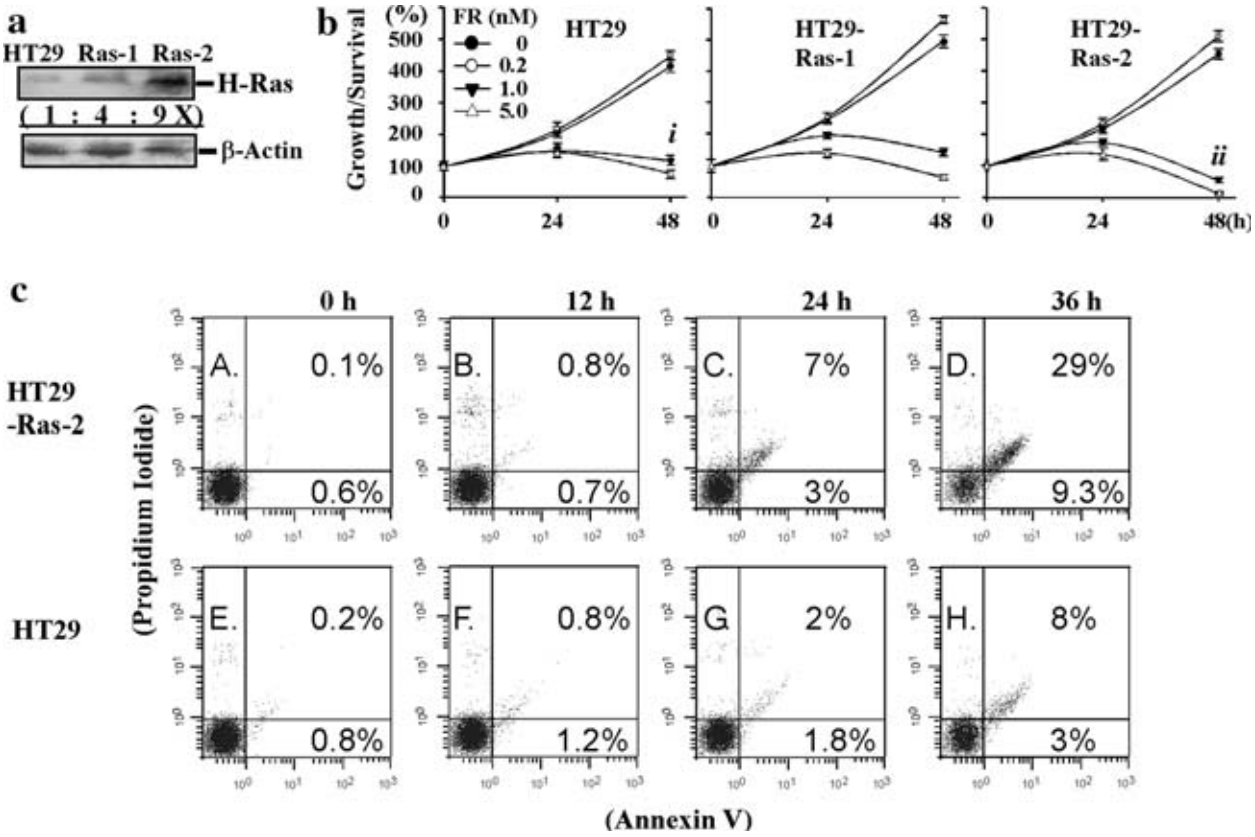
a
HT29 Ras-1 Ras-2
H-Ras
(1 : 4 : 9 X)
β-Actin
b
(%)
Growth/Survival
FR (nM)
0
0.2
1.0
5.0
HT29
HT29-
Ras-1
HT29-
Ras-2
i
ii
0
24
48
48(h)
c
0 h
12 h
24 h
36 h
HT29
-Ras-2
HT29
A. 0.1% 0.6%
B. 0.8% 0.7%
C. 7% 3%
D. 29% 9.3%
E. 0.2% 0.8%
F. 0.8% 1.2%
G 2% 1.8%
H. 8% 3%
(Propidium Iodide)
(Annexin V)

Fig. 2 Apoptotic pathways in FR901228-induced cell death. (**a**) Quantification of apoptotic-like cell death in cultures of HT29 and HT29-Ras-2 that were treated with 1 nM FR901228 for 48 h was determined using a Cell Death Detection ELISA kit. Relative cell death, as fold induction (X, arbitrary unit), was normalized by the value determined in untreated cells, set as 1. Each value represents a mean of triplicates, and error bars represent standard deviation. (**b**) HT29 and HT29-Ras-2 cultures were treated with 0 (lanes 1 and 4), 1 (lanes 2 and 5), and 5 (lanes 3 and 6) nM FR901228 for 48 h. Equal amounts of cellular proteins prepared from cell lysates were analyzed by Western immunoblotting using a specific antibody to detect levels of cleaved, active caspase-3. (**c-1** to **c-5**) HT29 and HT29-Ras-2 cultures were treated with 1 nM FR901228 for 0 (lanes 1 and 4), 24 (lanes 2 and 5), and 48 (lanes 3 and 6) h. Equal amounts of cellular proteins prepared from cell lysates were analyzed by Western immunoblotting using specific antibodies to detect levels of cleaved, active caspase-3 (**c-1**), active caspase-7 (**c-2**), cleaved PARP fragments (**c-3**), active caspase-8 (**c-4**), and β-Actin (**c-5**). (**d**) HT29 and HT29-Ras-2 cells were pretreated with 100 μM of caspase-3/-7 inhibitor Ac-DEVD-CHO (CI) or 100 μM of serine protease inhibitor AEBSF-HCl (SI) for 6 h. Then, HT29 and HT29-Ras-2 cultures were treated with 1 nM FR901228 for 48 h. Quantification of cell viability in these cultures was determined with an MTT assay kit. Relative cell viability was normalized by the value determined in untreated cells, set as 100%. Each value represents a mean of triplicates, and error bars represent standard deviation. The Student's *t*-test was used to analyze statistical significance of ***ii*** and ***iii*** versus ***i*** ($p < 0.01$). * indicates a non-specific protein.

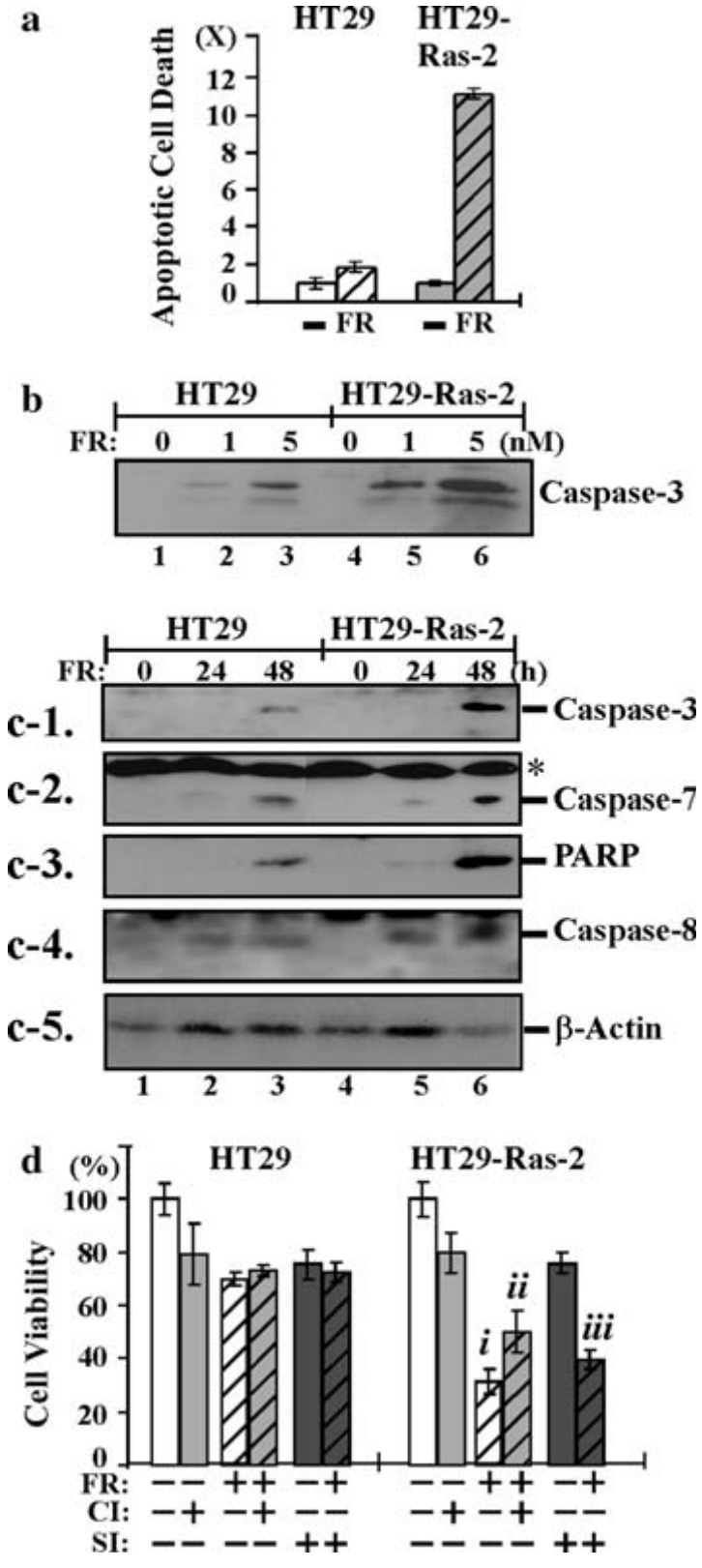
a
HT29
HT29-Ras-2
Apoptotic Cell Death
(X)
12
10
8
6
4
2
0
FR
FR
b
HT29
HT29-Ras-2
FR: 0 1 5 0 1 5 (nM)
Caspase-3
1 2 3 4 5 6
HT29
HT29-Ras-2
FR: 0 24 48 0 24 48 (h)
c-1.
Caspase-3
c-2.
*
Caspase-7
c-3.
PARP
c-4.
Caspase-8
c-5.
β-Actin
1 2 3 4 5 6
d
(%)
HT29
HT29-Ras-2
Cell Viability
100
80
60
40
20
0
i
ii
iii
FR: − − + + − + − − + + − +
CI: − + − + − − − + − + − −
SI: − − − − + + − − − − + +

Fig. 3 Death receptor family pathways involved in FR901228-induced cell death. HT29 and HT29-Ras-2 cells were treated with TRAIL (**a**), FasL (**b**), and TNFα (**c**) at indicated concentrations in the absence and presence of 1 nM FR901228 for 48 h. Quantification of cell viability in these cultures was determined with an MTT assay kit. Relative cell viability was normalized by the value determined in untreated cells, set as 100%. Each value represents a mean of triplicates, and error bars represent standard deviation. (**d-1** to **d-3**) HT29 and HT29-Ras-2 cells were treated with 1 nM FR901228 for 0 (lanes 1 and 4), 24 (lanes 2 and 5), and 48 (lanes 3 and 6) h. Equal amounts of cellular proteins prepared from cell lysates were analyzed by Western immunoblotting using specific antibodies to detect levels of Fas (**d-1**) and FasL (**d-2**) with β-Actin (**d-3**) as a control.

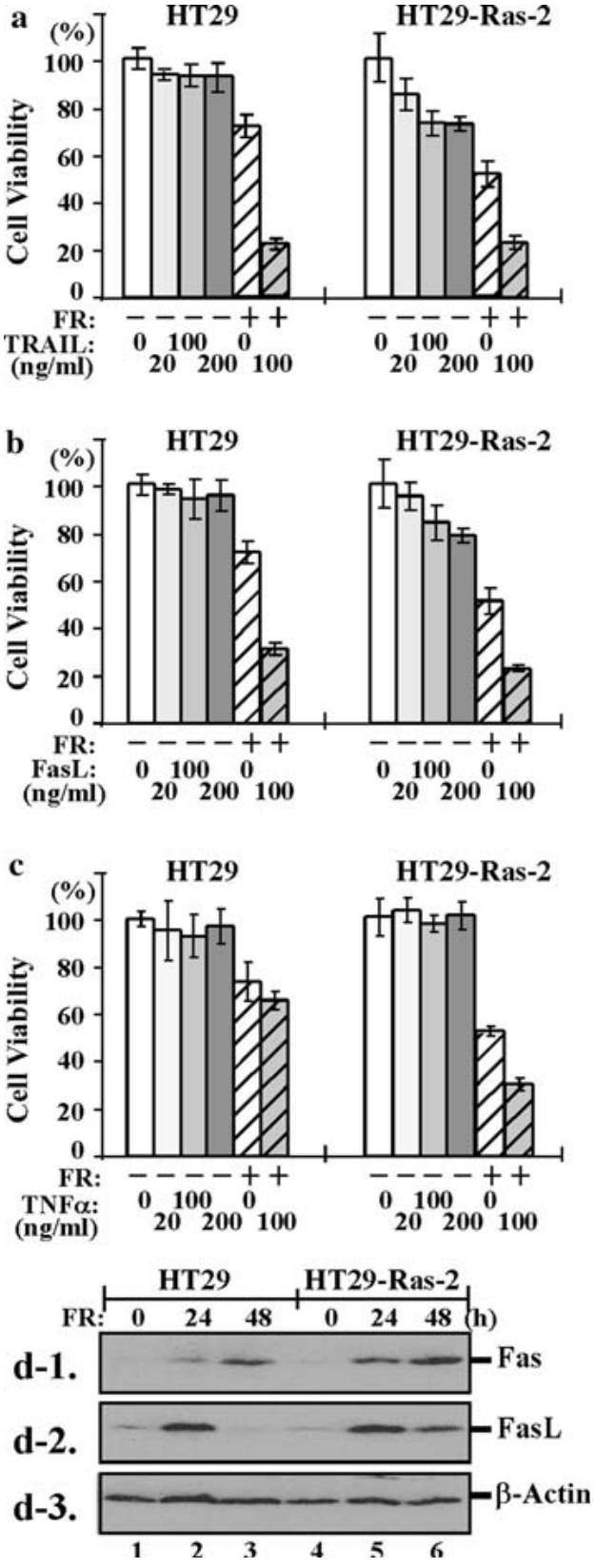
a
HT29
HT29-Ras-2
(%)
Cell Viability
100
80
60
40
20
0
FR:
TRAIL:
(ng/ml)
0 100 0
20 200 100
b
FasL:
c
TNFα:
HT29
HT29-Ras-2
FR: 0 24 48 0 24 48 (h)
d-1.
Fas
d-2.
FasL
d-3.
β-Actin
1 2 3 4 5 6

Fig. 4 Induction of CDK inhibitors in FR901228-arrested cells. (**a**) Inhibition of cell growth induced by FR901228 was determined by the blockage of BrdU incorporation into cellular DNA. HT29 and HT29-Ras-2 cells were treated with 1 nM FR901228 for 24 h. Cells were labeled with BrdU, incubated with peroxidase-conjugated BrdU-specific antibodies, and stained with peroxidase substrate. Relative cell growth rate was normalized by the value of BrdU detected in untreated cells, set as 100%. Each value represents a mean of triplicates, and error bars represent standard deviation. (**b** to **e**) HT29 and HT29-Ras-2 cells were treated with 1 nM FR901228 for 0 (lanes 1 and 4), 24 (lanes 2 and 5), and 48 (lanes 3 and 6) h. Equal amounts of cellular proteins prepared from cell lysates were analyzed by Western immunoblotting using specific antibodies to detect levels of p21^{Cip1} (**b**), p53 (**c**), and p27^{Kip1} (**d**), with β-Actin (**e**) as a control.

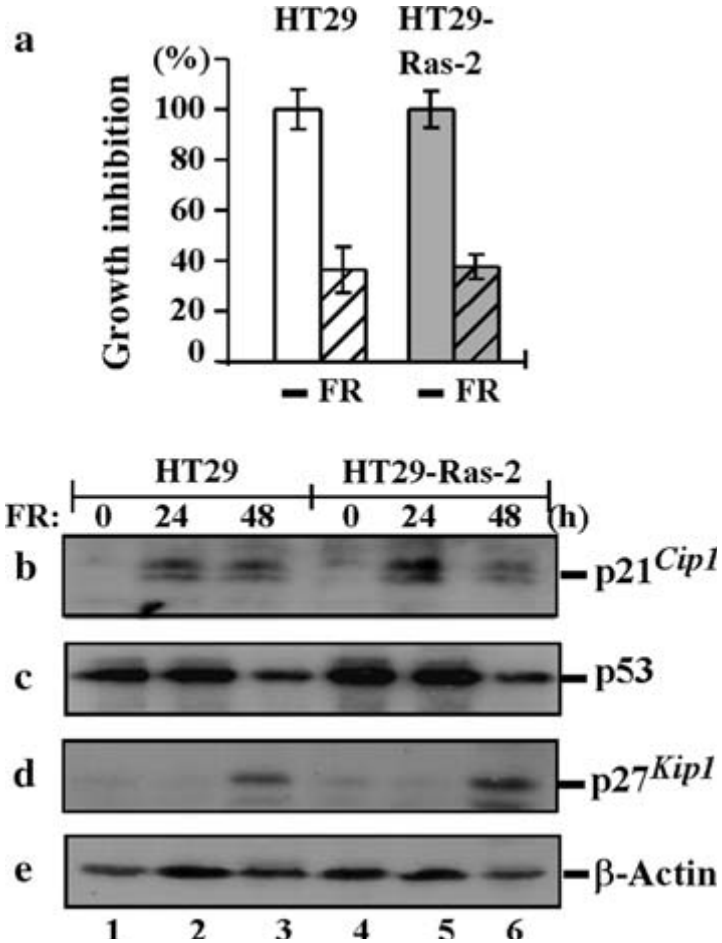
a
HT29
HT29-Ras-2
(%)
Growth inhibition
100
80
60
40
20
0
– FR
– FR
HT29
HT29-Ras-2
FR: 0 24 48 0 24 48 (h)
b
p21Cip1
c
p53
d
p27Kip1
e
β-Actin
1 2 3 4 5 6

Fig. 5 Modulation of the ERK and PI3-K pathways in FR901228-treated cells. (**a**) HT29 and HT29-Ras-2 cells were treated with 20 μM U0126 (U0) in the presence and absence of 1 nM FR901228 for 48 h. Quantification of cell viability was determined with an MTT assay kit. Relative cell viability was normalized by the value determined in untreated cells, set as 100%. Each value represents a mean of triplicates, and error bars represent standard deviation. The Student's *t*-test was used to analyze statistical significance of ***ii*** versus ***i*** ($p < 0.001$). (**b** to **i**) Cell lysates were prepared from HT29 and HT29-Ras-2 cells treated with 1 nM FR901228 for 0 (lanes 1 and 4), 24 (lanes 2 and 5), and 48 (lanes 3 and 6) h. Cell lysates were also prepared from growing J82 cultures for a comparison (**f** to **h**, lane 7). Equal amounts of cellular proteins prepared from cell lysates were analyzed by Western immunoblotting with specific antibodies to detect levels of phosphorylated B-Raf (**b-1**) and total B-Raf protein (**b-2**) , phosphorylated Raf-1 (**c-1**) and total Raf-1 protein (**c-2**), β-Actin (**d**), Rap1 (**e**), phosphorylated Mek1/2 (**f-1**) and total Mek1/2 proteins (**f-2**), phosphorylated Erk1/2 (**g-1**) and total Erk1/2 proteins (**g-2**), phosphorylated Akt (**h-1**) and total Akt proteins (**h-2**), and phosphorylated Bad (**i-1**) and total Bad protein (**i-2**). Levels of p-B-Raf, B-Raf, p-Raf-1, Raf-1, p-Bad, Bad, and β-Actin on radiograms were quantified by densitometry. The relative levels of specific phosphorylation of B-Raf (p/B-Raf), Raf-1 (p/Raf-1), and Bad (p/Bad) were calculated by normalizing the levels of p-B-Raf , p-Raf-1, and p-Bad with the levels of their cognate proteins, and then were normalized by the level in parental HT29 cells (lane 1), set as 1 (X, arbitrary unit). The relative levels of Raf-1 protein (Raf-1/Actin) were calculated by normalizing the levels of Raf-1 with the levels of β-Actin, and then were normalized by the level in parental HT29 cells (lane 1), set as 1 (X, arbitrary unit). The ratio of p/Bad in FR90122-treated HT29-Ras-2 cells (**i**, lanes 5 and 6) to

untreated cells (lane 4) was also calculated as shown in parenthesis.

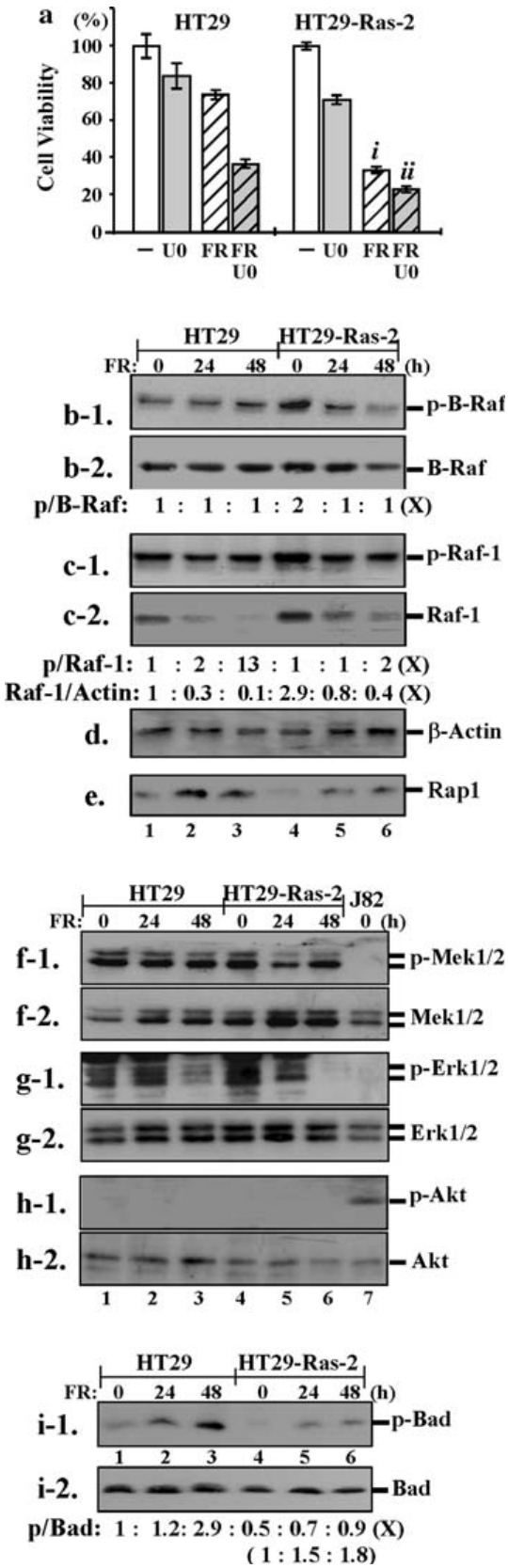
a
(%)
HT29
HT29-Ras-2
Cell Viability
100
80
60
40
20
0
i
ii
– U0 FR FR U0
– U0 FR FR U0
HT29
HT29-Ras-2
FR: 0 24 48 0 24 48 (h)
b-1.
p-B-Raf
b-2.
B-Raf
p/B-Raf: 1 : 1 : 1 : 2 : 1 : 1 (X)
c-1.
p-Raf-1
c-2.
Raf-1
p/Raf-1: 1 : 2 : 13 : 1 : 1 : 2 (X)
Raf-1/Actin: 1 : 0.3 : 0.1: 2.9: 0.8: 0.4 (X)
d.
β-Actin
e.
Rap1
1 2 3 4 5 6
HT29
HT29-Ras-2
J82
FR: 0 24 48 0 24 48 0 (h)
f-1.
p-Mek1/2
f-2.
Mek1/2
g-1.
p-Erk1/2
g-2.
Erk1/2
h-1.
p-Akt
h-2.
Akt
1 2 3 4 5 6 7
HT29
HT29-Ras-2
FR: 0 24 48 0 24 48 (h)
i-1.
p-Bad
1 2 3 4 5 6
i-2.
Bad
p/Bad: 1 : 1.2: 2.9 : 0.5 : 0.7 : 0.9 (X)
(1 : 1.5 : 1.8)

Fig. 6 Histone modulation in FR901228-treated cells. HT29 and HT29-Ras-2 cells were treated with 1 nM FR901228 for 0 (lanes 1 and 4), 24 (lanes 2 and 5), and 48 (lanes 3 and 6) h. Nuclear lysates were prepared, and equal amounts of cellular proteins in these nuclear lysates were analyzed by Western immunoblotting with specific antibodies to detect levels of acetylated H2B (**a-1**) and total H2B protein (**a-2**), and acetylated H3 (**b-1**) and total H3 protein (**b-2**).

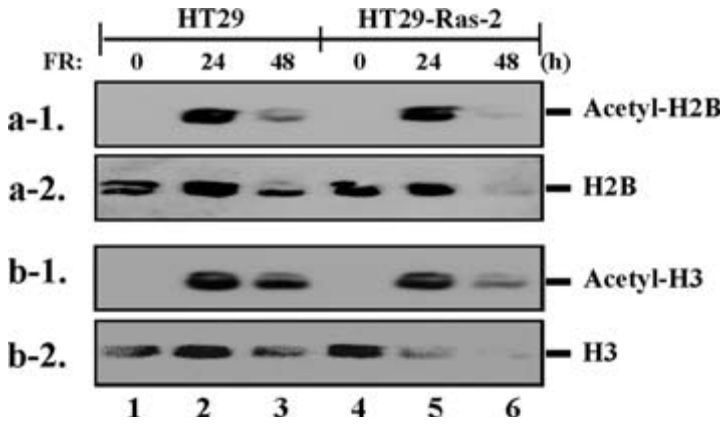

Fig. 7 Cell susceptibility to HDACI. HT29, HT29-Ras-2, and SW480 cells were treated with 0, 0.2, 1, 5, and 25 nM FR901228 (**a**) and 0, 1, 5, 25, and 100 nM TSA (**b**) for 48 h. Quantification of cell viability was determined with an MTT assay kit. Relative cell viability was normalized by the value determined in untreated cells, set as 100%. Each value represents a mean of triplicates, and error bars represent standard deviation. (**c**) 10T1/2-TR-H-*ras* cells were treated with 100 ng/ml tetracycline (Tet) to induce expression of H-Ras and cellular transformation for 72 h in the absence (-) and presence of 5 nM TSA. Every 24 h, live cells were counted in a hemocytometer. Relative cell growth and survival rates in cultures were normalized by the number of live cells determined at 0 hour, set as 100%. Each value represents a mean of triplicates, and error bars represent standard deviation. The Student's *t*-test was used to analyze statistical significance of ***ii*** versus ***i*** ($p < 0.001$).

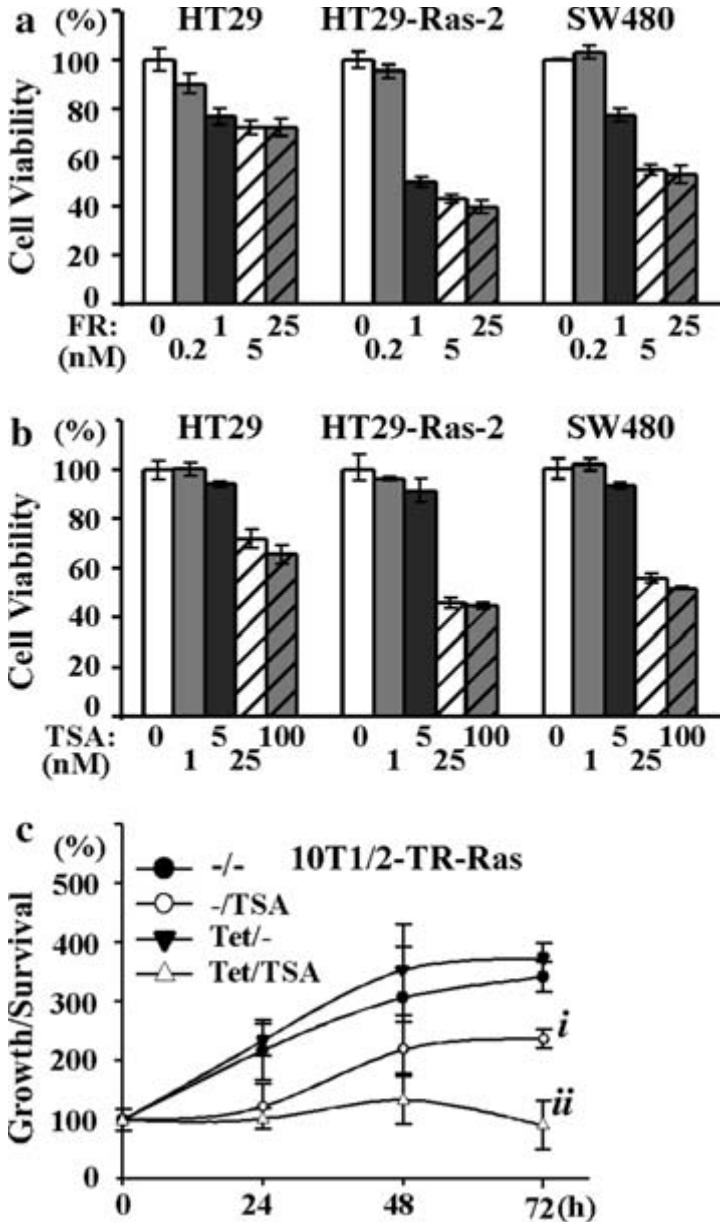
a
(%)
HT29
HT29-Ras-2
SW480
Cell Viability
100
80
60
40
20
0
FR:
0
1
25
(nM)
0.2
5
b
TSA:
100
c
Growth/Survival
500
400
300
200
10T1/2-TR-Ras
-/-
-/TSA
Tet/-
Tet/TSA
i
ii
0
24
48
72(h)

PART –IV

ROLE OF REACTIVE OXYGEN SPECIES IN THE ABILITY OF H-RAS TO ENHANCE CELL DEATH INDUCED BY HISTONE DEACETYLASE INHIBITORS

Research described in this chapter is slightly modified version of an article that is submitted for publication in International Journal of Cancer by Shambhunath Choudhary, Kusum Rathore, Xiaoyu Song, and Hwa-Chain Robert Wang.

Shambhunath Choudhary, Kusum Rathore, Xiaoyu Song, and Hwa-Chain Robert Wang. Role of reactive oxygen species in the ability of H-Ras to enhance cell death induced by histone deacetylase inhibitors (International Journal of Cancer-Submitted)

In this paper "our" and "we" refers to me and co-authors. My contribution in the paper includes (1) Selection of the topic (2) Compiling and interpretation of the literature (3) Designing experiments (4) understanding the literature and interpretation of the results (5) providing comprehensive structure to the paper (6) Preparation of the graphs and figures (7) Writing and editing

Abstract

Oncogenic induction of the *ras* genes is widely involved in human cancers. Expression of oncogenic H-Ras increases susceptibility of human and mouse cells to histone deacetylase inhibitors (HDACIs), such as FK228 and trichostatin A, for inducing caspase activation and selective apoptosis. HDACIs make up a new class of structurally diverse anticancer agents and have been shown to exhibit antimetastatic and antiangiogenic activities toward malignantly transformed cells. To understand the mechanisms behind the proapoptotic ability of oncogenic H-Ras to enhance cell susceptibility to HDACIs, we detected that expression of oncogenic H-Ras

potentiated intracellular reactive oxygen species (ROS) in human urinary bladder cancer J82, human colorectal cancer HT29, and mouse embryo fibroblast 10T1/2 cells to enhance HDACI-induced ROS, thereby contributing to the induction of selective apoptosis and caspase activation. Expression of oncogenic H-Ras also increased cell susceptibility to hydrogen peroxide (H_2O_2) for inducing apoptosis and caspase activation. By studying IC_{50} values of FK228 and H_2O_2 for oncogenic H-Ras-expressing and parental cells and by quantifying cell death and caspase activation induced by FK228 and H_2O_2, we demonstrated evidence to indicate, for the first time, that intracellular ROS was cooperatively up-regulated by oncogenic H-Ras and FK228 treatment to induce apoptosis and caspase activation in a dose-dependent manner. Considering the role of intracellular ROS as a potential target of the novel proapoptotic activity of oncogenic H-Ras is important in developing therapeutic strategies to control oncogenic H-Ras-involved human cancers.

Introduction

Induction of *ras* genes is frequently detected in human cancers (1). Both clinical and basic studies suggest that activation of H-Ras accompanied by inactivation of tumor suppressor p53 may play important roles in tumorigenesis in high-grade, invasive urothelial tumors (2,3). In fact, an activating mutation in codon 12 of the H-*ras* gene is detected in more than 35% of patients with urinary bladder cancers (1). The human urinary bladder transitional carcinoma J82 cell line hosts wild-type *ras* and the inactive mutant *Rb* and *p53* genes with deletion of the *pTEN* gene (4,5). We have shown that ectopic expression of oncogenic H-Ras promotes acquired tumorigenicity in J82 cells, mimicking an acquisition of H-*ras* gene activation in tumor development (6). We have also shown that expression of oncogenic H-Ras in J82 (6), human colorectal adenocarcinoma HT29 (7), and mouse embryo fibroblast 10T1/2 (8,9) cells increases their susceptibility to the histone deacetylase inhibitors (HDACIs) FK228 and trichostatin A (TSA) for inducing apoptosis. Expression of oncogenic H-Ras also results in reducing clonogenic resistance of J82 cells to HDACIs (6). Our results of the ability of oncogenic H-Ras to increase cell susceptibility to HDACIs for inducing selective apoptosis lead us to suggest that oncogenic H-Ras possesses a proapoptotic ability to facilitate HDACI-induced apoptosis.

Ectopic expression of oncogenic H-Ras has been shown to elevate intracellular ROS, including superoxide and H_2O_2, in mouse and rat fibroblast cells (10,11) and ovarian epithelial cells (12). Several studies have indicated that the Ras-induced membrane NADPH-oxidase complex plays an important role in producing ROS for Ras-induced transformation phenotypes (13-18). Increased ROS reportedly mediates changes of cell morphology and motility in Ras-transformed fibroblast cells (11), and increased ROS is required for Ras-induced cell growth

(10,19) and DNA repair (13) in mouse embryo fibroblast cells. In addition, oncogenic Ras-increased ROS may cause DNA damage, contributing to Ras-induced mutagenesis in cells lacking the tumor suppressor p53 (20). On the other hand, increased intracellular ROS has been postulated to play a role in the increased susceptibility of H-Ras-expressing ovarian and breast epithelial cells to β-phenylethyl isothiocyanate (12) and to capsaicin (21) for inducing cell death, respectively. However, whether increased ROS may also play a role in the increased susceptibility of H-Ras-expressing human cancer cells to HDACIs for inducing selective apoptosis remains to be clarified.

HDACIs make up a new class of structurally diverse anticancer agents and have been shown to exhibit antimetastatic and antiangiogenic activities toward malignantly transformed cells in vitro and *in vivo* (22,23). Growing evidence indicates transformed cells are much more sensitive than normal cells to growth-inhibitory and apoptotic effects of HDACIs (22,24). Some studies have suggested that Class I histone deacetylases (HDACs) are important in the regulation of proliferation and survival in cancer cells (23,25,26). FK228, a depsipeptide also known as FR901228 and romidepsin (NSC-630176) (27), has been shown to exhibit strong activity inhibiting Class I HDAC-1 and HDAC-2, mild activity inhibiting Class II HDAC-4, and weak activity inhibiting Class II HDAC-6, assayed *in vitro* (28). Selective inhibition of Class I HDACs by FK228 may contribute to its selectivity in control of cancer cells. In addition, FK228 treatment has been shown to result in elevated ROS in gastrointestinal cancer cells for inducing cell death (29). However, whether FK228 treatment is able to induce elevated ROS contributing to selective apoptosis of oncogenic H-Ras-expressing human cancer cells remains to be clarified.

In this report, we present evidence to reveal, for the first time, that intracellular ROS was

cooperatively increased by ectopic expression of oncogenic H-Ras and FK228 treatment in increasing cell susceptibility for inducing selective apoptosis and profound caspase activation in oncogenic H-Ras-expressing cells versus parental cells in a dose-dependent manner. Our results show the contributing role of elevated ROS in the proapoptotic ability of oncogenic H-Ras to increase susceptibilities of human urinary bladder and colorectal cancer cells as well as mouse embryo fibroblast cells to HDACIs for inducing selective apoptosis.

Materials and Methods

Cell Cultures and Reagents

J82 and HT29 cells (ATCC, Rockville, MD) and oncogenic H-Ras-expressing, J82-Ras (6) and HT29-Ras (7) cells were maintained in DMEM supplemented with 10% fetal bovine serum. 10T1/2 and oncogenic H-Ras-expressing, 10T1/2-Ras cells (8) were maintained in Basal Medium Eagle supplemented with 10% fetal bovine serum. All cultures were maintained in medium supplemented with 100 U/ml penicillin and 100 μg/ml streptomycin in 7% CO_2 at 37°C and routinely subcultured every 2 to 3 days. Stock aqueous solutions of FK228 (National Cancer Institute, Chemistry and Synthesis Branch, collaboration with Dr. KK Chan, The Ohio State University), chloromethyl-dichlorodihydrofluorescein-diacetate (CM-H_2DCF-DA) (Invitrogen/Molecular Probes, Carlsbad, CA), rhodamine-123 (Rho-123), rotenone (ROT) (Sigma, St. Louis, MO), and TSA (Wako, Richmond, VA) were prepared in DMSO and diluted in culture medium for assays. Stock aqueous solutions of *N*-acetyl-*L*-cysteine (NAC) (Alexis, San Diego, CA) and 10-*N*-nonyl acridine orange (NAO) (Sigma) were prepared in distilled water and diluted in culture media for assays. Stock aqueous solution of H_2O_2 (Cumberland Swan,

Smyrna, TN) was diluted directly in culture medium for assays.

Cell Viability Assay

A Methyl Thiazolyl Tetrazolium (MTT) assay kit (ATCC) was used to measure cell viability in cultures (6,7). Five x 10^4 cells were seeded into each well of 96-well culture plates for 24 h. After indicated treatments, cells were incubated with MTT reagent for 4 h, followed by incubation with detergent reagent for 24 h. Reduced MTT reagent in cultures was quantified with an ELISA reader (Bio-Tek, Winooski, VT).

Annexin-V Apoptosis Assay

An annexin-V-fluorescein isothiocyanate (FITC) apoptosis detection kit with propidium iodide (BD Biosciences, San Jose, CA) was used to detect apoptotic cell death by flow cytometry (6,7). In brief, cells were collected after trypsinization and washed with PBS. Cells were then incubated with annexin V-FITC and propidium iodide in a binding buffer (10 mmol/L Hepes-KOH, pH 7.4, 150 mmol/L NaCl, 1.8 mmol/L $CaCl_2$) for 20 min at ambient temperature in the dark. Flow cytometric analysis was performed on the Coulter EPICS Elite Cytometer (Hialeah, FL) at the excitation and emission wavelengths of 488 and 550 nm, respectively, for FITC measurements, and at 488 and 645 nm for propidium iodide measurements. Both subpopulations of annexin V-FITC-labeled cells and propidium iodide-labeled cells were considered together to determine the percentage of cells undergoing apoptotic cell death using Multicycle software.

Measurement of Intracellular ROS

To measure intracellular ROS levels, cells were incubated with 5 μmol/L CM-H_2DCF-DA in 7% CO_2 at 37ºC for 1 h (12). Cells were rinsed with Ca^{++} and Mg^{++} free PBS, trypsinized from cultures, and resuspended in PBS for analysis of intracellular ROS by flow cytometry. Flow cytometric analysis was performed, as described above (6,7), by using a 15 milliwatt air-cooled argon laser to produce 488 nm light. DCF fluorescence emission was collected with a 529 nm band pass filter. The mean fluorescence intensity of 2 x 10^4 cells was quantified using Multicycle software (Phoenix Flow System, San Diego, CA).

Measurement of Mitochondrial Membrane Potential ($\Delta\psi$m) and Mitochondrial Membrane Lipid Peroxidation

To measure mitochondrial membrane potential, cells were incubated with 1 μmol/L Rho-123 in 7% CO_2 at 37ºC for 1 h (12). To measure mitochondrial membrane lipid peroxidation, cells were incubated with 50 nmol/L NAO in 7% CO_2 at 37ºC for 15 min (12). Cells were rinsed with PBS, trypsinized from cultures, and resuspended in PBS for flow cytometric analysis, as described above, at the excitation and emission wavelengths of 488 and 529 nm, respectively, for Rho-123 or NAO fluorescence measurements.

Determination of Caspase Activity by Luminescence Spectroscopy

Caspase-3/7 activity was measured using a Caspase-Glo assay kit (Promega, Madison, WI). Cells were lysed in a buffer (10 mmol/L Tris–HCl, 150 mmol/L NaCl, 1% Triton X-100, 5 mmol/L EDTA, 10 mmol/L sodium pyrophosphate, 10% glycerol, 0.1% Na_3VO_4, 50 mmol/L

NaF, pH 7.4) (6,7). Whole cell lysates were isolated from the supernatants after centrifugation of crude cell lysates at 20,000 x g for 20 min. Protein concentrations in cell lysates were measured using the BCA assay (Pierce, Rockford, IL). Cell lysates containing 30 μg of protein were incubated with a proluminescent substrate specific for caspase-3/7 in white-walled 384-well plates at ambient temperature for 1 h. The released luminescence in each reaction was measured in a luminometer plate-reader (Bio-Tek).

Statistical Analysis

Statistical significance was analyzed by the Student *t* test. A *P*-value of ≤ 0.05 was considered significant.

Results

Intracellular ROS Increase by Oncogenic H-Ras and HDACIs in Human Urinary Bladder Cancer Cells

To determine whether expression of oncogenic H-Ras and HDACI treatment resulted in increasing intracellular ROS contributing to selective apoptosis of human cancer cells, we used CM-H_2DCF-DA (30) to measure the overall intracellular ROS levels by flow cytometry in FK228-treated cells. As shown in Fig. 1A, FK228 treatment significantly increased ROS in both parental J82 and J82-Ras cells, and co-treatment of cells with the antioxidant NAC (11,12,31) significantly reduced FK228-induced ROS. The basal level of ROS was detectably higher in J82-Ras cells than in J82 cells, and FK228 treatment induced significantly higher levels of ROS in J82-Ras cells compared to J82 cells in a time-dependent manner (Fig. 1B). These results

verified that expression of oncogenic H-Ras or FK228 treatment resulted in increases of ROS; expression of oncogenic H-Ras enhanced FK228-increased ROS in J82 cells. In addition, higher levels of ROS (Fig. 1C) correlated with higher degrees of FK228-induced apoptosis (Fig. 1D) of J82-Ras cells versus J82 cells. Reduction of FK228-induced ROS from approximately 1.9- to 1.4-fold and from approximately 3.3- to 2.4-fold by NAC (Fig. 1C) significantly reduced FK228-induced apoptosis from approximately 14% to 10% and from approximately 37% to 27% in parental J82 and J82-Ras cells (Fig. 1D), respectively, though NAC treatment was able to only partially suppress FK228-induced ROS and apoptosis in J82 and J82-Ras cells.

Using another HDACI, TSA (22,23), which is structurally unrelated from depsipeptide FK228, we detected that TSA treatment also induced significantly higher levels of ROS (Fig. 2A), apoptosis (Fig. 2B), and caspase-3/7 activity (Fig. 2C) in J82-Ras cells compared to J82 cells. Co-treatment with NAC resulted in a significant reduction of TSA-increased ROS from approximately 1.6- to 1.3-fold and from approximately 2.7- to 1.9-fold (Fig. 2A), a reduction in apoptosis from approximately 12% to 9% and from approximately 33% to 26% (Fig. 2B), and in caspase-3/7 activity from approximately 2.7- to 2-fold and from approximately 9- to 5.9-fold (Fig. 2C) in J82 and J82-Ras cells, respectively. Thus, increased intracellular ROS played an important role in selective apoptosis of oncogenic H-Ras-expressing, J82-Ras versus parental J82 cells induced by both HDACIs FK228 and TSA. In addition, using an unbiased anticancer agent to induce apoptosis of J82-Ras and parental J82 cells as a control, we did not detect any differentially up-regulated ROS induced by 5-Fluorouracil in J82-Ras versus J82 cells (data not shown).

ROS-Mediated Oxidative Damage in FK228-Induced Cell Death

In investigating the involvement of mitochondrial membrane damage in FK228-induced apoptosis, we labeled cells with Rho-123 to measure mitochondrial membrane potential in FK228-treated cells. We detected that FK228 treatment resulted in reduction of mitochondrial membrane potential, which was indicated by reduction of Rho-123 labeling down to approximately 95% and 75% in J82 and J82-Ras cells, respectively (Fig. 3A), indicating a possible mitochondrial membrane damage induced by FK228. To investigate whether FK228-induced ROS was involved in mitochondrial membrane damage, we used NAO to measure lipid peroxidation of mitochondrial membrane in FK228-treated cells. NAO has been shown to specifically interact with a mitochondrial membrane lipid component cardiolipin; and cardiolipin peroxidation induced by oxidative damage to mitochondrial membrane reduces the NAO-labeling of cardiolipin (32). As shown in Fig. 3B, FK228 treatment significantly reduced NAO-labeling to approximately 79% and 59% in parental J82 and J82-Ras cells, respectively; and, co-treatment with NAC significantly reversed the FK228-reduced NAO-labeling back to approximately 92% and 83% in parental J82 and J82-Ras cells, respectively. FK228 treatment appeared to result in higher oxidative damage to mitochondrial membrane in J82-Ras cells than in parental J82 cells. Using rotenone to block mitochondrial ROS (33,34), we detected that rotenone treatment resulted in modest but significant reduction of FK228-increased ROS from approximately 1.3- to 1.1-fold and from approximately 2.2- to 1.9-fold (Fig. 3C) and resulted in significant reversal of FK228-decreased cell viability from approximately 73% back to 86% and from approximately 51% back to 72% (Fig. 3D) in parental J82 and J82-Ras cells, respectively. Apparently, FK228-induced ROS was involved in mitochondrial membrane damage, and reduction of FK228-induced mitochondrial ROS reduced FK228-induced cell death.

Dose-Dependent Induction of Cell Death and Caspases by FK228 and ROS

To measure oncogenic H-Ras-enhanced susceptibility of J82 cells to FK228 for inducing cell death, we compared IC_{50} values of FK228 for J82 and J82-Ras cells. As shown in Fig. 4A, IC_{50} values of FK228 for J82 and J82-Ras cells were determined at concentrations of 500±50 nmol/L and 5±2 nmol/L, respectively. Accordingly, expression of oncogenic H-Ras in J82 cells resulted in an approximate 100-fold increase of cell susceptibility to FK228 for inducing cell death.

To measure ROS levels potentiated by oncogenic H-Ras for inducing cell death, we compared IC_{50} values of H_2O_2 for J82-Ras and J82 cells. As shown in Fig. 4B, IC_{50} values of H_2O_2 for J82 and J82-Ras cells were determined at concentrations of 2±0.15 mmol/L and 1±0.15 mmol/L, respectively. Accordingly, the result indicated that expression of oncogenic H-Ras-potentiated endogenous ROS resulted in an approximate 2-fold increase of cell susceptibility to H_2O_2 for inducing cell death.

Combined results from the above studies indicated that expression of oncogenic H-Ras in cells resulted in elevated ROS, enhanced FK228-induced ROS, and increased susceptibility to H_2O_2 for inducing cell death. J82-Ras cells with a higher endogenous level of ROS than J82 cells required less H_2O_2 for inducing cell death. Based on IC_{50} values of FK228 and H_2O_2 for J82 and J82-Ras cells, we tested whether distinguishable degrees of cell death and caspase activation were induced by FK228 in combination with H_2O_2 in a dose-dependent manner. As shown in Fig. 4C, treatment of J82 cells with FK228 at 5 nmol/L, which was the IC_{50} value of FK228 for J82-Ras cells (*column 8*), reduced cell viability to approximately 70% (*column 4*). Similarly, treatment of J82 cells with H_2O_2 at 1 mmol/L, which was the IC_{50} value of H_2O_2 for

J82-Ras cells (*column 9*), reduced cell viability to approximately 70% (*column 5*). Noteworthy is the difference between IC_{50} values of H_2O_2 for J82 (2 mmol/L) and J82-Ras (1 mmol/L): 1 mmol/L. The additional 1 mmol/L H_2O_2 appeared to be sufficient to enhance the activity of 5 nmol/L FK228 to reduce cell viability to 50% (*column 6*), as induced by 500 nmol/L FK228 in J82 cells (*column 2*). Accordingly, H_2O_2 was able to enhance FK228-induced cell death in a dose-dependent manner; treatment with both FK228 and H_2O_2 cooperatively induced death of J82 cells.

To verify whether caspase-3/7 activity was increased by the addition of H_2O_2 to FK228 treatment, we treated J82 and J82-Ras cells with FK228 in the presence of additional H_2O_2. As shown in Fig. 4D, treatment of J82 cells with FK228 at 500 nmol/L (*column 3*) or H_2O_2 at 2 mmol/L (*column 5*) significantly induced caspase-3/7 activity to approximately 8- and 6-fold, respectively. Treatment of J82 cells with FK228 at 5 nmol/L (*column 7*) or H_2O_2 at 1 mmol/L (*column 9*) significantly induced an approximate 3-fold increase in caspase-3/7 activity. Interestingly, treatment of J82 cells with 5 nmol/L FK228 and an additional 1 mmol/L H_2O_2 significantly induced an increase in caspase-3/7 activity by approximately 7-fold (*column 11*); thus, treating cells with FK228 and H_2O_2 additively increased caspase-3/7 activity in J82 cells. The additional 1 mmol/L H_2O_2 appeared to be sufficient to enhance the activity of 5 nmol/L FK228 to induce caspase activity to a level similar to that induced by 500 nmol/L FK228 in J82 cells. In contrast, treating J82-Ras cells with 5 nmol/L FK228 (*column 15*) or 1 mmol/L H_2O_2 (*column 17*) alone significantly induced an increase in caspase-3/7 activity by approximately 9- and 11-fold, respectively. All FK228- and/or H_2O_2-increased caspase-3/7 activity was

significantly suppressed by co-treatment with the antioxidant NAC (*even columns*). H_2O_2-induced cell death was also significantly suppressed by NAC (data not shown). Accordingly, H_2O_2 was able to play a contributing role in FK228-induced activation of caspases for inducing cell death in a dose-dependent manner. Oncogenic H-Ras-increased susceptibility of J82 cells to FK228 from IC_{50} values of 500 nmol/L to 5 nmol/L could be alternately achieved by an additional 1-fold increase of 1 mmol/L H_2O_2. These results indicated that differentially up-regulated ROS quantitatively contributed to the proapoptotic ability of oncogenic H-Ras to enhance FK228-induced cell death and caspase activation.

ROS Increase by Oncogenic H-Ras and FK228 in Human Colorectal Cancer Cells and Mouse Embryo Fibroblast Cells

To determine whether increases of ROS also played an important role in FK228-induced selective apoptosis of human cancer cells other than J82 cells, we treated human colorectal adenocarcinoma HT29 cells and oncogenic H-Ras-expressing, HT29-Ras cells (7) with FK228 in the presence of NAC (Fig. 5A to 5C). To determine whether an increase of ROS played an important role in FK228-induced selective apoptosis of cells other than human cells, we treated mouse embryo fibroblast 10T1/2 cells and oncogenic H-Ras-expressing, 10T1/2-Ras cells (8) with FK228 in the presence of NAC (Fig. 6A to 6C). We detected that FK228 treatment induced significantly higher levels of ROS to approximately 2.7- and 2.4-fold (Fig. 5A and 6A), apoptosis to approximately 40% and 37% (Fig. 5B and 6B), and caspase-3/7 activity to approximately 8- and 9-fold (Fig. 5C and 6C) in HT29-Ras and 10T1/2-Ras cells, respectively, compared to the FK228-induced ROS to approximately 1.6- and 1.4-fold (Fig. 5A and 6A),

apoptosis to approximately 13% and 11% (Fig. 5B and 6B), and caspase-3/7 activity to approximately 3-fold (Fig. 5C and 6C) in parental HT29 and 10T1/2 cells, respectively. NAC treatment resulted in a significant reduction of FK228-increased ROS down to approximately 1.8-fold (Fig. 5A and 6A) and apoptosis down to approximately 28% (Fig. 5B and 6B) in both oncogenic H-Ras-expressing, HT29-Ras and 10T1/2-Ras cells, and a significant reduction of caspase-3/7 activity down to approximately 4.4- and 5.7-fold (Fig. 5C and 6C) in HT29-Ras and 10T1/2-Ras cells, respectively. In addition, NAC treatment resulted in a significant reduction of FK228-increased ROS down to approximately 1.3- and 1.2-fold (Fig. 5A and 6A), apoptosis down to approximately 9% and 8% (Fig. 5B and 6B) in parental HT29 and 10T1/2 cells, respectively, and caspase-3/7 activity down to approximately 2-fold (Fig. 5C and 6C) in both types of cells. Accordingly, increased intracellular ROS also played an important role in FK228-induced selective apoptosis of oncogenic H-Ras-expressing human colorectal cancer cells and oncogenic H-Ras-expressing mouse embryo fibroblast cells versus their parental counterpart cells in addition to human urinary bladder cancer cells.

Discussion

In this communication, our studies show that differentially up-regulated intracellular ROS played a pivotal role in selective apoptosis induced by the HDACIs FK228 and TSA and profound activation of caspases in oncogenic H-Ras-expressing human urinary bladder cancer J82, human colorectal cancer HT29, and mouse embryo fibroblast 10T1/2 cells versus their parental counterpart cells. Expression of oncogenic H-Ras resulted in elevation of intracellular ROS in cells, as did treatment of cells with HDACIs; as a result, expression of oncogenic H-Ras

in cells and FK228 treatment resulted in cooperative elevation of intracellular ROS in cells. FK228 treatment profoundly increased ROS in all the oncogenic H-Ras-expressing, J82-Ras, HT29-Ras, and 10T1/2-Ras cells and modestly increased ROS in parental counterpart cells, which led to induction of profound and modest mitochondrial membrane damage, caspases, and apoptosis in oncogenic H-Ras-expressing cells and parental counterpart cells, respectively. Blockage of ROS production resulted in suppression of FK228-induced mitochondrial membrane damage, apoptosis, and caspase activation, indicating an important role of intracellular ROS in FK228-induced selective apoptosis of oncogenic H-Ras-expressing cells versus their parental counterpart cells. Although ROS has been reportedly shown to induce DNA damage through p53 activity, leading to apoptosis (35), it is unlikely to be involved in HDACI-induced cell death of either J82 or HT29 cells, which host the inactive mutant p53 genes (4, 36).

Expression of oncogenic H-Ras in J82 cells increased cell susceptibility not only to HDACIs but also to H_2O_2 for inducing apoptosis and caspase activation. Elevation of H_2O_2 has been postulated to facilitate apoptosis (37,38). It has also been postulated that the high levels of H_2O_2 frequently detected in cancer cells may potentiate cancer cells to be more susceptible to H_2O_2-induced apoptosis than normal counterpart cells (39). Our studies showed that expression of oncogenic H-Ras in J82 cells resulted in a 100-fold increase of cell susceptibility to FK228 and a 2-fold increase of cell susceptibility to H_2O_2 for inducing cell death. The IC_{50} values of FK228 for J82 and J82-Ras were 500 and 5 nmol/L, respectively. The difference between IC_{50} values of H_2O_2 for J82 (2 mmol/L) and J82-Ras (1 mmol/L) was 1 mmol/L. Treatment of J82 cells with FK228 at 5 nmol/L or H_2O_2 at 1 mmol/L alone resulted in a reduction of cell viability to 70%. Treatment with 5 nmol/L FK228 and an additional 1 mmol/L H_2O_2 resulted in a

reduction of cell viability to 50% and was sufficient to induce activation of caspases to levels similar to those induced by either 500 nmol/L FK228 or 2 mmol/L H_2O_2 alone. Thus, the oncogenic H-Ras-increased susceptibility of J82 cells to FK228 from IC_{50} values of 500 nmol/L to 5 nmol/L could be alternately achieved by an additional 1-fold increase of 1 mmol/L H_2O_2. Our semi-quantitative study verified that differentially up-regulated intracellular ROS played a contributing role in the proapoptotic ability of oncogenic H-Ras to increase cell susceptibility to HDACIs for inducing apoptosis and caspase activation in a dose-dependent manner.

Although differential regulation of ROS played an important role, other mechanisms are also involved in HDACI-induced selective apoptosis of oncogenic H-Ras-expressing cells versus parental counterpart cells. Previously, we reported that differential regulation of the caspase pathways, the Raf and ERK pathway, the p38/SAPK pathway, $p21^{Cip1}$ and $p27^{Kip1}$, and core histone contents contributes to FK228-induced selective apoptosis of oncogenic H-Ras-expressing, J82-Ras, HT29-Ras, and 10T1/2-Ras cells versus their parental counterpart cells (6-9), though some discrepancies in regulation of the downstream ERK pathway and PI3K pathway are detectable between these cell lines. As a consequence, reduction of ROS by either NAC or rotenone may not be able to completely suppress FK228-induced cell death. However, we also experienced incomplete blockage of FK228-induced ROS by using NAC and rotenone, though both NAC and rotenone are recognized to exhibit potent activity in blocking intracellular ROS (40). Whether complete blockage of FK228-induced ROS may result in completely suppressing FK228-induced cell death remains to be clarified.

NAC, a precursor of glutathione (40), was able to significantly reduce FK228- and TSA-induced ROS and apoptosis in oncogenic H-Ras-expressing and parental counterpart cells.

HDACIs have been shown to deplete cellular glutathione (41), depletion of cellular glutathione results in ROS accumulation (12,41), and NAC is able to suppress glutathione depletion and ROS accumulation (12). HDACI has also been shown to up-regulate thioredoxin-binding protein-2, resulting in suppression of thioredoxin, which is a major intracellular scavenger of ROS, and leading to excessive accumulation of intracellular ROS (42). Whether depletion of cellular glutathione, up-regulation of thioredoxin-binding protein-2, and down-regulation of thiroredoxin are involved in profound increases of ROS by FK228 as well as TSA in selective induction of apoptosis in oncogenic H-Ras-expressing cells remains to be determined.

In conclusion, our study revealed profound increases of intracellular ROS cooperatively induced by expression of oncogenic H-Ras and treatment with HDACIs FK228 and TSA, leading to selective induction of apoptosis of oncogenic H-Ras-expressing cancer cells versus their parental counterpart cells. It is important to utilize the cell killing potential of ROS in control of oncogenic Ras-expressing cancer cells and any cancer cells with potential to generate high levels of ROS by using ROS-inducing anticancer agents, such as HDACIs, to increase intracellular ROS to induce selective cell death of target cancer cells. The proapoptotic ability of oncogenic H-Ras, through increases of intracellular ROS, to increase cell susceptibility to HDACIs should be seriously considered in developing anticancer therapeutics against Ras-related human cancers and any other types of human cancers with intrinsic ability to generate toxic levels of ROS induced by HDACIs.

LIST OF REFERENCES

1. Buyru N, Tigli H, Ozcan F, Dalay N. Ras oncogene mutations in urine sediments of patients with bladder cancer. J Biochem Mol Biol 2003;36:399-402.
2. Oxford G, Theodorescu D. The role of Ras superfamily proteins in bladder cancer progression. J Urol 2003;170:1987-93.
3. Wu XR. Urothelial tumorigenesis: a tale of divergent pathways. Nat Rev Cancer 2005;5:713-25.
4. Cheng YT, Li YL, Wu JD, et al. Overexpression of MDM-2 mRNA and mutation of the p53tumor suppressor gene in bladder carcinoma cell lines. Mol Carcinog 1995;13:173-81.
5. Wang DS, Rieger-Christ K, Latini JM, et al. Molecular analysis of PTEN and MXI1 in primary bladder carcinoma. Int J Cancer 2000;88:620-5.
6. Choudhary S, Wang HCR. Proapoptotic ability of oncogenic H-Ras to facilitate apoptosis induced by histone deacetylase inhibitors in human cancer cells. Mol Cancer Ther 2007;6:1099-111.
7. Choudhary S, Wang HCR. Pro-apoptotic activity of oncogenic H-Ras for histone deacetylase inhibitor to induce apoptosis of human cancer HT29 cells. J Cancer Res Clin Oncol 2007;133:725-39.
8. Fecteau KA, Mei J, Wang HCR. Differential modulation of signaling pathways and apoptosis of ras-transformed cells by a depsipeptide FK228. J Pharmacol Exp Ther 2002;300:890-9.

9. Song P, Wei J, Wang HCR. Distinct roles of the ERK pathway in modulating apoptosis of Ras-transformed and non-transformed cells induced by anticancer agent FK228. FEBS Lett 2005;579:90-4.

10. Irani K, Xia Y, Zweier JL, et al. Mitogenic signaling mediated by oxidants in Ras-transformed fibroblasts. Science 1997;275:1649-52.

11. Alexandrova AY, Kopnin PB, Vasiliev JM, Kopnin BP. ROS up-regulation mediates Ras-induced changes of cell morphology and motility. Exp Cell Res 2006;312:2066-73.

12. Trachootham D, Zhou Y, Zhang H, et al. Selective killing of oncogenically transformed cells through a ROS-mediated mechanism by β-phenylethyl isothiocyanate. Cancer Cell 2006;10:241-52.

13. Cho HJ, Jeong HG, Lee JS, et al. Oncogenic H-Ras enhances DNA repair through the Ras/phosphatidylinositol 3-kinase/Rac1 pathway in NIH3T3 cells. Evidence for association with reactive oxygen species. J Biol Chem 2002;277:19358-66.

14. Yang JQ, Li S, Domann FE, Buettner GR, Oberley LW. Superoxide generation in v-Ha-ras-transduced human keratinocyte HaCaT cells. Mol Carcinog 1999;26:180-8.

15. Santillo M, Mondola P, Serù R, et al. Opposing functions of Ki- and Ha-Ras genes in the regulation of redox signals. Curr Biol 2001;11:614-9.

16. Liu R, Li B, Qiu M. Elevated superoxide production by active H-ras enhances human lung WI-38VA-13 cell proliferation, migration and resistance to TNF-alpha. Oncogene 2001;20:1486-96.

17. Mitsushita J, Lambeth JD, Kamata T. The superoxide-generating oxidase Nox1 is functionally required for Ras oncogene transformation. Cancer Res 2004;64:3580-5.

18. Shinohara M, Shang WH, Kubodera M, et al. Nox1 redox signaling mediates oncogenic Ras-induced disruption of stress fibers and focal adhesions by down-regulating Rho. J Biol Chem 2007;282:17640-8.
19. Chuang JI, Chang TY, Liu HS. Glutathione depletion-induced apoptosis of Ha-ras-transformed NIH3T3 cells can be prevented by melatonin. Oncogene 2003;22:1349-57.
20. Kopnin PB, Agapova LS, Kopnin BP, Chumakov PM. Repression of sestrin family genes contributes to oncogenic Ras-induced reactive oxygen species up-regulation and genetic instability. Cancer Res 2007;67:4671-8.
21. Kim S, Moon A. Capsaicin-induced apoptosis of H-ras-transformed human breast epithelial cells is Rac-dependent via ROS generation. Arch Pharm Res 2004;27:845-9.
22. Marks PA, Miller T, Richon VM. Histone deacetylases. Current Opin Pharmacol 2003;3:344-51.
23. Dokmanovic M, Marks PA. Prospects: histone deacetylase inhibitors. J Cell Biochem 2005;96:293-304.
24. Espino PS, Drobic B, Dunn KL ,Davie JR. Histone modifications as a platform for cancer therapy. J Cell Biochem 2005;94:1088-102.
25. Glaser KB, Li J, Staver MJ, et al. Role of Class I and Class II histone deacetylases in carcinoma cells using siRNA. Biochem Biophys Res Comm 2003;310:529-36.
26. Bolden JE, Peart MJ, Johnstone RW. Anticancer activities of histone deacetylase inhibitors. Nat Rev Drug Discov 2006;5:769-83.
27. Vigushin DM. FR-901228 (Fujisawa/National Cancer Institute). Curr Opin Investig Drugs 2002;3:1396-402.

28. Furumai R, Matsuyama A, Kobashi N, et al. FK228 (depsipeptide) as a natural prodrug that inhibits class I histone deacetylases. Cancer Res 2002;62:4916-21.
29. Adachi M, Zhang Y, Zhao X, et al. Synergistic effect of histone deacetylase inhibitors FK228 and m-carboxycinnamic acid bis-hydroxamide with proteasome inhibitors PSI and PS-341 against gastrointestinal adenocarcinoma cells. Clin Cancer Res 2004;10:3853-62.
30. Jakubowski W, Bartosz G. 2,7-dichlorofluorescin oxidation and reactive oxygen species: what does it measure? Cell Biol Int 2000;24:757-60.
31. Sadowska AM, Manuel-Y-Keenoy B, De Backer WA. Antioxidant and anti-inflammatory efficacy of NAC in the treatment of COPD: discordant in vitro and in vivo dose-effects: a review. Pulm Pharmacol Ther 2007;20:9-22.
32. Nomura K, Imai H, Koumura T, Kobayashi T, Nakagawa Y. Mitochondrial phospholipid hydroperoxide glutathione peroxidase inhibits the release of cytochrome c from mitochondria by suppressing the peroxidation of cardiolipin in hypoglycaemia-induced apoptosis. Biochem J 2000;351:183-93.
33. Barrientos A, Moraes CT. Titrating the effects of mitochondrial complex I impairment in the cell physiology. J Biol Chem 1999;274:16188-97.
34. Benard G, Bellance N, James D, et al. Mitochondrial bioenergetics and structural network organization. J Cell Sci 2007;120:838-48.
35. Cardaci S, Filomeni G, Rotilio G, Ciriolo MR**.** Reactive oxygen species mediate p53 activation and apoptosis induced by sodium nitroprusside in SH-SY5Y cells. Mol Pharmacol 2008;74:1234-45.

36. Huang F, Hsu S, Yan Z, Winawer S, Friedman E . The capacity for growth stimulation by TGF beta 1 seen only in advanced colon cancers cannot be ascribed to mutations in APC, DCC, p53 or ras. Oncogene 1994;9:3701–6.
37. Alexandre J, Batteux F, Nicco C, et al. Accumulation of hydrogen peroxide is an early and crucial step for paclitaxel-induced cancer cell death both in vitro and in vivo. Int J Cancer 2006;119:41-8.
38. Pervaiz S, Clement MV. Superoxide anion: oncogenic reactive oxygen species? Int J Biochem Cell Biol 2007;39:1297-304.
39. López-Lázaro M. Dual role of hydrogen peroxide in cancer: possible relevance to cancer chemoprevention and therapy. Cancer Lett 2007;252:1-8.
40. Deneke SM. Thiol based antioxidant. Curr Top Cell Regul 2000;36:151-80.
41. Rikiishi H, Shinohara F, Sato T, Sato Y, Suzuki M, Echigo S. Chemosensitization of oral squamous cell carcinoma cells to cisplatin by histone deacetylase inhibitor, suberoylanilide hydroxamic acid. Int J Oncol 2007;30:1181-8.
42. Xu WS, Parmigiani RB, Marks PA. Histone deacetylase inhibitors: molecular mechanisms of action. Oncogene 2007;26:5541-52.

APPENDIX

Figure 1. Oncogenic H-Ras- and FK228-induced ROS and apoptosis in human urinary bladder cancer J82 cells. **A,** J82 and J82-Ras cells were treated with 0 and 5 nmol/L FK228 (FK) in the presence or absence of 5 mmol/L NAC for 24 h. **B**, J82 and J82-Ras cells were treated with 5 nmol/L FK228 for 0, 12, 24, and 36 h. **C and D**, J82 (white *columns*) and J82-Ras (dark *columns*) cells were treated with 5 nmol/L FK228 in the presence or absence of 5 mmol/L NAC for 36 h. **A, B, and C**, cultures were then labeled with CM-H_2DCF-DA for flow cytometric analysis of intracellular ROS levels. Relative fluorescence intensity, as fold induction (X, arbitrary unit), was normalized by the fluorescence intensity determined in the untreated J82 cells, set as 1. *Points*, mean of triplicates; *bars*, SD. **D**, apoptotic cell population (%) was measured by flow cytometry with an Annexin-V-FITC Apoptosis Detection Kit. *Columns*, mean of triplicates; *bars*, SD. The Student *t* test was used to analyze statistical significance, indicated by * $P<0.05$, ** $P<0.01$, *** $P<0.001$. All results are representative of three independent experiments.

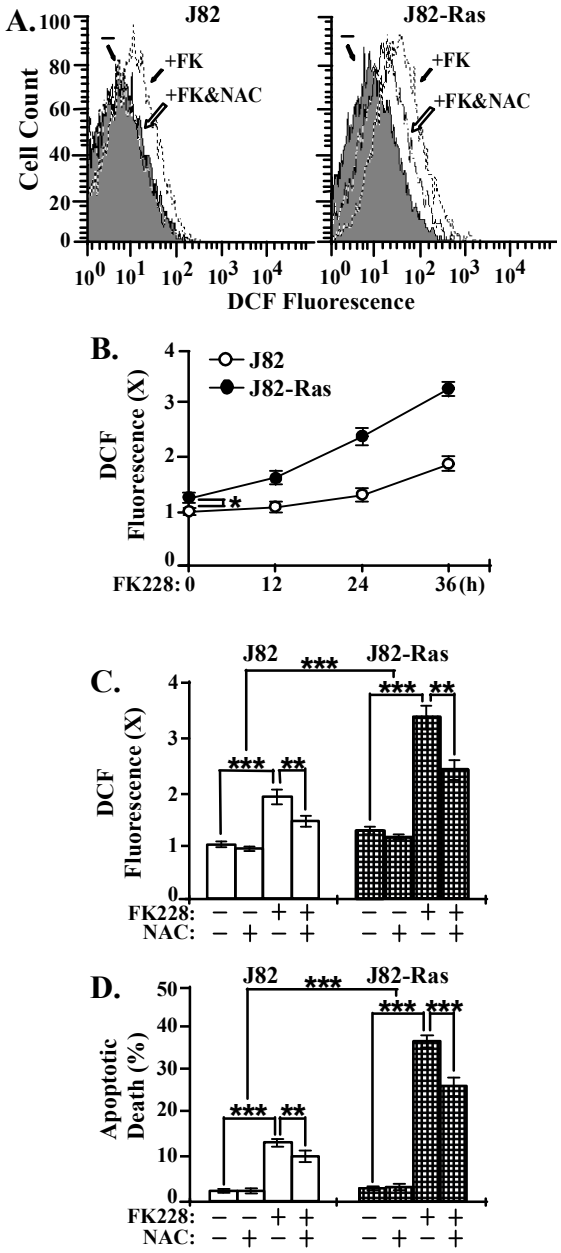
A.
J82
J82-Ras
Cell Count
+FK
+FK&NAC
DCF Fluorescence
B.
J82
J82-Ras
DCF Fluorescence (X)
FK228: 0 12 24 36 (h)
C.
J82
J82-Ras
DCF Fluorescence (X)
FK228:
NAC:
D.
J82
J82-Ras
Apoptotic Death (%)
FK228:
NAC:

Figure 2. ROS in TSA-induced apoptosis of J82 and J82-Ras cells. J82 (white *columns*) and J82-Ras (dark *columns*) cells were treated with 25 nmol/L TSA in the presence or absence of 5 mmol/L NAC for 48 h. **A**, cultures were then labeled with CM-H_2DCF-DA for flow cytometric analysis of intracellular ROS levels. Relative fluorescence intensity, as fold induction (X, arbitrary unit), was normalized by the fluorescence intensity determined in the untreated J82 cells, set as 1. *Columns*, mean of triplicates; *bars*, SD. **B**, apoptotic cell population (%) was measured by flow cytometry with an Annexin-V-FITC Apoptosis Detection Kit. *Columns*, mean of triplicates; *bars*, SD. **C**, a Caspase-Glo luminescence assay kit was used to measure the activity of caspase-3/7. Relative caspase activity, as fold induction (X, arbitrary unit), was normalized by the values determined in the untreated counterpart J82 and J82-Ras cells, set as 1. *Columns*, mean of triplicates; *bars*, SD. The Student *t* test was used to analyze statistical significance, indicated by * $P<0.05$, ** $P<0.01$, *** $P<0.001$. All results are representative of three independent experiments.

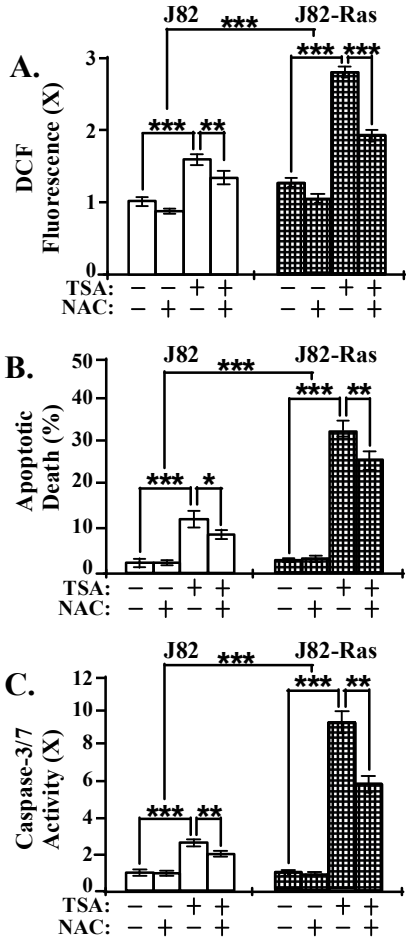
A.
DCF Fluorescence (X)
J82
J82-Ras
***
***
***
***
***
**
3
2
1
0
TSA: − − + + − − + +
NAC: − + − + − + − +
B.
Apoptotic Death (%)
J82
J82-Ras
***
***
***
**
*
50
40
30
20
10
0
TSA: − − + + − − + +
NAC: − + − + − + − +
C.
Caspase-3/7 Activity (X)
J82
J82-Ras
***
***
***
**
**
12
10
8
6
4
2
0
TSA: − − + + − − + +
NAC: − + − + − + − +

Figure 3. ROS-mediated oxidative damage in FK228-induced cell death. **A,** J82 (white *columns*) and J82-Ras (dark *columns*) cells were treated with 0 and 5 nmol/L FK228 for 36 h. Cultures were then labeled with Rho-123 for flow cytometric analysis of mitochondrial membrane potential. Relative fluorescence intensities in FK228-treated J82 cells and J82-Ras cells were normalized by the fluorescence intensities determined in the untreated counterpart J82 and J82-Ras cells, set as 100%. *Columns*, mean of triplicates; *bars*, SD. **B,** J82 and J82-Ras cells were treated with 0 and 5 nmol/L FK228 in the presence or absence of 5 mmol/L NAC for 36 h. Cultures were then labeled with NAO for flow cytometric analysis of mitochondrial membrane oxidative damage. Relative fluorescence intensities in FK228-treated J82 cells and J82-Ras cells were normalized by the fluorescence intensities determined in the untreated counterpart J82 and J82-Ras cells, set as 100%. *Columns*, mean of triplicates; *bars*, SD. **C,** J82 and J82-Ras cells were treated with 5 nmol/L FK228 in the presence or absence of 1 μmol/L rotenone (ROT) for 24 h. Cultures were then labeled with CM-H$_2$DCF-DA for flow cytometric analysis of intracellular ROS levels. Relative fluorescence intensity, as fold induction (X, arbitrary unit), was normalized by the fluorescence intensity determined in the untreated J82 cells, set as 1. *Columns*, mean of triplicates; *bars*, SD. **D,** J82 and J82-Ras cells were treated with 5 nmol/L FK228 in the presence or absence of 1 μmol/L rotenone for 36 h. Quantification of cell viability was determined with an MTT assay kit, and relative cell viability was normalized by the value determined in untreated counterpart J82 and J82-Ras cells, set as 100%. *Columns*, mean of tetraplicates; *bars*, SD. The Student *t* test was used to analyze statistical significance, indicated by * $P<0.05$, ** $P<0.01$, *** $P<0.001$. All results are representative of three independent experiments.

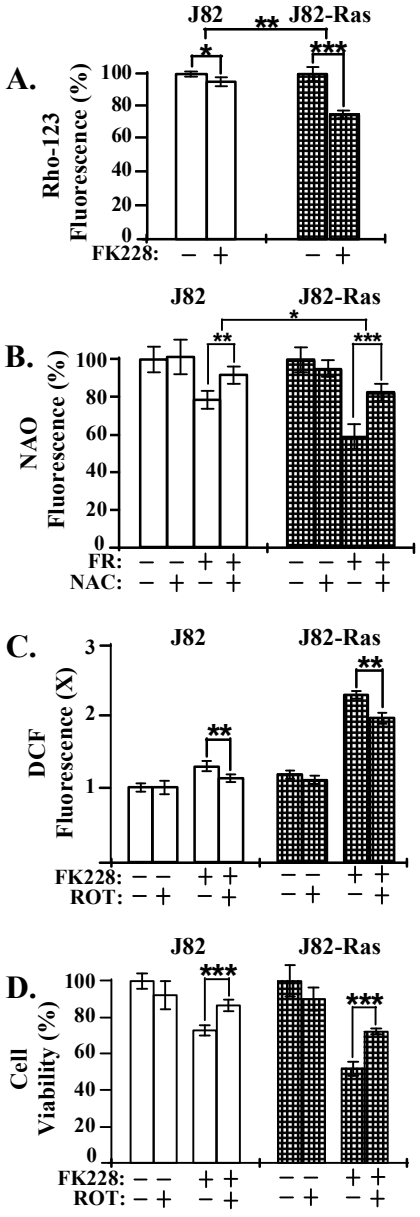
A.
J82
J82-Ras
Rho-123 Fluorescence (%)
FK228:
B.
NAO Fluorescence (%)
FR:
NAC:
C.
DCF Fluorescence (X)
FK228:
ROT:
D.
Cell Viability (%)
FK228:
ROT:

Figure 4. Dose-dependent enhancement of cell death and caspase activity by combined FK228 and H_2O_2. **A**, J82 and J82-Ras cells were treated with FK228 at a range of concentrations from 0.1 to 5000 nmol/L (nM) for 48 h, followed by MTT assay for revealing dose-response curves of cell viability in response to FK228. **B**, J82 and J82-Ras cells were treated with H_2O_2 at a range of concentrations from 0.1 to 500 mmol/L (mM) for 24 h, followed by MTT assay to reveal dose-response curves of cell viability in response to H_2O_2. *Points*, mean of triplicates. IC_{50} values of FK228 at 500±50 nmol/L and 5±2 nmol/L and IC_{50} values of H_2O_2 at 2±0.15 mmol/L and 1±0.15 mmol/L were determined for J82 and J82-Ras cells, respectively, from the semi-logarithmic dose-response curves of cell viability. All results are representative of three independent experiments. **C**, J82 (*columns* 1 to 6) and J82-Ras (*columns* 7 to 9) cells were treated with FK228 at 0, 5, or 500 nmol/L (nM) in the presence and absence of 1 or 2 mmol/L (mM) H_2O_2 for 48 h. Cell viability was measured with an MTT assay kit, and relative cell viability was normalized by the value determined in untreated counterpart J82 (*column* 1) and J82-Ras (*column* 7) cells, set as 100%. *Columns*, mean of tetraplicates; *bars*, SD. **D**, J82 (*columns* 1 to 12) and J82-Ras (*columns* 13 to 18) cells were treated with FK228 at 0, 5, or 500 nmol/L in the presence and absence of 1 or 2 mmol/L H_2O_2 and 5 mmol/L NAC (even *columns*) for 24 h. A Caspase-Glo luminescence assay kit was used to measure the activity of caspase-3/7. Relative caspase activity, as fold induction (X, arbitrary unit), was normalized by the values determined in the untreated counterpart J82 (*column* 1) and J82-Ras (*column* 13) cells, set as 1. *Columns*, mean of triplicates; *bars*, SD. The Student *t* test was used to analyze statistical significance, indicated by *** $P<0.001$. All results are representative of three independent experiments.

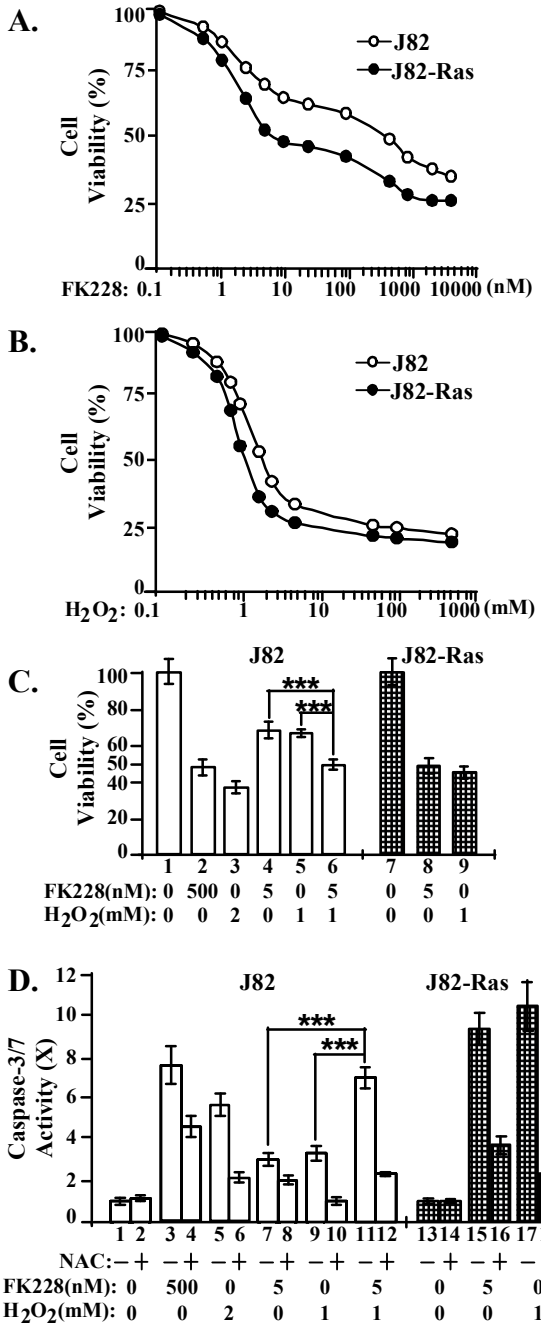
A.
Cell Viability (%)
J82
J82-Ras
FK228: 0.1 1 10 100 1000 10000 (nM)
B.
Cell Viability (%)
J82
J82-Ras
H2O2: 0.1 1 10 100 1000 (mM)
C.
J82
J82-Ras
Cell Viability (%)
***
***
1 2 3 4 5 6 7 8 9
FK228(nM): 0 500 0 5 0 5 0 5 0
H2O2(mM): 0 0 2 0 1 1 0 0 1
D.
J82
J82-Ras
Caspase-3/7 Activity (X)
***
***
1 2 3 4 5 6 7 8 9 10 11 12 13 14 15 16 17 18
NAC: − + − + − + − + − + − + − + − + − +
FK228(nM): 0 500 0 5 0 5 0 5 0
H2O2(mM): 0 0 2 0 1 1 0 0 1

Figure 5. Oncogenic H-Ras- and FK228-induced ROS and apoptosis of human colorectal cancer HT29 cells. HT29 (white *columns*) and HT29-Ras (dark *columns*) cells were treated with 1 nmol/L FK228 in the presence or absence of 5 mmol/L NAC for 48 h. **A**, cultures were then labeled with CM-H$_2$DCF-DA for flow cytometric analysis of ROS levels. Relative fluorescence intensity, as fold induction (X, arbitrary unit), was normalized by the fluorescence intensity determined in the untreated HT29 cells, set as 1. *Columns*, mean of triplicates; *bars*, SD. **B**, apoptotic population (%) was measured by flow cytometry with an Annexin-V-FITC Apoptosis Detection Kit. *Columns*, mean of triplicates; *bars*, SD. **C**, a Caspase-Glo luminescence assay kit was used to measure the activity of caspase-3/7. Relative caspase activity, as fold induction (X, arbitrary unit), was normalized by the values determined in the untreated counterpart HT29 and HT29-Ras cells, set as 1. *Columns*, mean of triplicates; *bars*, SD. The Student *t* test was used to analyze statistical significance, indicated by * $P<0.05$, ** $P<0.01$, *** $P<0.001$. All results are representative of three independent experiments.

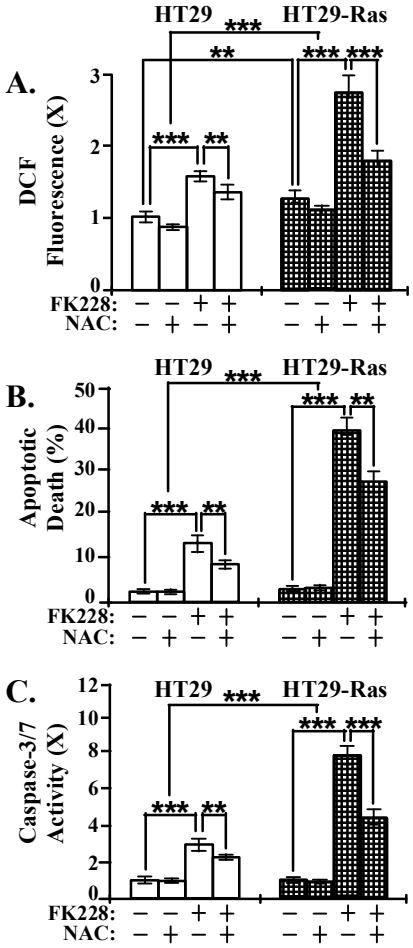
A.
HT29
HT29-Ras
DCF Fluorescence (X)
B.
Apoptotic Death (%)
C.
Caspase-3/7 Activity (X)
FK228:
NAC:

Figure 6. Oncogenic H-Ras- and FK228-induced ROS and apoptosis of mouse embryo fibroblast 10T1/2 cells. 10T1/2(white *columns*) and 10T1/2-Ras (dark *columns*) cells were treated with 1 nmol/L FK228 in the presence or absence of 5 mmol/L NAC for 48 h. **A**, cultures were then labeled with CM-H_2DCF-DA for flow cytometric analysis of intracellular ROS levels. Relative fluorescence intensity, as fold induction (X, arbitrary unit), was normalized by the fluorescence intensity determined in the untreated 10T1/2 cells, set as 1. *Columns*, mean of triplicates; *bars*, SD. **B**, apoptotic cell population (%) was measured by flow cytometry with an Annexin-V-FITC Apoptosis Detection Kit. *Columns*, mean of triplicates; *bars*, SD. **C**, a Caspase-Glo luminescence assay kit was used to measure the activity of caspase-3/7. Relative caspase activity, as fold induction (X, arbitrary unit), was normalized by the values determined in the untreated counterpart 10T1/2 and 10T1/2-Ras cells, set as 1. *Columns*, mean of triplicates; *bars*, SD. The Student *t* test was used to analyze statistical significance, indicated by * $P<0.05$, ** $P<0.01$, *** $P<0.001$. All results are representative of three independent experiments.

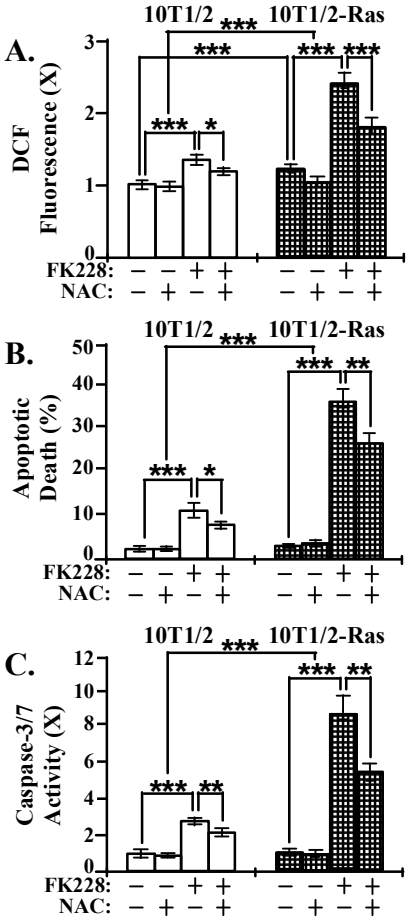
A.
DCF Fluorescence (X)
10T1/2
10T1/2-Ras
***
***
***
***
***
*
***
3
2
1
0
FK228: − − + + − − + +
NAC: − + − + − + − +
B.
Apoptotic Death (%)
10T1/2
10T1/2-Ras
***
***
**
***
*
50
40
30
20
10
0
FK228: − − + + − − + +
NAC: − + − + − + − +
C.
Caspase-3/7 Activity (X)
10T1/2
10T1/2-Ras
***
***
**
***
**
12
10
8
6
4
2
0
FK228: − − + + − − + +
NAC: − + − + − + − +

PART-V

General Discussion

General Discussion

The study presented in this dissertation was designed to (1) investigate the pro-apoptotic activity of oncogenic H-Ras in human cancer cells that allows HDACIs to induce selective apoptosis and, (2) show that elevated intracellular reactive oxygen species (ROS) play an important role in the pro-apoptotic ability of oncogenic H-Ras to enhance cell death induced by HDACIs.

Importance of the novel pro-apoptotic ability of oncogenic H-Ras in developing anticancer therapeutics against Ras-related cancers

Oncogenic Ras is widely involved in human cancers (1). Activating mutation of the K-*ras* gene is frequently detected in pancreatic and colonic carcinomas. H-*ras* mutations are commonly seen in bladder carcinomas, whereas lymphoid malignancies and melanomas frequently harbor activating mutations of the N-*ras* gene (1,2). Hence, it is important develop selective anticancer therapeutics against Ras-related human cancers by identifying anticancer agents and their molecular targets to selectively induce apoptosis of Ras-related cancer cells to increase the effectiveness of chemotherapy.

In our studies, introduction of the oncogenic H-*ras* gene into J82 cells promoted cells to acquire the tumorigenic ability to develop xenograft tumors in immune-deficient mice; however, it was also accompanied by the novel pro-apoptotic property which allowed FR901228 and TSA to induce selective apoptosis in these cells. The human urinary bladder carcinoma T24 cell line, in which oncogenic H-Ras is endogenously expressed (3), showed a comparable level of susceptibility with J82-Ras cells to both FR901228 and TSA for inducing cell death. We have also shown that expression of oncogenic H-Ras in human colorectal adenocarcinoma HT29, and

mouse embryo fibroblast 10T1/2 cells increases their susceptibility to the HDACIs FR901228 and TSA for inducing apoptosis. The observed ability of oncogenic H-Ras to increase cell susceptibility to HDACIs for inducing selective apoptosis lead us to suggest that oncogenic H-Ras possesses a pro-apoptotic ability to facilitate HDACI-induced apoptosis. However, expression of oncogenic H-Ras in any of these cells did not increase susceptibility to other agents, including U0126, LY294002, SB203580, SP600125, and Ac-DEVD-CHO. Therefore, the pro-apoptotic ability of oncogenic H-Ras that facilitates agents to induce cell death is HDACI-specific, but is not a cell type-specific property. In addition, our results also suggest that selectivity of HDACI to induce cell death in oncogenic H-Ras-expressing cells may be applicable to other Ras family proteins, such as K-Ras, as evident by a high susceptibility of SW480 cell line, which hosts the oncogenic K-*ras* gene, to both FR901228 and TSA for inducing cell death. However, whether the selectivity of HDACIs to induce cell death of oncogenic H-Ras-expressed cells is applicable to human cancers involving H-Ras overexpression or other oncogene-expressed cells needs to be broadly investigated.

Current Ras-targeted anticancer approaches are mainly based on understanding the roles of oncogenic Ras in tumorigenesis, such as inhibition of Ras protein synthesis, interference with Ras processing to functional sites, or blockage of downstream Ras effectors (4). However, agents targeting the pro-apoptotic activity of oncogenic Ras are still overlooked. Our studies verified the pro-apoptotic activity of oncogenic H-Ras that allows HDACIs to induce cell death of human cancer cells. Our results indicate the ability of HDACIs to discriminate between oncogenic H-Ras-expressed and counterpart human cells, and suggest a potential value of HDACIs in treating Ras-related human cancers. The values of the ERK, p38/SAPK and PI3-K

pathways, the death receptor family pathways, caspase-3, caspase-7, and caspase-8, and Cdk inhibitors as molecular targets need to be considered individually for designing therapeutic protocols using HDACI in combination with other agents to assure the effectiveness of target therapies for treat human cancer involving Ras or Raf activation.

Elevated intracellular reactive oxygen species (ROS) has a pivotal role in the pro-apoptotic ability of oncogenic H-Ras

Ectopic expression of oncogenic H-Ras has been shown to elevate intracellular ROS, including superoxide and hydrogen peroxide. Increased ROS is reportedly required for the Ras-induced increase in cell growth (5,6) and DNA repair (7) in mouse embryo fibroblast NIH3T3 cells. On the other hand, increased intracellular ROS has been postulated to play a role in the increased susceptibility of H-Ras-expressing ovarian and breast epithelial cells to β-phenylethyl isothiocyanate (8) and to capsaicin (9) for inducing cell death, respectively. However, whether increased ROS may also have played a role in the increased susceptibility of H-Ras-expressing human cancer cells to HDACIs for inducing selective apoptosis remained to be clarified. In addition, HDACIs treatment has been shown to result in elevated ROS in gastrointestinal cancer cells for inducing cell death (4). However, whether HDACI treatment was able to induce elevated ROS contributing to selective apoptosis of oncogenic H-Ras-expressing human cancer cells remained to be clarified.

In our studies, HDACIs treatment significantly increased ROS in all the oncogenic H-Ras-expressing cells (J82-Ras, HT29-Ras, and 10T1/2-Ras cells) compared to their parental counterpart cells. Severe accumulation of intracellular ROS in oncogenic H-Ras-expressing cells

caused profound induction of mitochondrial membrane damage, caspases, and apoptosis. In contrast, HDACIs treatment caused only modest increase in ROS insufficient to cause significant apoptosis in parental counterpart cells. Blockage of ROS production resulted in suppression of HDACI-induced mitochondrial membrane damage, apoptosis, and caspase activation, indicating an important role of intracellular ROS in HDACI-induced selective apoptosis of oncogenic H-Ras-expressing cells versus their parental counterpart cells. Although ROS has been reportedly shown to induce DNA damage through p53 activity, leading to apoptosis (10), it is unlikely to be involved in HDACI-induced cell death of either J82 or HT29 cells, which host the inactive mutant p53 genes (11,12).

In conclusion, our results show the contributing role of elevated ROS in the pro-apoptotic ability of oncogenic H-Ras to increase susceptibilities of human urinary bladder and colorectal cancer cells as well as mouse embryo fibroblast cells to HDACIs for inducing selective apoptosis. It is important to utilize the cell killing potential of ROS in control of oncogenic Ras-expressing cancer cells and any cancer cells with potential to generate high levels of ROS by using ROS-inducing anticancer agents, such as HDACIs, to increase intracellular ROS to induce selective cell death of target cancer cells. The pro-apoptotic ability of oncogenic H-Ras, through increases of intracellular ROS, to increase cell susceptibility to HDACIs should be seriously considered in developing anticancer therapeutics against Ras-related human cancers and any other types of human cancers with intrinsic ability to generate toxic levels of ROS induced by HDACIs.

Summary

These studies demonstrate that oncogenic H-Ras has a pro-apoptotic activity that allows histone deacetylase inhibitors (HDACIs) to induce selective apoptosis of oncogenic H-Ras-expressed cells (J82-Ras, HT29-Ras, and 10T1/2-Ras). H-Ras-potentiated ROS plays a pivotal role in the pro-apoptotic ability of oncogenic H-Ras to facilitate HDACI-induced, ROS-dependent mitochondrial damage, activation of caspase pathways and selective apoptosis of oncogenic H-Ras expressed cells. The interplay of above discussed factors can be summarized by the scheme shown in Figure 1.

Data also indicate that besides differential regulation of ROS, other mechanisms such as differential regulation of the caspase pathways, the Raf and ERK pathway, the p38/SAPK pathway, $p21^{Cip1}$ and $p27^{Kip1}$, and core histone contents also contributes to FR901228-induced selective apoptosis of oncogenic H-Ras-expressing, J82-Ras, HT29-Ras, and 10T1/2-Ras cells versus their parental counterpart cells, though some discrepancies in regulation of the downstream ERK pathway and PI3K pathway are detectable between these cell lines.

Prospects

Investigate the mechanisms for synergy between oncogenic H-Ras and HDACI in ROS mediated dell death

Our study revealed significant increases of intracellular ROS cooperatively induced by expression of oncogenic H-Ras and treatment with HDACIs FR901228 and TSA, leading to selective induction of apoptosis of oncogenic H-Ras-expressing cancer cells versus their parental

counterpart cells. However, a mechanism for synergy between oncogenic H-Ras and HDACI in ROS mediated dell death is not clear and warrant further investigations.

(1) **Investigating the antioxidant system of the cell.** HDACIs have been shown to deplete cellular glutathione (13), depletion of cellular glutathione results in ROS accumulation (8,13). HDACI has also been shown to up-regulate thioredoxin-binding protein-2, resulting in suppression of thioredoxin, which is a major intracellular scavenger of ROS, and leading to excessive accumulation of intracellular ROS (14). Glutathione and thioredoxin represents the two major antioxidant systems of the cells which neutralizes the cytotoxic effects of ROS (15). Whether depletion of cellular glutathione, up-regulation of thioredoxin-binding protein-2, and down-regulation of thiroredoxin are involved in profound increases of ROS by HDACIs in selective induction of apoptosis in oncogenic H-Ras-expressing cells remains to be determined.

(2) **Investigating the connection between Ras signaling pathways and ROS.** Our data suggest that the Ras-Raf-MEK1/2-ERK1/2 and the p38/SAPK pathways are differentially regulated in HDACI-induced selective apoptosis of oncogenic H-Ras-expressing cells. HDACI treatment stimulated the survival role of the ERK pathway and pro-apoptotic role of the p38/SAPK pathway in oncogenic H-Ras-expressing cells. Recent studies have shown that ROS participate in both Ras-Raf-MEK1/2-ERK1/2 signaling and the p38 MAPK pathway. Increased intracellular levels of ROS, induced by the Ras-Raf-MEK-ERK signaling cascade, may mediate the activation of the p38 pathway and act as an

intermediate signal between the MEK-ERK and MKK3/6-p38 pathways (16). On the other hand, the activation of p38 mitogen-activated protein kinase (MAPK) has been shown to be a prerequisite for ROS-mediated functions such as apoptotic cell death in cancer cells (17). Whether ROS directly mediate the Ras-Raf-MEK1/2-ERK1/2 and p38 MAPK signaling pathways in HDACI-induced selective apoptosis of oncogenic H-Ras-expressing cells remains to be determined.

LIST OF REFERENCES

1. Bos JL. Ras oncogenes in human cancer: a review. Cancer Res 1989; 49:4682–9.
2. Karnoub AE & Weinberg RA. Ras oncogenes: split personalities. Nature Reviews Molecular Cell Biology 9, 517-531 (July 2008)
3. Taparowsky E, Suard Y, Fasano O, Shimizu K, Goldfarb M, Wigler M. Activation of the T24 bladder carcinoma transformingg ene is linked to a single amino acid change. Nature 1982;300:762–5.
4. Adjei AA. Blocking oncogenic Ras signaling for cancer therapy. J Natl Cancer Inst 2001;93:1062–74.
5. Irani K, Xia Y, Zweier JL, et al. Mitogenic signaling mediated by oxidants in Ras-transformed fibroblasts. Science 1997;275:1649-52.
6. Chuang JI, Chang TY, Liu HS. Glutathione depletion-induced apoptosis of Ha-ras-transformed NIH3T3 cells can be prevented by melatonin. Oncogene 2003;22:1349-57.
7. Cho HJ, Jeong HG, Lee JS, et al. Oncogenic H-Ras enhances DNA repair through the Ras/phosphatidylinositol 3-kinase/Rac1 pathway in NIH3T3 cells. Evidence for association with reactive oxygen species. J Biol Chem 2002;277:19358-66.
8. Trachootham D, Zhou Y, Zhang H, et al. Selective killing of oncogenically transformed cells through a ROS-mediated mechanism by β-phenylethyl isothiocyanate. Cancer Cell 2006;10:241-52.
9. Kim S, Moon A. Capsaicin-induced apoptosis of H-ras-transformed human breast epithelial cells is Rac-dependent via ROS generation. Arch Pharm Res 2004;27:845-9.

10. Cardaci S, Filomeni G, Rotilio G, Ciriolo MR. Reactive oxygen species mediate p53 activation and apoptosis induced by sodium nitroprusside in SH-SY5Y cells. Mol Pharmacol 2008;74:1234-45.

11. Cheng YT, Li YL, Wu JD, et al. Overexpression of MDM-2 mRNA and mutation of the p53tumor suppressor gene in bladder carcinoma cell lines. Mol Carcinog 1995;13:173-81.

12. Huang F, Hsu S, Yan Z, Winawer S, Friedman E . The capacity for growth stimulation by TGF beta 1 seen only in advanced colon cancers cannot be ascribed to mutations in APC, DCC, p53 or ras. Oncogene 1994;9:3701–6.

13. Rikiishi H, Shinohara F, Sato T, Sato Y, Suzuki M, Echigo S. Chemosensitization of oral squamous cell carcinoma cells to cisplatin by histone deacetylase inhibitor, suberoylanilide hydroxamic acid. Int J Oncol 2007;30:1181-8.

14. Xu WS, Parmigiani RB, Marks PA. Histone deacetylase inhibitors: molecular mechanisms of action. Oncogene 2007;26:5541-52.

15. Klaunig JE, Kamendulis LM. 2004. The role of oxidative stress in carcinogenesis. Annu Rev Pharmacol Toxicol 44: 239-267.

16. Pan JS, Hong MZ, and Ren JL. Reactive oxygen species: A double-edged sword in oncogenesis. World J Gastroenterol. 2009 April 14; 15(14): 1702–1707.

17. Kang YH, Lee SJ. The role of p38 MAPK and JNK in Arsenic trioxide-induced mitochondrial cell death in human cervical cancer cells. J Cell Physiol. 2008;217:23–33.

APPENDIX

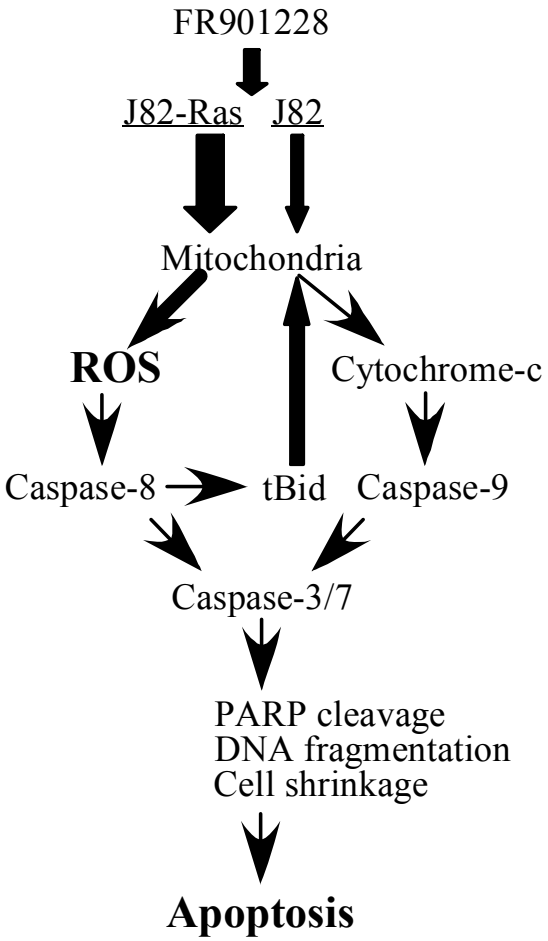

Figure 1.
Hypothetical scheme of FR901228-induced ROS-dependent, oncogenic H-Ras-enhanced caspase pathways for selective apoptosis.

VITA

Shambhunath Choudhary was born in Sindri, Bihar, India on the 5th of December, 1978, and was raised in Patna, Bihar. He completed his primary and advanced level education in Modern Public School and Government Boy's High School, respectively, in the same city. He earned his BVSc & AH (DVM) from the College of Veterinary Medicine & Animal Sciences, Kerala Agricultural University, Mannuthy, India, in June, 2004. In August 2004, he joined the University of Tennessee, Knoxville, USA, and received a Doctor of Philosophy (Ph.D) in Comparative and Experimental Medicine, from the Department of Comparative Medicine, College of Veterinary Medicine in May 2008. He plans to pursue his post doctoral training.